Application of adsorption on activated carbons and natural zeolite for the removal of lincomycin from wastewater of swine production industry

A Thesis Submitted to the College of

Graduate and Postdoctoral Studies

In Partial Fulfillment of the Requirements

For the Degree of

Master of Science

In the Department of Chemical and Biological Engineering

University of Saskatchewan

Saskatoon, Saskatchewan

Canada

By

Oscar Balladares Moyano

PERMISSION TO USE

In presenting this thesis in partial fulfillment of the requirements for a Postgraduate degree from the University of Saskatchewan, I agree that the Libraries of this University may make it freely available for inspection. I further agree that permission for copying of this thesis/dissertation in any manner, in whole or in part, for scholarly purposes may be granted by the professor or professors who supervised my thesis work or, in their absence, by the Head of the Department or the Dean of the College in which my thesis work was done. It is understood that any copying or publication or use of this thesis or parts thereof for financial gain shall not be allowed without my written permission. It is also understood that due recognition shall be given to me and to the University of Saskatchewan in any scholarly use which may be made of any material in my thesis.

Requests for permission to copy or to make other use of material in this thesis in whole or in part should be addressed to:

Head of the Department of Chemical and Biological Engineering

College of Engineering, 57 Campus Drive

University of Saskatchewan

Canada S7N 5A9

ABSTRACT

The occurrence of antibiotics in natural water bodies have concerned the scientific community because of the potential development of antibiotic resistance in bacteria. Lincomycin is a lincosamide antibiotic used in the Saskatchewan swine industry for infection treatment, prevention, and possibly weight gain. The dose recommended for swine contains 22 g of lincomycin per metric ton of feed. Due to partial metabolization, part of the lincomycin is excreted through manure. It has been reported that after 5 weeks of storage, 74 % of this compound is degraded by natural processes in the manure. Therefore, it is important to remove the remaining lincomycin from manure before its application to land.

Adsorption on activated carbons and zeolites was used for removing lincomycin from water and synthetic manure. For activated carbons, lincomycin adsorption was greater at solution initial pH 10, above the lincomycin's pKa (7.8), than at initial neutral pH of 6.5. On the other hand, increasing the pH value reduced the adsorption capacity in the natural zeolite. The presence of NaCl did not affect the adsorption capacity of activated carbons because non-electrostatic interactions controlled the process. Conversely, for natural zeolite, increasing ionic strength decreased the adsorption capacity, probably, because the cationic exchange process was affected. From the thermodynamic characterization, it was determined that the adsorption, on both activated carbons and zeolites, was endothermic and spontaneous.

The better performance adsorbents were evaluated in the removal of lincomycin from synthetic and real manure. In synthetic manure, the adsorption capacities were similar to the ones found at pH 10 in deionized water. The lack of solids and compounds competing for active sites, in the synthetic manure formulation, contributed to the unaltered adsorption capacities. On the other hand, in the real manure, due to competition and the presence of solids, the concentration of activated carbon used in the experiments with deionized water (50 mg/L) was insufficient for separating lincomycin. Different doses of activated carbon were tested and the simplified background equivalent compound model was used for predicting the lincomycin removal efficiency based on the used adsorbent dose. Activated carbon 1240 showed higher lincomycin

adsorption capacity than F400 in real manure. As a comparison, for 60% lincomycin removal, doses of 900 mg/L and 1300 mg/L of 1240 and F400 can be used, respectively.

ACKNOWLEDGEMENTS

First, I would like to thank my supervisor Dr. Jafar Soltan, who guided me through this important part of my life. More than my supervisor, he has been a friend and someone whom I can count on. Thank you for showing me that being a good person is more important than any academic degree. Finally, thank you for being such a nice person. I'll always remember you as one of the coolest guys I have ever met.

Also, I would like to acknowledge my graduate advisory committee members, Dr. Catherine Niu and Dr. Lifeng Zhang. Your knowledge and advice were fundamental for the completion of this research.

I want to acknowledge my family. They have been the biggest support in every step of my life. Thank you for your encouragement to follow my dreams.

Thanks to Jack (Zhuoyue), my Chinese little brother. He was my best friend in the most difficult part of this stage. Also, thanks to my research group colleagues, Mosi and Zahra. Their knowledge and experience were invaluable. I would like to acknowledge Mr. Richard Blondin and Ms. Heli Eunike for its assistance in the technical part of this project.

Finally, special gratitude to the Secretaría Nacional de Educación Superior, Ciencia, Tecnología e Innovacion (SENESCYT) for the complete financial support for completing my degree.

DEDICATION

To my parents, Sixto and Celida, and my sister Viviana.

TABLE OF CONTENTS

LIST OF TABLES

LIST OF FIGURES

NOMENCLATURE AND ABBREVIATIONS

NOMENCLATURE:

ΔG	Gibbs free energy change of adsorption (kJ/mol)
$\Delta H°$	Standard enthalpy change of adsorption (kJ/mol)
$\Delta S°$	Standard entropy change of adsorption (J/mol.K)
C_e	Concentration of adsorbate in solution (mg/L)
K_c	Thermodynamic equilibrium constant
K_L	Langmuir model constant ($L*mg^{-1}$)
K_S	Sips model constant ($L*mg^{-1}$)
K_f	Freundlich model constant $(mg/g)(L/mg)^{1/n}$
K_{ow}	Octanol-water partition coefficient
pKa	Acid dissociation constant
q_e	Adsorption capacity (mg adsorbate/mg adsorbent)
q_{max}	Monolayer maximum capacity in the Langmuir model (mg /mg adsorbent)
q_m	Monolayer maximum capacity in the Sips model (mg /mg adsorbent)
R	Universal gas constant ($8.314\ J\ K^{-1}\ mol^{-1}$)
R^2	Determination coefficient
rpm	revolutions per minute
T	Absolute temperature (K)
V	Volume of the solution (L)

W	Weight of adsorbent (g)

ABBREVIATIONS

1240	Cabot Norit 1240 granular activated carbon
ANOVA	Analysis of variance
ASAP	Accelerated surface area and porosimeter system
BET	Brunauer-Emmett-Teller
BJH	Barrett-Joyner-Halenda
EBCM	Equivalent background compound model
F400	Filtrasorb 400 granular activated carbon
GAC	Granular activated carbon
HDTMA	Hexadecyltrimethyl ammonium surfactant
HPLC	High-performance liquid chromatography
IAST	Ideal adsorbed solution theory
LSD	Least Significant Difference
n	Freundlich adsorption affinity parameter
NOM	Natural organic matter
NR	Norit Row 0.8 granular activated carbon
NZ	Clinoptilolite natural zeolite
NZH	Modified clinoptilolite by acid treatment
PAC	Powdered activated carbon
PSD	Pore size distribution

PZC	Point of zero charge
SAD	Sigma Aldrich Darco granular activated carbon
SAN	Sigma Aldrich Norit granular activated carbon
SEBCM	Simplified equivalent background compound model
SRC	Saskatchewan Research Council
TRM	The tracer model
UV-Vis	Ultraviolet and visible light
WDXRF	Wavelength dispersive X-ray fluorescence
XRF	X-ray fluorescence

CHAPTER 1
INTRODUCTION

In recent years, the occurrence, at low concentrations, of some emerging pollutants in water bodies has attracted the attention of the scientific community. Some examples of emerging pollutants are pharmaceutical compounds, hormones, personal care products, and pesticides that have been detected in nature. Particular attention has been placed on pharmaceutical compounds because problems like chronic toxicity, endocrine disruption and the development of pathogen resistance are associated with their occurrence [1].

The presence of antibiotics in water bodies, due to human and animal consumption [2], provides a suitable condition for bacteria to develop antibiotic resistance genes. In the livestock production industry, antibiotics are used mostly for disease treatment and prevention and occasionally weight gain. However, due to incomplete metabolization, in some cases, as much as 90% of the administered antibiotics doses are excreted through manure [3,4]. Only in Canada in 2014, around 1.5 million kg of antibiotic active compounds were used in the animal production industry [5]. From this amount, 7% was employed in Saskatchewan [5]. In the Canadian swine production industry, tetracyclines and lincosamides are the most popular groups of antibiotics for disease treatment and prevention applications [5].

Lincomycin is a lincosamide antibiotic used in the Saskatchewan swine production industry [6,7]. It has been reported that in swine liquid manure, after five of storage, 74% of this antibiotic is degraded by natural means [6]. Hence, when manure is applied to the land as natural fertilizer, the residual lincomycin may be transported to surface water bodies and, eventually, to rivers [7]. Experimental evidence has shown that lincomycin is one of the most frequently

detected antibiotics in the North American streams [8,9]. Due to these reasons, it is necessary to develop techniques for degrading or, at least, removing this compound from manure.

Several techniques like conventional oxidation [10], advanced oxidation [1,8,11], and membrane filtration [12] have been applied to remove antibiotics from water. However, low efficiency or generation of toxic by-products have been identified as shortcomings of these processes [13]. An alternative which avoids these problems is adsorption. The main advantage of this technique is that toxic or pharmacologically active products are not generated because pollutants are removed from the water matrix by the adsorbent [14]. On the other hand, it means the pollutant is only transferred from one media to another; therefore, a post-treatment is necessary [15].

The most common adsorbents are granular activated carbons that provide high surface area and removal capacity for organic compounds [14]. However, adsorption by activated carbons has limitations such as low selectivity, variable pore size distribution [14], and complicated regeneration processes [16]. Other materials for antibiotics removal are natural zeolites. These materials have been extensively used for pollutants removal [17]. However, the main limitation for their use is their low hydrophobicity [18]. For this reason, pre-treatments, like acid and surfactants addition, can be carried out to improve this property [17,19,20].

In this work, commercial activated carbons and natural zeolite were evaluated in the removal of lincomycin from deionized water and, in a second stage, from synthetic and real liquid swine manure. The influence of factors such as temperature, pH, and ionic strength was investigated. Finally, the adsorption isotherms were obtained and modeled through two, and three-parameter adsorption models and the thermodynamic characterization of the process was carried out.

The present thesis consists of six chapters including introduction, literature review and research objectives, materials and methods, results regarding the adsorption of lincomycin in deionized water, results about the adsorption of lincomycin from synthetic and real manure and conclusions and recommendations for future work.

CHAPTER 2
LITERATURE REVIEW

This chapter provides a brief literature review related to the occurrence of emerging pollutants in water bodies and relevant results obtained about their removal from water matrices by adsorption. Later, the mathematical modeling for adsorption equilibrium data is presented for both, isotherm models and thermodynamic characterization.

2.1 Occurrence of pharmaceuticals in water

Among emerging contaminants, pharmaceutical compounds cause a great deal of concern. In recent years the frequency of detection of pharmaceutical compounds has increased, and many countries have developed programs to study the effects of their presence in the environment [13]. The effects associated with their use are aquatic toxicity, resistance development in bacteria, genotoxicity and endocrine disruption [21]. Besides, the long-term consequences of the presence of traces of mixtures of these compounds in drinking water are not entirely clear [22].

One of the problems associated with the occurrence of antibiotics in water bodies is the development of antibiotics resistance in bacteria (ARB) [23]. The concept of ARB refers to the characteristics that bacteria develop to resist traditional antimicrobial effect due to a selective pressure process [24]. In the development of ARB, two elements are combined: an antibiotic and a bacteria colony where at least one bacteria resists the antibiotic effect. Hence, the vast majority of bacteria die but the resistant strain survives, and the genetic information contained in its organism is spread to other bacteria [25]. It has been determined that, in seawater, more than

90% of bacteria have developed antibiotic resistance characteristics [26]. Due to the severity of the problem, the World Health Organization considers this threat as a critical global public health issue [27]. Moreover, the Antimicrobial Resistance Global Report indicates that ARB has reached alarming levels in parts of the world where traditional antibiotics are becoming insufficient for treating common infections [27].

Pharmaceutical compounds in the environment are caused mainly by human consumption and also by their application in veterinary medicine and animal production industries [2,23]. In the livestock production industry, antibiotics are used mostly for disease treatment and prevention and occasionally weight gain. However, due to incomplete metabolization, in some cases, as much as 90% of the antibiotics doses are excreted through manure [4]. Only in Canada in 2014, around 1.5 million kg of antibiotic active compounds were used in the animal production industry [5]. From this amount, 7% were employed in Saskatchewan [5]. For these reasons, in surface water, concentrations from nanograms to low micrograms per liter have been detected. Also, low nanograms per liter contamination in drinking water have been reported in the literature [2]. In the Canadian swine production industry, tetracyclines and lincosamides are the most popular groups of antibiotics for disease treatment and prevention applications [5].

2.2 Lincomycin and its relevance as an emerging pollutant

Lincomycin is a compound classified into the lincosamides antibiotics [21]. However, the activity of lincomycin is similar to the ones found in macrolide antibiotics, and due to this reason, sometimes it is classified as one of them [21]. Lincomycin hydrochloride is employed for the treatment of gram-positive pathogens like streptococci, pneumococci, and staphylococci by blocking protein synthesis [28,29].

In the environment, lincomycin is one of the most common antibiotics detected in U.S. streams [30] and in treated wastewaters and in manures [28]. In Canada, samples from the Grand River in Southern Ontario were analyzed, and more than 90% of them contained lincomycin [31]. Furthermore, lincomycin has been detected in effluents from wastewater treatment plants,

where only 11% of this compound was removed through the treatment process [32]. Figure 1.1 presents the molecular structure of a lincomycin molecule [28].

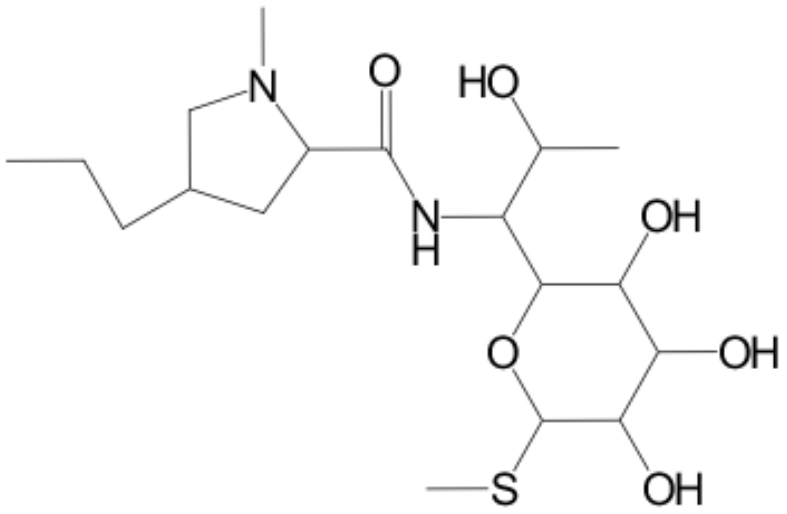

Figure 1.1. Molecular structure of the lincomycin molecule

Lincomycin molecule contains three main structures, a pyranose ring, an amide group, and a pyrrolidine ring [9]. The pyrrolidine ring is an organic base with a pKa between 7.6 and 7.8 [11], so, in natural water bodies, lincomycin is found as a combination of both neutral and cationic species. Lincomycin molecular weight is 406.53 g/mol, its Stokes diameter is 5.8 Å, and its molecular dimensions are 5.3*7.2*15.6 $Å^3$ [33]. It is bigger than other typical pharmaceutical compounds like carbamazepine, naproxen and ketoprofen [33]. Figure 1.2 shows the fractions of cationic and neutral lincomycin in solution as a function of the solution pH [34].

The use of lincomycin is not limited to treatment of human diseases, but also it is used in swine production, to control dysentery that results in weight gain [35]. Lincomycin is commonly employed in the Saskatchewan swine production industry [6]. It is mixed with spectinomycin and commercially is available as premix L-S 20 [36]. As a consequence, the combination of both antibiotics provides a broader antimicrobial activity [36]. The dose recommended for swine, up to 57 kg weight, contains 22 g of lincomycin per metric ton of feed [36]. After excretion, it was determined that the concentration of lincomycin in fresh swine liquid manure is 9.78 ppm,

and after 5 weeks of storage, it is reduced to 2.52 ppm [6]. Consequently, when manure is applied to the land as natural fertilizer, the residual lincomycin may be transported to surface water bodies and, eventually, to rivers [7]. Therefore, it is necessary to develop techniques for degrading or, at least, removing this compound from manure before its application to land.

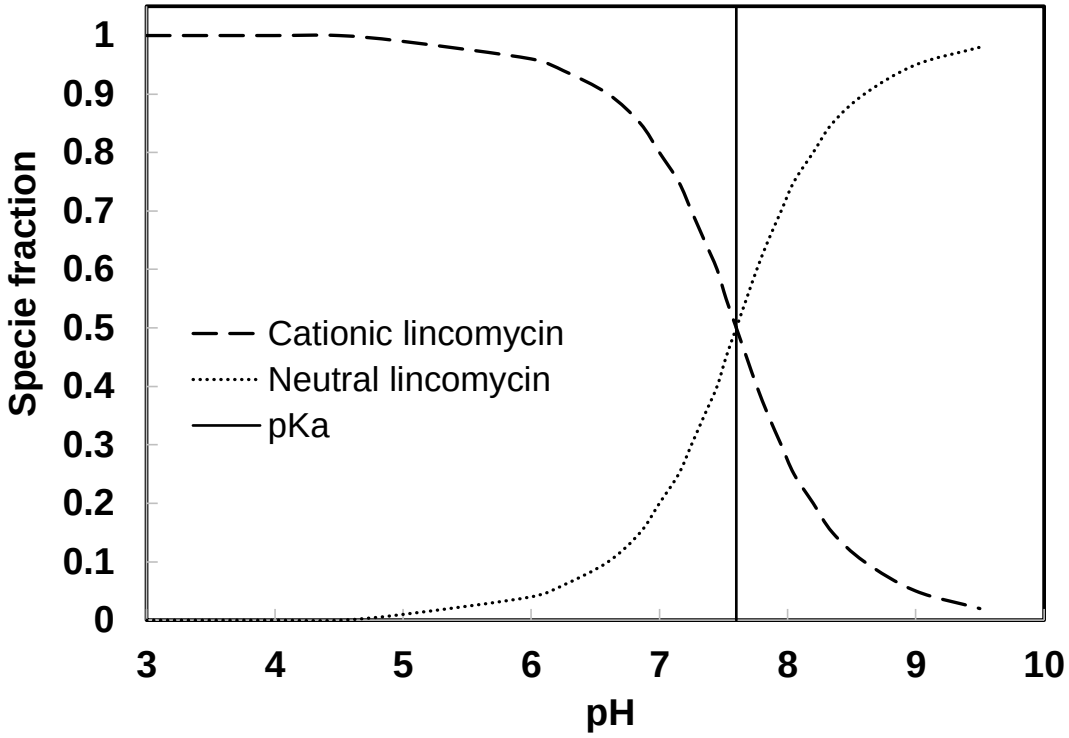

Figure 1.2. Fractions of cationic and neutral lincomycin in solution as a function of solution pH

2.3 Adsorption of pharmaceuticals from water on activated carbons and zeolites

Adsorption is a transfer process between phases. Molecules from a liquid or gas phase are attached on the solid adsorbent surface, by the chemical or physical interactions between the adsorbent and adsorbate [37]. The adsorption process occurs by the transport from the bulk to the surroundings of the adsorbent, the diffusion along the film, diffusion into the pores and, finally, the attachment of some molecules to the adsorbent surface [37]. Physical or chemical adsorption can take place depending on the bonding strength associated with the process. Physical

interactions are weak and mainly exist due to Van der Waals forces. In chemical interactions bonds formation have been identified; for this reason, interactions are stronger, and monolayer adsorption is predominant [15].

The most significant advantage of adsorption, over oxidation techniques, is that new metabolites are not generated. However, in adsorption the pollutants are transferred from liquid phase to solid phase, and post-treatment may be required [37]. Besides, regeneration of adsorbents is required to avoid efficiency decrease [15]. In environmental applications, adsorption has been widely used for water treatment. Activated carbon is the most important adsorbent, and it has been employed in different matrices such as drinking water, wastewater, groundwater, landfill and leachate [37]. However, commercial activated carbon is expensive, and its regeneration is complicated [15]. For this reason, other materials are studied as alternative adsorbents. Among the substitute materials, zeolites which provide high surface area and defined pore dimensions have been extensively used in the removal of undesired compounds [37,38]. Zeolites can be continuously regenerated without changing their structure as much as activated carbon [37,38]. The mechanisms that control the adsorption of compounds from water matrices on activated carbons and natural zeolites are presented below.

2.3.1 Adsorption on activated carbon

Adsorption on activated carbon is controlled by electrostatic and non-electrostatic interactions [39]. On the one hand, electrostatic interactions are defined as the attraction or repulsion taking place between the adsorbent and the adsorbate due to the total charge on the surface of both species. On the other hand, non-electrostatic interactions refer to the attraction caused by the surface properties of activated carbon, principally related to the presence of oxygen groups [39–41]. A detailed description of both interaction types and parameters influencing each one is presented below.

Electrostatic interactions in the adsorption on activated carbon

Electrostatic interactions refer to the attraction or repulsion developed between the activated carbon and the selected adsorbate based on their overall charge [39]. In aqueous phase, antibiotics can have a total charge due to the existence of dissociative functional groups in their structure [42]. For example, lincomycin is a weak organic base, and the pyrrolidine group in its structure has a pKa value of 7.6-7.8 [11]. Therefore, below this pH value, the lincomycin molecule is positively charged, and electrostatic interactions may play a role in the adsorption process [11]. On the other hand, above the pKa value, lincomycin is present mainly in its neutral form, and electrostatic interactions are negligible [11].

Regarding the adsorbent, activated carbons are amphoteric materials [43]. Hence, due to the presence of oxygen groups, these materials develop a total charge on their surface [43]. The presence of carboxylic, lactone and phenolic groups is related to the acidic properties of the material [39]. Conversely, electron rich zones, chromene and pyrone groups justify the basic character [39]. The pH value at which the charge density caused by the presence of acid and basic groups is in equilibrium is called the point of zero charge (PZC) [39]. At this pH value, the total charge density on the activated carbon surface is zero [40]. Moreover, below this value, the surface is positively charged and, on the contrary, pH values above the PZC produce a total negative charge [40].

In the previous paragraphs, it can be noted that the most important parameter affecting the electrostatic interactions is the pH value. Thus, depending on the pH of the aqueous matrix, several scenarios can take place in the same system. For example, Carrales, Ocampo, Leyva and Rivera [44] studied the effect of the pH value in the adsorption of metronidazole on activated carbon (PZC=9.4), activated carbon fibers and carbon nanotubes. Metronidazole molecule presents two pKa values corresponding to 2.6 and 14.4. At pH 2, metronidazole and activated carbon were positively charged. Hence, electrostatic repulsions took place, and the adsorption capacity was affected. At pH values greater than 4, the molecule was only in its neutral form, and the activated carbon was positively charged. Due to the neutral adsorbate charge, no electrostatic interactions occurred. Therefore, the adsorption capacity was greater than that at acidic pH

values. It is because electrostatic repulsions were avoided and other non-electrostatic interactions promoted the adsorption of metronidazole.

Another factor influencing the electrostatic interactions in the system is ionic strength [39]. In general, the addition of electrolytes to the system reduces the electrostatic interactions [45]. It means that attractive and repulsive interactions are affected by the presence of an electrolyte in the solution. Consequently, the adsorption capacity can be increased or decreased depending on the net adsorbent and adsorbate charges at the selected pH value [45]. For example, Bautista and colleagues [40] studied the effect of ionic strength in the adsorption of bisphenol A on activated carbon. At pH 7, activated carbons were positively charged, and the adsorbate was in its neutral form. The addition of NaCl to the system produced a screening effect reducing the activated carbon net charge and improved the dispersion or non-electrostatic interactions. As a consequence, the adsorption capacity increased. In contrast, if electrostatic attractions are taking place in the system and salts are added, a subsequent decrease in the adsorption capacity will be observed. It can be explained because the overall adsorbent attractive charge will be reduced by the binding of ionic species [39].

Non-electrostatic interactions in the adsorption on activated carbon

The non-electrostatic interactions are the second type of bonding that can take place between adsorbates and the surface of activated carbons. Properties like the carbon surface chemistry and the structure functional groups in the adsorbate affect the affinity in adsorbate-activated carbon [39] system. Several types of non-electrostatic interactions have been identified. Among them, hydrophobic bonding, π-π interactions, hydrogen bonds, and electron donor–acceptor complex systems can be mentioned [39]. Below, a brief discussion of each type of bonding is provided.

Hydrophobic interactions refer to the attractions occurring between a hydrophobic adsorbate and a hydrophobic carbon surface, produced by the low affinity that both adsorbate and adsorbent have with water [39]. Hydrophobic activated carbons are characterized by low acidic oxygen-groups content. It avoids the binding of water molecules in the active sites on

carbon surface [46]. The hydrophobicity of the adsorbate can be characterized by the n-octanol or water -partitioning coefficient (K_{OW}), high K_{OW} values represent high hydrophobicity in water media [47]. The hydrophobic bonding mechanism has been used for predicting the adsorption of low solubility species on activated carbons. For example, Mendez et al. [46] studied the adsorption of nitroimidazole on activated carbons and determined an indirect relation between the oxygen content and the adsorption capacity. Hence, hydrophobic carbons with low oxygen content showed higher adsorption capacity than the activated carbons with high oxygen content. It was because low oxygen-content carbons avoided the formation of hydrogen bonds between carbon surface groups and water. Therefore, the accessibility of nitroimidazole to the adsorption sites is not reduced by the presence of adsorbed water molecules.

Another type of non-electrostatic bonding is the π-π interactions. This kind of attachment occurs between the π electrons available in the aromatic rings in the adsorbate structure and the π electrons in the graphene structure on the activated carbon surface [48]. Hence, the molecules containing aromatic rings are adsorbed in flat position over the basal planes on carbon surface [39]. From this theory, it can be implied that the presence of acidic oxygen groups removes π electrons from the activated carbon surface and decreases the interactions by this mechanism, with a subsequent reduction in the adsorption capacity [39]. Peng et al. [48] studied the adsorption of antibiotics on graphene and biochar and determined that the adsorption rate is positively influenced by the number of aromatic rings in the antibiotics molecules. Besides, increasing the number of available π rings increased the adsorption energy. They concluded that π- π interactions played the major role in the adsorption process. However, others types of non-electrostatic interactions may contribute as support adsorption mechanisms.

A mechanism similar to the one suggested for π- π interactions was proposed by Mattson [49]. Mattson and colleagues introduced the concept of the formation of complex electron donor-acceptor systems [39,49]. In this case, carbonyl groups on the carbon surface share an electron with the acceptor species, located in the aromatic structure of an adsorbate [50]. This theory explained the decrease in the phenol uptake when oxidized carbons are used because while carbonyl groups can act as electron donors, it is not the case for carboxylic groups [39]. This mechanism by itself has not been widely used, but the main concept of acceptor and donor

systems is the same as the one proposed for π- π interactions [51]. Therefore, names of both mechanisms are used in the same way in the literature [51].

Hydrogen bonding is the last type of non-electrostatic interaction mentioned in this section. This kind of bonding occurs when the oxygen groups on the activated carbon surface interact with the hydroxyl groups in the adsorbate molecule and form a hydrogen bond [50]. As mentioned before, water can also interact with the surface of activated carbons and form hydrogen bonds [39]. Therefore, when hydrogen bonding takes place in the system, a competition for the adsorption sites between water and the adsorbate occurs [43]. Salvador and Merchan [52] studied the desorption of phenol on activated carbon. Phenol contains one hydroxyl group in its structure. They determined that the range of energy of bonding in the desorption process correspond to the ones of hydrogen-bonds. Besides, in the adsorption of lincomycin on carbonaceous materials, it is expected that hydrogen bonding takes place because the pyranose ring in lincomycin's structure contains three hydroxyl groups that can interact with the oxygen groups on the carbon surface [53,54].

Finally, it is important to mention that, in many cases, the adsorption process on activated carbons is not controlled by only one mechanism. Thus, some adsorbates can interact with activated carbon by different combined electrostatic and non-electrostatic interactions [39,43,50].

2.3.2 Adsorption on zeolites

Zeolites are crystalline and hydrated minerals that contain alkali and alkaline earth metals in their structure. Their frameworks are composed of $[SiO_4]^{4-}$ and $[AlO_4]^{5-}$ tetrahedral structures that form cages connected by windows of defined sizes [55]. Natural zeolites present low surface areas ranging from 10 to 40 m^2/g. According to pore size distribution, the majority of zeolites structure are mesopores (2-5 nm) [55]. Natural zeolites are used in applications such as adsorption, catalysis, building industry, agriculture, soil remediation and energy [17]. In general, natural zeolites are hydrophilic materials suitable for ion exchange processes, ammonium, and heavy metal removal, but not for the adsorption of non-polar organic substances [17,37,56].

In the adsorption of antibiotics on natural zeolite, Li et al. [57] studied the adsorption of sulfadiazine sulfonamide from water by hydrophilic non-treated clinoptilolite. They determined that the adsorption of this antibiotic is favored at pH values below the sulfadiazine pKa. At this pH, sulfadiazine is positively charged, and ionic exchange was the controlling adsorption mechanism. Conversely, at pH values higher than the sulfadiazine pKa, no electrostatic interactions occurred and, subsequently, low adsorption capacity values were detected. In this study, hydrophobic interactions were not strong enough to compensate for the reduction in the adsorption capacity caused by the reduction in the concentration of adsorbate ionic species. Moreover, Otker and Akmehmet-Balcıoglu [58] studied the adsorption of enrofloxacin on natural zeolite and determined that the adsorption capacity is directly affected by the concentration of charged enrofloxacin. These results confirm that the mechanism controlling the adsorption of antibiotics on natural zeolite is ionic exchange, and it is only possible when antibiotics are electrolytes that can be dissociated and positively charged in the aqueous phase.

One important characteristic in natural zeolites is the hydrophobic character. This property is represented by the Si/Al ratio (varies from 4.0 to 5.3 in clinoptilolite), that determines the overall negative charge of the material [20]. Increasing the Si/Al ratio enhances the hydrophobic character of these aluminosilicates [56]. Several methods have been tested for modifying the hydrophilic/hydrophobic properties of zeolite, among them acidic washing, surfactants addition and ammonium exchange followed by calcination can be mentioned [17,18,59].

Acid washing is applied to eliminate cations, such as Na, Mg, K and Ca, and also to remove alumina from the structure [17]. Besides, the surface area and pore size distribution are also modified [59]. On the other hand, thermal stability can be reduced in this process [17]. Kurama, Zimmer, and Reschetilowski [59] studied the effect of acid washing on the adsorption capacity of natural clinoptilolite. Acid washing increased the ratio of Si/Al and, subsequently, offered better adsorption of neutral molecules. Besides, surface area increased from 35 m^2/g in raw material to 315 m^2/g in the acid treated sample. The effect of the temperature in the modification process has also been studied. Cakicioglu-Ozkan and Ulku [60] treated clinoptilolite at different hydrochloric acid concentrations ranging from 0.032 M to 5 M and different temperatures ranging from 25 °C to 100 °C. They determined that increasing the

temperature and acid concentration removed cations such as Mg, Fe and Ca and increased the surface area. However, above 40% alumina removal, the surface area decreased because the framework structure was affected.

Another method used for modifying the overall negative charge of zeolites is the addition of surfactants to the surface of the adsorbent [20]. In this case, cationic surfactants are used and the positively charged side of the surfactant is attached to the polar surface of zeolite, and the hydrophobic chain side interacts with the adsorbates [56]. The efficiency of the process depends on the degree of surfactant adsorption and surface coverage [17,20]. Li, Dong, Peng and Kong [61] used Hexadecyltrimethyl ammonium surfactant (HDTMA) to modify zeolite in the removal of humic acid. The original zeolite provided low adsorption capacity. However, the modified zeolite provided adsorption capacities similar to the ones found in activated carbon and clays. On the downside, the detachment of surfactants from the zeolite surface can lead to indirect contamination and reduced adsorption capacity.

2.4 Adsorption of lincomycin from water matrices

Lincomycin is one of the most common antibiotics used in the animal production industry [34]. In fresh swine manure, lincomycin has shown high persistence in storage conditions [6]. After being excreted, the concentration of lincomycin was 9.76 ppm in the waste stream, and after 5 weeks of storage, it was reduced to 2.52 ppm [6]. Due to the resistant properties of lincomycin, its removal from water bodies by adsorption has been studied [33,34,54,62]. A brief summary is provided below.

Wang, and colleagues [34] studied the adsorption of lincomycin on smectite and determined that the main mechanism controlling the adsorption process is cationic exchange. This conclusion was obtained by studying the effect of pH and ionic strength on the adsorption capacity. Thus, the adsorption capacity was favored at acidic pH values because lincomycin was in its cationic form. However, at pH values near the lincomycin pKa (7.6), the adsorption capacity was drastically reduced because the concentration of cationic lincomycin decreased

significantly. Besides, the addition of cations like Ca^{2+} affected the adsorption capacity due to the competition for cationic exchange sites on the smectite surface.

To improve the adsorption by electrostatic interactions, Liu and colleagues [62] used biochars for removing lincomycin from deionized water. These biochars were pyrolyzed from solid manure and presented acidic properties. Thus, at neutral pH, the biochar surface was negatively charged. In this study, the effect of pH, adsorbent particle size and ionic strength were studied. The maximum adsorption capacity identified in this study corresponded to 697 μg/g at pH 6.9. They determined that the adsorption capacity at pH values below the pKa is greater than at basic values. This behavior was attributed to the positive charge of lincomycin and negative surface charge that enhanced the electrostatic interactions. Conversely, at pH values above the pKa lincomycin was in its neutral form. Therefore, the adsorption capacity was affected because electrostatic attraction did not take place in the system. Besides, the addition of electrolytes to the system reduced the adsorption capacity. Regarding the adsorption mechanism, a combination of electrostatic and non-electrostatic interactions was proposed. In the case of non-electrostatic interactions, hydrogen bonding and Van der Waals forces are mentioned as the possible adsorption mechanisms. However, they mention that the mechanism should be elucidated by experimental evidence in the future.

Carbon nanotubes have shown potential in environmental remediation applications. These materials are highly hydrophobic and can interact with aromatic compounds mainly by π interactions due to the high concentration of sp^2 carbon atoms on the graphite surface [54]. Kim, Hwang, and Sharma [54] studied the adsorption of lincomycin on carbon nanotubes and compared their performance with commercial powdered activated carbons (PAC). The adsorption of lincomycin was completed at 100 hours of stirring. Besides, Langmuir model did not predict well the equilibrium data (R^2<0.70). The authors proposed it was due to the fact that the adsorption of lincomycin was not purely monolayer type. Therefore, Freundlich model was used for modeling the adsorption process. This model provided good fitting results (R^2>0.96) with n values greater than 1, suggesting non-linear heterogeneous adsorption. For carbon nanotubes and activated carbon, the Freundlich constants for the adsorption of lincomycin were $1.03*10^3$ and $1.00*10^3$ $mmol^{1-n}L^nkg^{-1}$ respectively. The authors remarked that the adsorption on carbon nanotubes was mainly controlled by the surface area of the adsorbent.

2.5 Adsorption equilibrium data modeling

An adsorption system can be characterized by studying both the equilibrium and kinetics data [37,63]. Equilibrium data provides information about the adsorbent loading capacity for a specific adsorbate and the bonding strength [37]. On the other hand, kinetic analysis relates the adsorbent loading rate with the contact time [37]. Therefore, in the practical application, information about both the equilibrium and kinetics is necessary for designing adsorption systems [63]. For example, using a material with high adsorption capacity but a low adsorption rate would take a long time to reach the equilibrium adsorption capacity, implying longer residence time and low processed flow in a continuous system [63].

In a pure component system, the uptake or adsorption capacity of a certain solute depends on the concentration of adsorbate in solution and the temperature of the process [37,64]. However, to simplify the characterization, the process can be carried out at a single temperature and, subsequently, the adsorption capacity only depends on the concentration in solution of the adsorbate [37]. The relation between the solute concentration and the adsorption capacity at a specific temperature is called adsorption isotherm [63].

To predict the adsorption capacity, at a specific solute concentration, a vast number of adsorption isotherms models have been developed [65]. Two-parameter models such as Langmuir and Freundlich models have been traditionally used for describing the adsorption of antibiotics on various adsorbent materials [14,42,66,67]. However, the application of these models may not describe well the adsorption process due to the assumptions made in each case [63,64]. For example, Langmuir model considers a homogeneous distribution of the adsorption sites. This assumption is not necessarily true for activated carbons [63]. On the other hand, Freundlich model does not consider a saturation capacity. It can be a weakness for monolayer adsorption systems [64]. Therefore, other models that address the deficiencies of Langmuir and Freundlich models have been developed [68]. In this research, a three-parameter model such as Sips was used to simulate the adsorption process. This model is considered as a combination of the two-parameters models of Langmuir and Freundlich [63]. The following sections provide a brief description of each model.

In a multicomponent system such as real liquid swine manure, micro-pollutants like lincomycin compete for active sites with the natural organic matter present in the manure composition [69]. As a consequence, the adsorption capacity determined from pure component systems can be significantly decreased [70] in a multicomponent system. The ideal adsorbed solution theory (IAST) has been used traditionally for modeling multicomponent adsorption [37]. However, its application requires the knowledge of the composition of the components, the initial concentration, and the single-solute isotherm parameters of each component [37]. Therefore, the direct applicability of this model is not feasible for real manure. A derived methodology for predicting the removal of micro pollutants from high content natural matter called simplified equivalent background compound model (SEBCM) is used in this study. This model is presented in Section 2.5.3.

2.5.1 Langmuir and Freundlich two parameters adsorption isotherms models

Langmuir proposed a theory based on the kinetic viewpoint of the adsorption process [63]. At equilibrium, a continuous process of molecules bombardment onto the surface and a corresponding desorption to maintain zero rate of accumulation is considered [71]. Besides, Langmuir considered that the energy distribution on the surface is homogeneous. Therefore, specific adsorption sites accommodate only one molecule, and a monolayer is formed when the adsorbent is saturated [63]. The developed model is presented in equation (2.1).

$$q_e = \frac{C_e K_L q_{max}}{1 + C_e K_L} \tag{2.1}$$

Where q_e is the adsorption capacity determined at a certain adsorbate concentration in solution (C_e). Besides, K_L is a direct measure of the affinity of adsorbent and adsorbate, and q_{max} is the monolayer maximum capacity in the Langmuir model [50]. The Langmuir equation reduces to the Henry law isotherm when the concentration is very low [63]. Thus, the amount adsorbed increases linearly with concentration [63]. However, at high concentration the amount adsorbed reaches the saturation capacity and, subsequently, multilayer adsorption can't be described by this model [50,63].

Freundlich developed another popular two-parameter adsorption model. Freundlich model has been widely used for describing adsorption data on activated carbons [63]. This model is not restricted to monolayer and considers the non-uniform distribution of adsorption sites [37]. However, very low and very high concentrations are not well described by this model. This is because at low concentration this model does not follow Henry's law. Besides, at high concentrations, the lack of a maximum adsorption capacity parameter does not consider the saturation of active sites on the solid surface [63,65]. Equation (2.2) shows the form of Freundlich model.

$$q_e = K_F C_e^{1/n} \quad (2.2)$$

Where K_F is the relative adsorption maximum capacity and 1/n indicates the surface heterogeneity. Hence, larger values of n indicates more heterogeneous distribution of the adsorption sites on the solid [65]. Freundlich equation has been used mainly for the adsorption of organic compounds on activated carbon [63,65].

In adsorption of lincomycin on carbonaceous materials, Kim et al., [54] found that Freundlich model (R^2<0.96) described the adsorption isotherms better than Langmuir model (R^2<0.70) based on the determination coefficient value. It was proposed that the adsorption of lincomycin is not pure monolayer type. Besides, adsorption was non-linear, and n values in the Freundlich model were greater than 1. Therefore, it was suggested that the distribution of adsorption sites on the carbon nanotubes surface was heterogeneous, as proposed by Freundlich model [65].

2.5.2 Sips three-parameter adsorption isotherm model

Freundlich model does not consider a maximum saturation capacity of adsorption [63] and Langmuir model is not suitable for heterogeneous adsorbent surfaces [71]. Therefore, Sips proposed a model similar to Langmuir model but introduced a third parameter (n), analogous to the n parameter in Freundlich model, which refers to the heterogeneity of specific adsorption systems [37,63,65]. Sips model is presented in equation (2.3).

$$q_e = \frac{q_m * K_S * C_e^{\frac{1}{n}}}{1 + \left(K_S * C_e^{\frac{1}{n}}\right)} \quad (2.3)$$

Where qm is the monolayer maximum capacity, K_S is the Sips constant and 1/n indicates the affinity or surface heterogeneity [63,72]. Sips model describes the monolayer saturation capacity of an adsorbent ($q_e = q_m$) at high concentrations ($K_S * C_e^{\frac{1}{n}} \gg 1$) and at low concentrations ($K_S * C_e^{\frac{1}{n}} \ll 1$) it is reduced to the Freundlich model [37]. Besides, if the adsorption sites distribution is homogeneous ($n \approx 1$) the model is reduced to Langmuir equation [63]. On the other hand, n values greater than 1 represents high heterogeneity in the system [63]. Sips adsorption isotherm model is also called Langmuir-Freundlich model due to the similarities described before [63].

Hindarso et al. [73] studied the adsorption of aromatic compounds on activated carbon. Sips and Toth [50] three-parameter models described the adsorption isotherms better than Freundlich and Langmuir two-parameter models based on the normalized residuals. Authors attributed these results to the specificity that Sips and Toth models provide for describing adsorption on heterogeneous materials like activated carbon. Sips model has also been used in the adsorption of antibiotics. For example, Attallah et al. [74] studied the adsorption of fluoroquinolones on magnetic nanoparticles and determined that Sips model provides better fitting results than Langmuir and Freundlich models based on the determination coefficient.

Due to the combination of Langmuir maximum adsorption capacity and Freundlich model's capacity to describe heterogeneous systems, Sips three parameters equation will be used in this research for modeling the adsorption of lincomycin on activated carbons and natural zeolite.

2.5.3 Simplified equivalent background compound model (SEBCM)

Equivalent background compound model (EBCM) is a simplification of IAST model [70] used for describing the adsorption of a micro-pollutant from an aqueous matrix containing NOM [69]. EBCM considers the NOM as a single component called the equivalent background

compound (EBC). Hence, a competitive bi-component adsorption system formed by the EBC and the micropollutant is obtained [75]. Therefore, only the isotherms parameters for single-solute adsorption and initial concentration of both components (EBC and micro-pollutant) are necessary for characterizing the adsorption process [69].

The EBCM can be simplified when the concentration of the micropollutant is much lower than the NOM concentration, as in the case of antibiotics in liquid manure [69]. At this condition, the adsorption capacity of NOM is dominant in the system ($q_{NOM} >> q_{pollutant}$) [76]. As a consequence, the removal efficiency (C_e/C_o) of the process is independent of the initial concentration of the micropollutant and the obtained isotherms follow the behavior of the linear isotherm [69].

The obtained simplified model was proposed by Qi et al. [70] and allows the prediction of the micropollutant removal only based on the activated carbon dose. Equation (2.4) represents the simplified equivalent background compound model (SEBCM).

$$\frac{C_e}{C_o} = \frac{1}{A}\left(\frac{m_A}{V}\right)^{1/n_1} + 1 \tag{2.4}$$

Where Ce is the residual concentration of the micro-pollutant in solution, m_A is the adsorbent weight and V is the solution volume. Besides, n_1 is the Freundlich exponent of the micropollutant single-solute adsorption, and A is a parameter that includes the adsorption parameters of the trace compound and the NOM. From the linearization of Equation (2.3), it is possible to determine the characteristic parameters that relates the adsorbent dose and the removal percentage.

This model eliminates the necessity of knowing the adsorption parameters of NOM and depends only on the micro-pollutant adsorption isotherm [69]. On the other hand, it is important to remark that the SEBCM considers that the removal ratio C_e/C_o is independent of the initial micropollutant concentration [70]. This assumption is only valid in matrices with much higher concentration of NOM than the micro-pollutant [70]. In the present study, the adsorption process takes place in real liquid manure with very high content of NOM. Therefore, the application of

SEBCM constitutes a feasible option for simulating the adsorption of lincomycin contained in liquid swine manure.

2.6 Adsorption thermodynamic characterization

The equilibrium state is the most important aspect of adsorption because it studies the loading capacity of an adsorbent for a specific adsorbate and the strength of its interaction [63]. In equilibrium, in addition to using established or created isotherm models that provide valuable information about the mechanisms involved, it is necessary to study the thermodynamic characteristics of the system [77]. Parameters like enthalpy, entropy and Gibbs free energy of adsorption that can provide information about the endothermic or exothermic character, the strength of bonding, spontaneity, and mechanism of the process should be determined [77].

The determination of thermodynamic parameters depends strongly on the equilibrium constant value. Hence, the selection of one method for its determination directly affects the results obtained [77]. Even though several methods have been proposed for calculating this constant value, the selection of one of the adsorption models should be carried out carefully, and it needs to be theoretically justified. Problems associated with the determination of equilibrium constant are related to the selected method, the non-consideration of the dimensionless character of the equilibrium constant and inappropriate range of data used.

The following sections will present a short review of the significance of thermodynamic parameters. Special focus will be given to the methods employed for the determination of the thermodynamic equilibrium constant.

2.6.1 Fundamentals of the adsorption thermodynamics in equilibrium

The most important thermodynamic parameters that characterize an adsorption process are the Gibbs free energy, adsorption enthalpy, and entropy changes. The thermodynamic laws can be used for determining these parameters through the following equations [77,78]:

$$\Delta G^\circ = -RT\ln K_c \quad (2.5)$$

$$\ln K_c = -\frac{\Delta H^\circ}{RT} + \frac{\Delta S^\circ}{R} \quad (2.6)$$

$$\Delta G^\circ = \Delta H^\circ - T\Delta S^\circ \quad (2.7)$$

Where K_c is the thermodynamic equilibrium constant (dimensionless) [79], R is the universal gas constant (8.314 $Jmol^{-1}\ K^{-1}$), and T is the temperature in Kelvin. Van't Hoff equation (2.6) is used to determine the enthalpy and entropy variations by the determination of the slope and the intercept of the linear variation of ln K_c with 1/T.

Gibbs free energy is related to the spontaneity of the process. For a spontaneous adsorption system, this value must be negative at the experimental conditions. In general, a higher negative absolute value of this energy change indicates a more energetically favorable adsorption. In contrast, the process will not be spontaneous if this value is positive [4].

Enthalpy change or heat of adsorption explains the exothermic or endothermic nature of the process and gives information about the type of bonding [79]. A negative enthalpy value change reflects exothermicity, and a positive enthalpy change represents an endothermic phenomenon. When differentiating between chemical and physical adsorption, it is necessary to analyze the value of the enthalpy change. In general, it is stated that low values correspond to physisorption and high values correspond to chemisorption. However, this definition is vague and does not permit the unification of criteria to characterize each process. To address this issue, different ranges of enthalpy change values have been established for differentiating chemisorption and physisorption. Nevertheless, important differences are found in the literature. Table 2.1 summarizes the broad variety of values mentioned in the literature.

Table 2.1 shows the absolute enthalpy change ranges for physical and chemical adsorption for different adsorption processes. There is not agreement when discriminating one process from another. Hence, to select one of the ranges to explain experimental results, it is necessary to analyze the possible mechanisms of adsorption by analyzing the structure of the

adsorbate and adsorbent involved in the process. In the particular case of adsorption on activated carbons, lower values represent physisorption characterized by weak dispersion forces like π- π interactions and chemisorption is represented by the formation of hydrogen bonds or electron donor–acceptor complex systems [39].

Table 2.1. Absolute value of enthalpy change ranges for physical and chemical adsorption for different adsorption processes

Physisorption ($KJ*mol^{-1}$)	**Chemisorption ($KJ*mol^{-1}$)**	**References**
2.1 - 20.9	80 - 200	[79–81]
0 – 40	40 - 120	[58,82]
5 – 40	40 - 800	[83]
0 – 80	80 - 400	[84]

Another factor in interpreting the enthalpy change values is related to the sign of it. It is assumed that the adsorption process is exothermic by nature [85–87]. It means that due to the bonding of adsorbed molecules on the adsorbent surface there is a subsequent energy release. This statement is only true for physical adsorption. In the case of chemisorption where rupture and creation of chemical bonds can take place some of these reactions can be of endothermic nature, providing an endothermic character to the complete process [85]. Even though in the past, the possibility of an endothermic adsorption process was not considered, at present, several scientific documents have reported this phenomenon [58,72,80,83,86,88–90].

Equation (2.5) shows the relation between the Gibbs free energy change and enthalpy and entropy changes in an adsorption process. At normal experimental conditions (e.g. room temperature around 293 K, pressure around 1 atm) and spontaneous adsorption, the Gibbs free

energy change is negative. It has been stated that the entropy change should always be negative because this process implies accommodation of molecules over the adsorbent surface, in a so-called more stable state (e.g. condensation on the solid surface) [85]. However, this statement is only true for physical adsorption. In the case of chemisorption, where rupture and creation of chemical bonds can happen, some of these reactions can be of endothermic nature, providing an endothermic character to the complete reaction [85]. If the global reaction is endothermic and Gibbs free energy change must always be negative for a spontaneous process, the only remaining parameter that must be positive is entropy [77,84,85].

One theory supporting this point states that, in this case, adsorption must be carried out by dissociative adsorption [77,84,85]. The proposed model implies that because the molecule is divided and adsorbed on different sites, the new two molecules replace two water molecules and have complete two-dimensional mobility, increasing one degree of freedom, with a resulting positive entropy change [85].

2.6.2 Determination of the thermodynamic equilibrium constant

As shown in equations (2.5) and (2.6) the complete determination of the thermodynamic parameters depends on the equilibrium constant and the temperature of the process. The latter parameter can be easily controlled, but the equilibrium constant value depends on the mathematical method selected for its determination.

One of the popular methods used for the determination of the thermodynamic equilibrium constant implies using the equilibrium constant from Langmuir isotherm model as the thermodynamic equilibrium constant [58,91–97]. However, Milonjic [98] analyzed this determination method and found incorrect values for the thermodynamic parameters reported in published articles. The error was caused by the use of the Langmuir constant as the thermodynamic equilibrium constant without considering the dimensions of this constant. Thus, dimmensions of volume of liquid solvent over mass of adsorbent ($mL*mg^{-1}$) were associated to the thermodynamic constant [98]. As mentioned before, the strict definition of the thermodynamic equilibrium constant used in Equation (2.6) considers this parameter as

dimensionless [99,100]. Besides, Nguyen [77] mentioned that even changing from one Langmuir model linearized form to another can result in different thermodynamic parameters values. Finally, Langmuir model considers the concentration in solution instead of the adsorbate activity [99].

A second method that considers the adsorbate activity was proposed by Khan & Singh (1987) and modified by Milonjić (2007). It has been used due to the consideration of the activity of the solute [72,102–105]. This method proposed the determination of the thermodynamic equilibrium constant from the distribution coefficient, shown in equation (2.6).

$$K_d = \frac{a_s}{a_e} = \frac{\gamma_s}{\gamma_e} * \frac{q_e}{C_e} \tag{2.6}$$

Where, a_s and a_e represent the activity of adsorbed solute and adsorbate in solution respectively, γ_s and γ_e are the activity coefficients of adsorbed solute and adsorbate in solution respectively and q_e and C_e represent the concentration of adsorbed solute and adsorbate in solution respectively. When the concentration of adsorbate in the solution approaches zero, the activity coefficients approaches unity, hence, it can be represented as follows:

$$\lim_{qe \to 0} \frac{q_e}{C_e} = K_d = \frac{a_s}{a_e} \tag{2.7}$$

The thermodynamic equilibrium constant can be determined by plotting $\ln(qe/Ce)$ vs qe and extrapolating qe to zero.

The same problem mentioned for Langmuir isotherm is associated with this method. The constant obtained has dimmensions of volume of solvent per mass of adsorbent. Hence, Milonjic [98] proposed that for solving this problem it was only necessary to multiply the constant value by the density of water (1000 g/L) if the Langmuir constant is expressed as grams of adsorbent per liter of solvent, so the obtained model is shown in equation (2.8).

$$\Delta G = -RT\ln(K_c) = -RT\ln(1000 * K_d) \tag{2.8}$$

Expression (2.8) includes the correction for the dimensionless character of the distribution coefficient and will be applied in the determination of the thermodynamic equilibrium constant in this study.

2.7 Knowledge gaps and research objectives

To evaluate the feasibility of using adsorption processes for removal of lincomycin from the waste stream of animal production industries, a number of knowledge gaps were identified:

1. Although previous studies regarding adsorption process have been conducted; a comparison between the adsorption capacity of activated carbon and zeolites under varying conditions of temperature, pH, and ionic strength has not been carried out.
2. The thermodynamic characterization of the process has not been made in the previous research on lincomycin. Parameters such as enthalpy, entropy and Gibbs free energy change of adsorption have not been determined for adsorption of lincomycin over activated carbons and natural zeolite.
3. Adsorption has been only applied to deionized water matrices. There is a lack of publications about the comparison of the performance of adsorbents in deionized water and real water matrices.

Against this background, the objectives of the present research are:

1. To characterize six commercial activated carbons and one natural zeolite. Surface area, pore-size distribution, the point of zero charge and oxygen content need to be determined in the case of activated carbons. Surface area, ratio Si/Al and average pore size need to be determined for natural and modified natural zeolites.
2. To model the adsorption of lincomycin on activated carbons and natural zeolite using established two-parameter isotherm models such as Langmuir and Freundlich models and a three parameter model such as Sips model.

3. To study the effect of the temperature in the adsorption capacity through the thermodynamic characterization of the process associated to each adsorbent.
4. To study the influence of operating parameters such as pH and ionic strength on the adsorption capacity of the adsorbents.
5. To analyze the efficiency of the adsorbents applied in synthetic and real liquid swine manure.

CHAPTER 3
MATERIALS AND METHODS

Chapter three details the materials used in this research. Besides, experimental procedures and equipment used are described in detail. Also, lincomycin concentration quantification is described, by both high-performance liquid chromatography (HPLC) and UV-Vis spectrometry analysis. Finally, methods and equipment used in the characterization of activated carbons and natural zeolite are described.

3.1 Materials

3.1.1 Target compound solutions

Lincomycin was obtained as lincomycin hydrochloride ($C_{18}H_{34}N_2O_6S$•HCl) crystalline powder, molecular weight of 443.0 g*mol^{-1}, pKa of 7.8 and melting point of 156 to 158°C from Alfa Aesar. Deionized water, with a resistivity of 18.2 MΩ.cm at 298 K, was used for preparing pure water and synthetic manure lincomycin solutions of 10, 17, 25, 33, 40, 50, 70 and 90 ppm in 1 L volumetric flasks. Stock solutions were prepared the day before the experiments and stored in a refrigerator at 4°C. Before its use; solutions were collocated into a Fisher Scientific Ultrasonic bath 1800 and sonicated for 1 min.

Deionized water solutions were prepared at two different initial pH values of 6.5 and 10.0. The first value of 6.5 was obtained without adding reagents to the solution. On the other hand, NaOH 1 N standard solution provided by Alfa Aesar was used for adjusting the pH value

to 10.0. The amount of NaOH varied depending on the lincomycin concentration. Table 3.1 details the volume added to each solution.

Table 3.1. Volume of NaOH 1 N added for adjusting pH to 1 L of lincomycin solution

Lincomycin concentration (ppm)	10	17	25	33	40	50	70	90
Volume (µL)	50	150	150	150	180	200	220	240

3.1.2 Adsorbents

Commercial activated carbons and zeolites were used in this research. To maintain particle size uniformity, all the samples were grounded to 60-120 mesh size and stored in different containers.

Activated carbons were selected based on their different acid and basic properties represented by their different points of zero charge. A brief description is provided below:

Cabot Norit (1240) was obtained from Cabot Corporation; it is recommended for decolorization and purification of pharmaceuticals and removal of impurities from industrial process water. Norit Row 0.8 (NR) was obtained from Alfa Aesar; this steam activated material is mainly recommended for gas phase applications such as automotive emission control but also for removing by-products in drinking water. Filtrasorb 400 (F400) and Filtrasorb 300 (F300) were obtained from Calgon Carbon; both are bituminous coals mainly different in their micropore content, and they are recommended for removal of organic compounds from water, wastewater, and industrial processing streams. Darco 12-20 (SAD) and Norit GAC 1240W (SAN) were obtained from Sigma-Aldrich, produced by Chemviron Carbon by activation of bituminous coal with steam. Both of them are acid activated carbons and are recommended for removal of pollutants.

In the case of zeolite (NZ), natural clinoptilolite was obtained from Canadian Mining in the form of stones. Samples were ground to the same particle size as activated carbon samples and washed carefully with deionized water. Afterwards, they were dried at 383 K for 24 h. This material has been used traditionally for molecular sieving, absorption, ion exchange, dehydration and re-hydration in physical and chemical processes.

3.1.3 Water matrices

Lincomycin removal was studied using three water matrices, deionized water, a synthetic manure, and a sample of real liquid manure obtained from Prairie Swine Centre. The composition of the synthetic manure was based on a mixture used by Raby and colleagues [106]; they studied the elimination of nitrogen present in swine manure using a biotrickling filter in Canada. The reference provides a list of the principal components of real liquid swine manure and the concentration of each one. Synthetic formulation, suppliers, and reagents characteristics are described in Table 3.2.

Table 3.2. Synthetic manure composition used in this research

Compound	Concentration (ppm)	Supplier	Purity (%)
Sodium propionate	2000	Alfa Aesar	99
Sodium acetate	2000	Alfa Aesar	99
Lactic acid	3300	Alfa Aesar	80-85
Ethanol	1700	Sigma-Aldrich	95-96
Ammonium bicarbonate	13000	Alfa Aesar	99
Potassium phosphate	360	Alfa Aesar	97
Potassium sulfate	4000	Alfa Aesar	99

3.2 Experimental procedures

3.2.1 Modification of natural zeolite

A clinoptilolite sample was obtained from Canadian Mining; samples were washed with deionized water and dried at 373 K for 12 hours and collocated in a desiccator. 5 grams of clinoptilolite was added to 100 mL of 5 M hydrochloric acid, stirred at 400 rpm and heated at 363 K for 3 hours. Treated natural zeolite was washed with deionized water until no Cl^- ions were detected in the washing water by using $AgNO_3$ solution [60]. Washed natural zeolite was dried again at 373 K for 24 hours and collocated in a desiccator; the final modified zeolite was stored and sealed to avoid moisture effects.

3.2.2 Equilibrium time determination and verification of adsorbents concentration validity

Before adsorption essays at different temperatures, the adsorbents concentration validity was verified and equilibrium time was determined. This stage was conducted at room temperature (296 K) to verify that the concentration of lincomycin does not reach a value of zero with the selected adsorbent concentration value.

Before use as adsorbents, both activated carbons and zeolites were ground to obtain a particle size of 60-120 mesh, washed with deionized water, dried in an oven at 383 K for 24 hours and stored in a desiccator.

The selected concentrations were 50 mg/L for 1240, NR, F400 and F300, 100 mg/L for SAN and 200 mg/L for SAD, NZ, and NZH. In these experiments, 5, 10 or 20 mg of every adsorbent were added to an Erlenmeyer containing 100 mL of 10 ppm lincomycin solution; this lincomycin concentration was the lowest value between the concentrations selected for adsorption essays. The solutions were stirred at 130 rpm for 20 days, using an orbital shaker, and lincomycin concentration was measured. The final concentration value was different from zero. The final concentration for each adsorbent is presented in Table 3.3.

Table 3.3. Equilibrium concentration of lincomycin, after 20 days of stirring at 130 rpm, with initial lincomycin concentration of 10 ppm, in deionized water at initial pH 6.5.

Adsorbent	Code	Adsorbent concentration (ppm)	Final concentration (ppm)
Alfa Aesar 1240	1240	50	1.9
Norit Row 0.8	NR		1.3
Filtrasorb F400	F400		1.9
Filtrasorb F300	F300		2.7
Sigma Aldrich Norit	SAN	100	3.7
Sigma Aldrich Darco	SAD	200	2.9
Natural zeolite	NZ		2.9
Modified natural zeolite	NZH		7.6

Later, the equilibrium adsorption time for every adsorbent was determined. The experiments were carried out at 280 K and using 50 ppm lincomycin solutions. For these experiments, 3 Erlenmeyer flasks of each adsorbent, containing 5, 10 or 20 mg of adsorbent (depending on the adsorbent as detailed in Table 3.3) and 100 mL of 50 ppm lincomycin solution were stirred at 130 rpm. Later, lincomycin concentration was measured every day, until 15 days by UV spectrometry using a MECASYS Optizen POP UV-Vis spectrophotometer at a detection wavelength of 200 nm.

A single factor ANOVA analysis with LSD multiple range tests (95% confidence), for means analysis, was carried out, using Statgraphics Centurion XVI software. It was used for determining the statistically significant differences between the treatment times, and the minimum time from which no significant differences were detected, was selected as the adsorption equilibrium time. This time corresponded to 7 days for the adsorbents that required the longest equilibrium time. To keep homogeneity, samples were stirred for eight days in the

adsorption essays. Figure 3.1 shows the obtained results for different stirring times. Statistical analysis results are available in Appendix A.

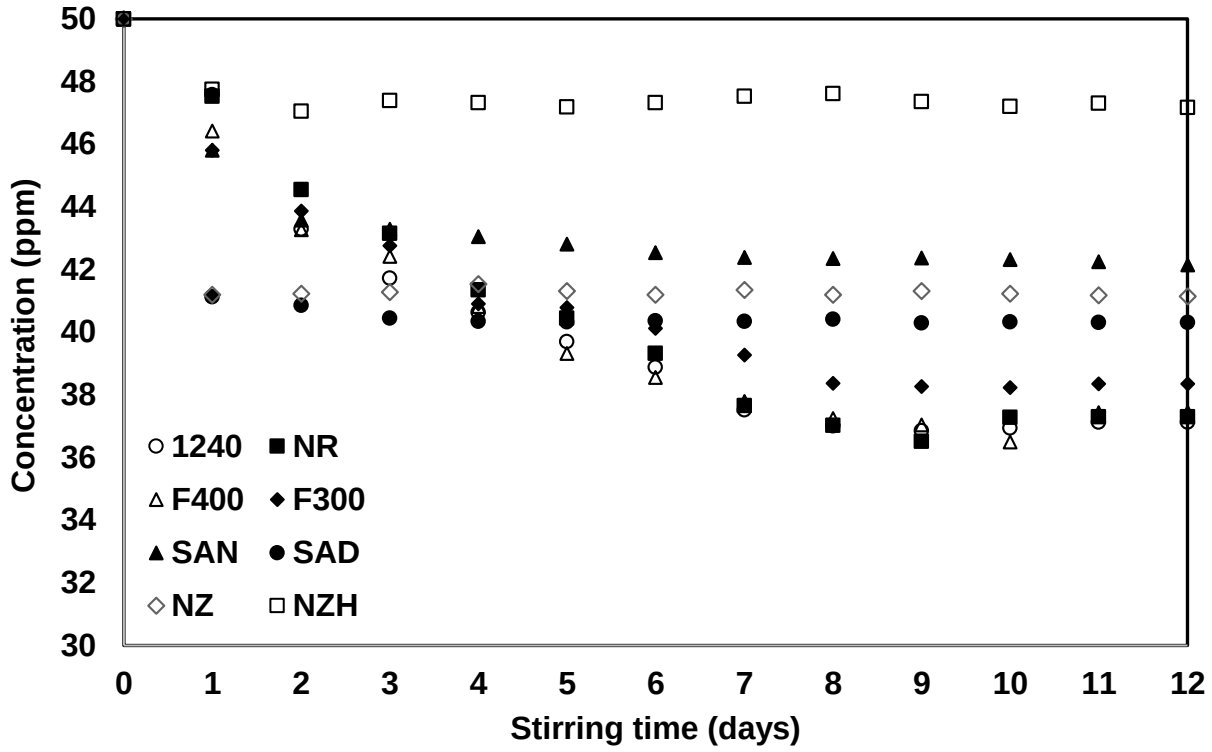

Figure 3.1. Concentration of lincomycin in solution as a function of stirring time, with initial lincomycin concentration of 50 ppm, at initial pH of 6.5 in deionized water

3.2.2 Adsorption of lincomycin from deionized water and synthetic manure experiments

Experimental adsorption experiments were carried out in sequential stages detailed below:

- First stage adsorption assays were performed using deionized water at four different temperatures (280, 288, 296 and 306 K) at the initial pH obtained without adding any reagent. This initial pH value corresponded to 6.5.
- The influence of pH was studied to analyze the effect of electrostatic interactions. Therefore, pH was adjusted to initial value of 10 using 1 N solution of NaOH as detailed

in Table 3.1. These experiments were carried out at four different temperatures (280, 288, 296 and 306 K).

- The final stage essays were conducted using synthetic and real swine manure. For synthetic manure, the experiments were carried out at four different temperatures (280, 288, 296 and 306 K). For real manure, experiments were conducted at room temperature (296 K).

The methodology for the preparation of all the samples is detailed below. Adsorption experiments were performed at four temperatures (280, 288, 296 and 306 K) to use conditions close to those in cold and hot regions respectively. Chemviron temperature controlled chambers at Pilot Plant were used for these experiments. Stock solutions were taken to the chambers the day before preparation of samples to avoid temperature fluctuations, and all the adsorption samples were prepared inside them. An initial amount of adsorbent, equivalent to 50 mg/L for 1240, NR, F400, and F300, 100 mg/L for SAN, and 200 mg/L for SAD and zeolites, was added into Erlenmeyer flasks containing 100 mL of 10, 17, 25, 33, 40, 50, 70 and 90 ppm lincomycin solutions. Flasks were sealed immediately to avoid the effect of CO_2. These solutions were stirred at 130 rpm for eight days, determined as the equilibrium time.

After flasks had been removed, samples were filtered using acetate syringe filters (0.45 µm) and injected into vials for HPLC analysis.

3.3 Analytical methods for determination of lincomycin concentration

Lincomycin concentration was quantified by UV-Visible spectrometry in the equilibrium time determination essays and by HPLC for adsorption assays at different temperatures. Both approaches provided calibration curves with correlation coefficients greater than 0.999.

UV-Visible spectrometry was useful in the determination of equilibrium time because it allowed returning the volume used for analysis to the essay Erlenmeyer flask without changing the sample volume. However, this method presented limitations in the quantification of high concentrated solutions (>50 ppm). Moreover, the presence of other compounds, especially in the synthetic and real manure, can interfere with the accurate quantification of the target compound.

Therefore, HPLC analysis was used because it allowed determining lincomycin concentration in highly concentrated solutions (90 ppm) and complex matrices. Furthermore, it provided better measurement precision.

3.3.1 Spectrometric detection of lincomycin

A MECASYS Optizen POP UV-Vis spectrophotometer was used for quantifying lincomycin concentration at the adsorption equilibrium time essays. The wavelength for lincomycin detection was reported at 210 nm [8]. To confirm this value a short range of wavelengths (195-220 nm) was scanned in the presence of lincomycin solutions. Absorbance curve produced by lincomycin in the selected range of wavelengths is presented in

Figure **3.2**.

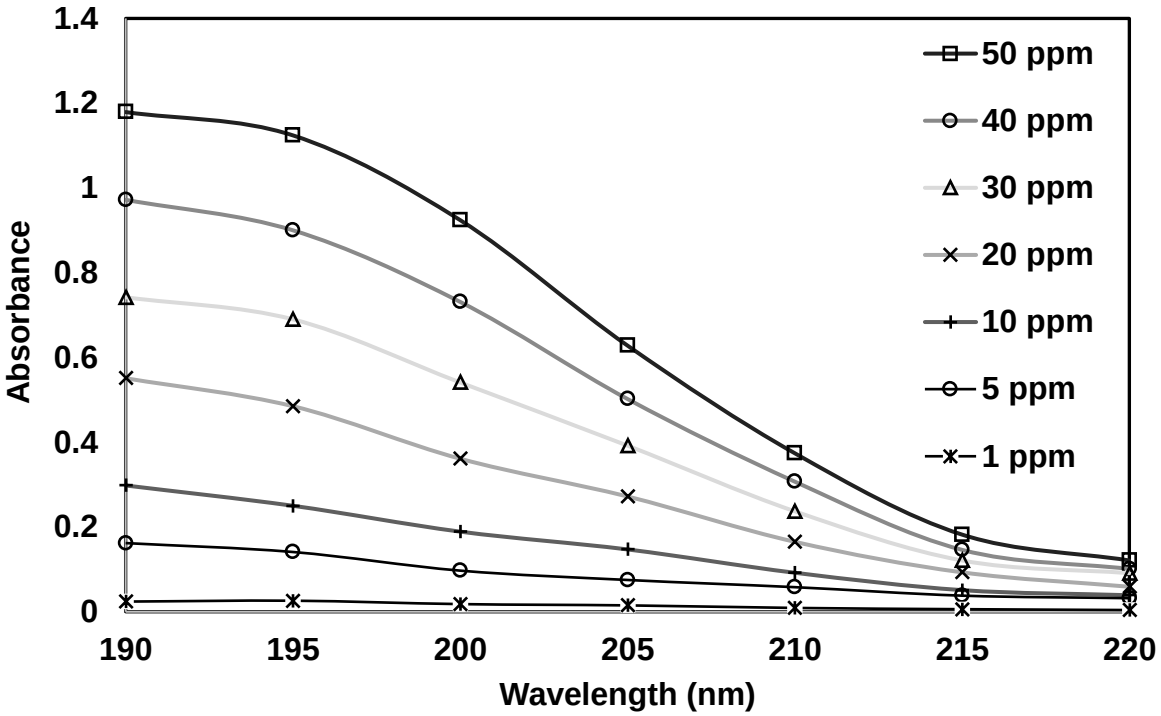

Figure 3.2. Absorbance of lincomycin solutions (1-50 ppm) in deionized water for the selected wavelength range between 195 and 220 nm

Lincomycin exhibited high absorbance values in the chosen range, however, to quantify low concentration values, 200 nm was selected as the working wavelength. From the data presented in

Figure **3.2**, it was possible to obtain the calibration curve and the relationship between absorbance and concentration of lincomycin in deionized water solutions. The upper and lower limits of quantification were 50 ppm and 1 ppm respectively. Figure 3.3 shows the obtained calibration curve at 200 nm.

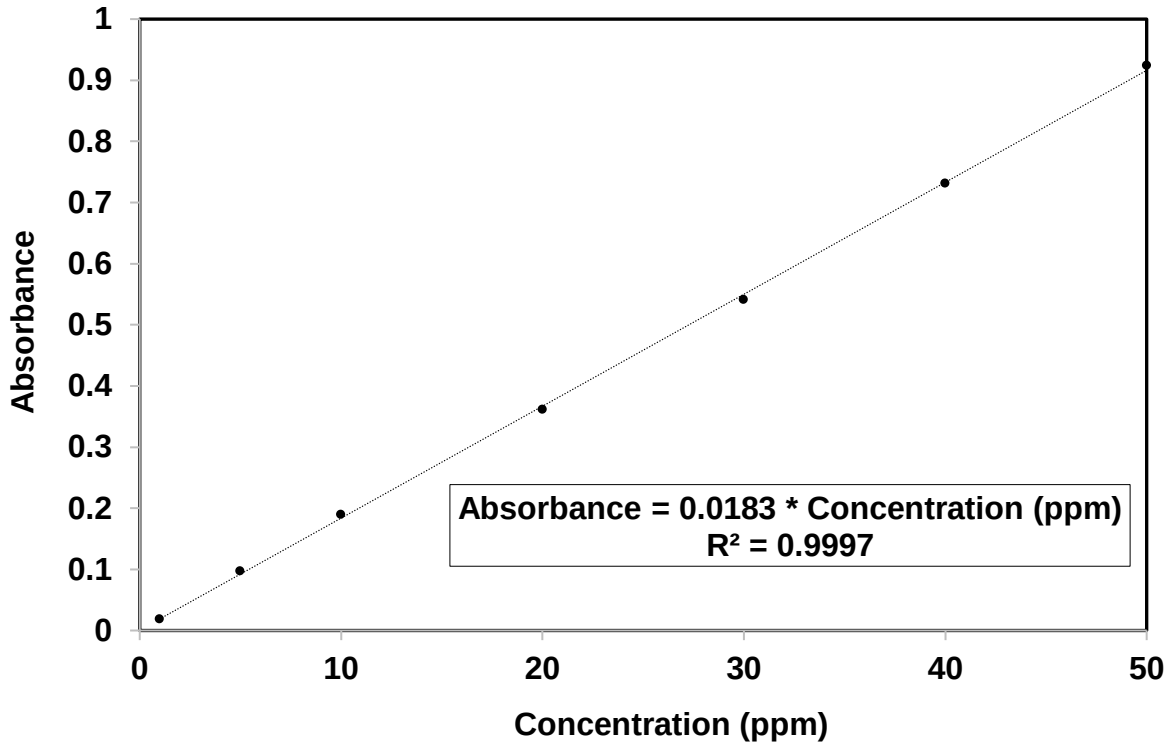

Figure 3.3. Lincomycin calibration curve for spectrometric lincomycin determination (wavelength = 220 nm)

3.3.2 Analysis of lincomycin with HPLC in deionized water

Thermo Scientific Ultimate 3000 HPLC coupled to a Diode array detector with a Thermo Scientific Acclaim 120 C18 (100mm*4.6mm, 5µm particle size) column was used for analysis of lincomycin. The detection was performed by measuring the absorption at 200 nm. The mobile phase used as eluent was 20 mM KH_2PO_4: acetonitrile (85:15) at a flow rate of 1 mL min^{-1} with an injection volume of 15 µL.

The upper and lower limits of quantification were 90 ppm and 1 ppm respectively. Figure 3.4 shows the obtained calibration curve at 200 nm.

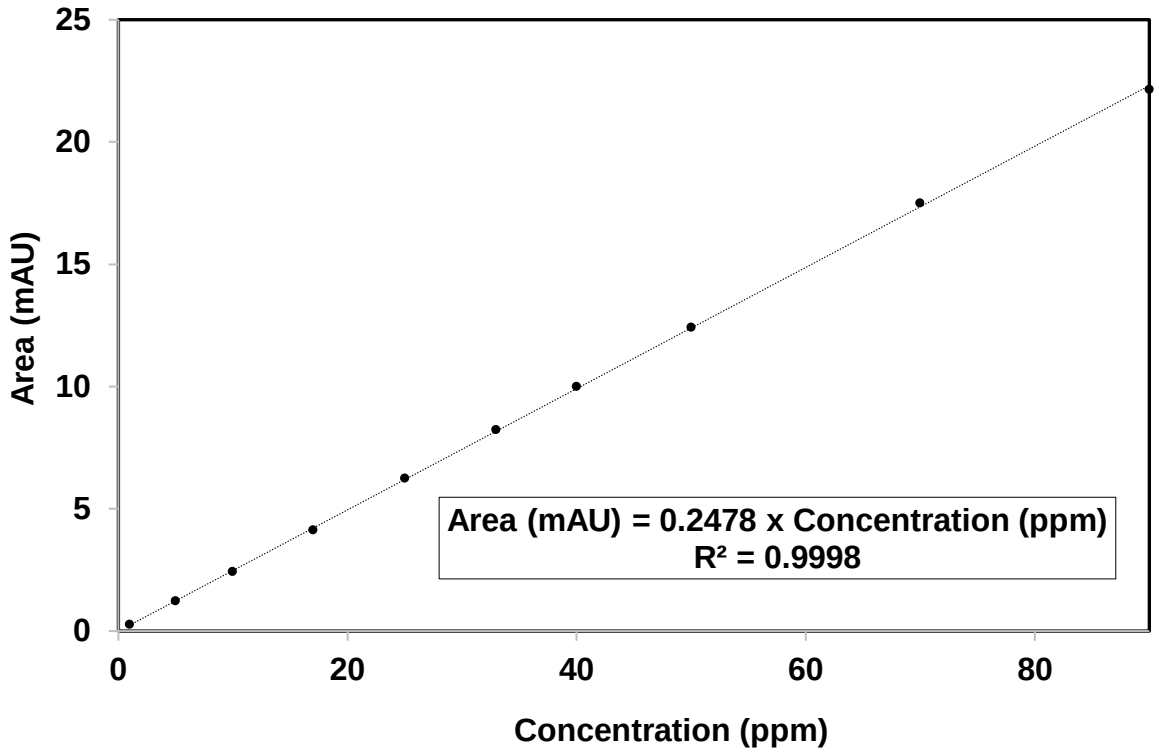

Figure 3.4. Lincomycin calibration curve for high-performance liquid chromatography lincomycin determination in deionized water (wavelength = 200 nm)

3.3.3 Analysis of lincomycin with HPLC in real manure

The method presented in section 3.3.2 was used for the detection of lincomycin in deionized water. However, in real manure, the presence of other organic compounds did not allow the detection using the same method. Therefore, a longer chromatographic column, lower

mobile phase flow, and different mobile phase composition were used to improve the quantification method. The separation was carried out using a Thermo Scientific Acclaim 120 C18 (250mm*4.6mm, 5µm particle size) column and the detection was performed by measuring the absorption at 200 nm. The mobile phase used as eluent was 20 mM KH_2PO_4: acetonitrile (90:10) at a flow rate of 0.8 mL min^{-1} with an injection volume of 15 µL. The upper and lower limits of quantification were 100 ppm and 5 ppm respectively. Figure 3.5 shows the obtained calibration curve at 200 nm.

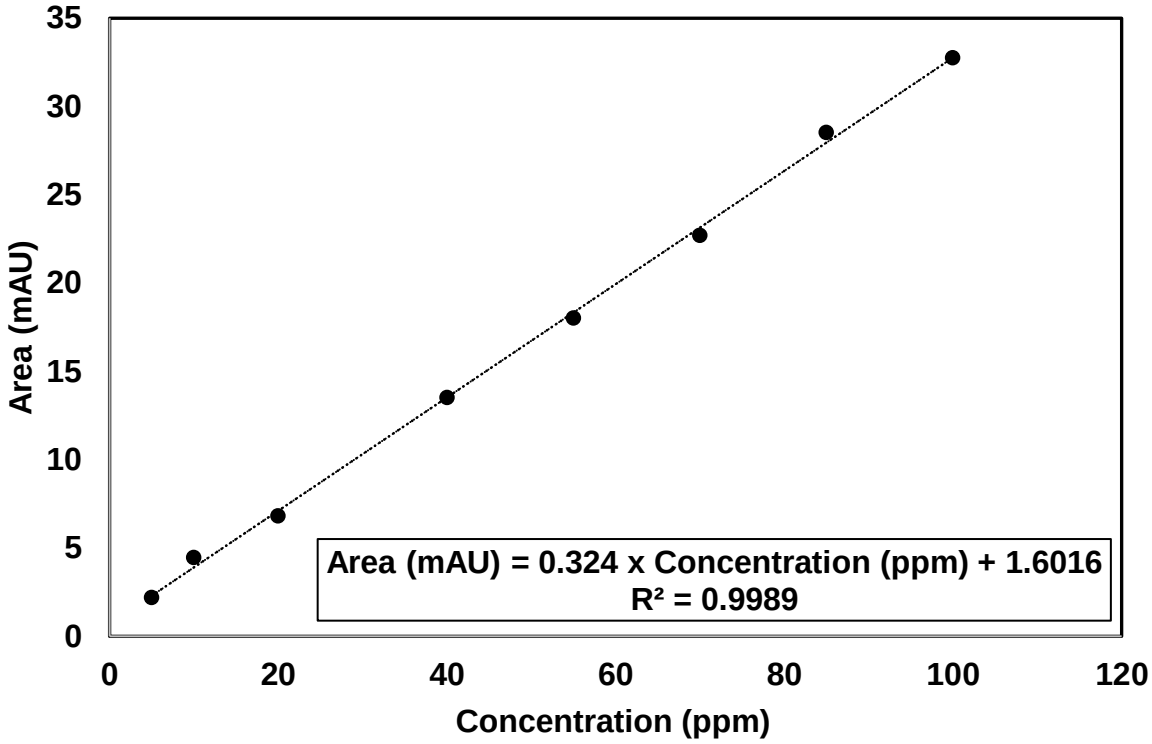

Figure 3.5. Lincomycin calibration curve for high-performance liquid chromatography lincomycin determination in real manure (wavelength = 200 nm)

3.4 Procedures for adsorbents characterizations

3.4.1 Measurement of adsorbents surface area and pore size distribution

The porosity characteristics of the adsorbents used in this study were determined by physical adsorption of nitrogen at 77 K using an Accelerated Surface Area and Porosimeter

system (ASAP 2020, Micromeritics, U.S.A.). Samples were previously washed with Millipore water and dried for two days at 383 K in an oven. Later, around 0.2 g of sample were collocated into the analysis chamber and degassed; this process helped to remove impurities attached to the surface and prepared the sample for nitrogen adsorption.

For the surface area measurement, desorption isotherms were analyzed by the Brunauer–Emmert– Teller (BET) equation. In the case of the pore size distribution, pores were classified as micropores (<2 nm), mesopores (2-50 nm) and macropores (>50 nm) [107] and determined by the t-method [108]. The obtained data was processed automatically by the software.

3.4.2 Measurement of the point of zero charge

The point of zero charge (PZC) was determined by the drift method [109]. NaCl 0.1 M was prepared. 40 mL of solution was added to 5 Erlenmeyer flasks with capacity of 125 mL. The pH of each container was adjusted to values of 5, 7, 9 and 11, using NaOH 0.5 N or HCl 0.5 N. Finally, 200 mg of adsorbent was added to each flask and covered with Parafilm. Samples were shaken for 48 hours at 200 rpm using an orbital shaker at room temperature (295 K). A Thermo Scientific pH meter was calibrated, samples were filtered using a 0.45 µm acetate syringe filter, and the final pH value was measured in each case. The point of zero charge corresponded to the pH at which the curve crosses the line pH final = pH initial.

3.4.3 Measurement of oxygen groups content on activated carbon

Standardization of solutions concentration

The content of oxygen groups on activated carbon was determined by Boehm's titration method following the methodology proposed by Goertzen, Theriault, Oickle, Tarasuk, & Andreas [110]. Acid groups were evaluated using basic solutions of different strengths ($NaHCO_3$, Na_2CO_3, and NaOH). On the other hand, basic properties were assessed using hydrochloric acid. The solutions concentration for all the cases was 0.05 M.

Standardized solutions of NaOH and HCl of concentration 1 M were obtained from Alfa Aesar. Solutions used for characterization were obtained diluting standardized solutions to a final concentration of 0.05 M for both reagents. Na_2CO_3 (99.5% purity) and $NaHCO_3$ (99.9% purity) were obtained from Sigma-Aldrich. Solutions of concentration 0.05 M were prepared, and real concentration was obtained titrating 10 mL of each solution. The methodology that was followed is detailed below:

- For Na_2CO_3, 30 mL of 0.05 M HCl were added and back titrated with NaOH 0.05 M.
- For $NaHCO_3$, 20 mL of 0.05 M HCl were added and back titrated with NaOH 0.05 M.

The endpoint of each test was determined by potentiometric titration using a pH meter when the pH value reached 7.0.

Preparation of samples and data processing

Each activated carbon was washed with Mili-Q water, dried at 383 K for 12 hours and collocated into a desiccator until its use. 1.5 g of each activated carbon was weighed, added to 50 mL of $NaHCO_3$, Na_2CO_3, NaOH and HCl 0.05 M, and sealed immediately with Parafilm. Samples were shaken for 24 hours at 130 rpm using an orbital shaker, filtered using a 0.45 µm syringe filter and degassed for 15 minutes by sonication. An aliquot of 10 mL was taken into an Erlenmeyer flask, previously washed with Mili-Q water, dried and sonicated for 10 min, and titrated as detailed below:

- For Na_2CO_3, 30 mL of 0.05 M HCl was added and back titrated with NaOH 0.05 M.
- For NaOH and $NaHCO_3$, 20 mL of 0.05 M HCl was added and back titrated with NaOH 0.05 M.
- For HCl, 20 mL of 0.05 M NaOH was added and back titrated with HCl 0.05 M.

The endpoint of each test was determined by potentiometric titration using a pH meter when the pH value was 7.0.

3.4.4 Determination of composition of natural and modified zeolites

The composition of the zeolites was determined by X-ray fluorescence (XRF). A Bruker S8 Tiger wavelength dispersive X-ray fluorescence (WDXRF) spectrometer was used, and analysis was carried out at Saskatchewan Research Council (SRC). X-ray fluorescence is a non-destructive and accurate technique that allowed determining the elemental composition of zeolites.

3.5 Real manure characterization

Liquid manure samples were obtained from the Prairie Swine Centre. Fresh samples were contained in 10 L containers and kept at refrigerated conditions (4°C) until its analysis.

3.5.1 Dissolved solids and total solids concentration

The dissolved and total solids in real manure were determined following the procedure suggested by HACH in the Handbook of Water Analysis [111]. For the determination of dissolved solids the manure was previously filtered using Whatman filter paper (8 μm).

An evaporating dish was collocated in a Lab Companion oven at 104°C for 1 hour and cooled in a desiccator until room temperature was achieved. The evaporating dish was weighed in an analytical balance, and the weight was recorded. Later, 35 mL of manure was added to the evaporating dish and put in the oven at 104°C for 6 hours. The evaporating dish was cooled in a desiccator and weighed. Finally, the sample was again placed in the oven and weighed every hour until results did not change more than 0.3 mg. The concentration of solids was determined by the difference of weights.

3.5.2 Dissolved organic carbon (DOC) determination

The dissolved organic carbon (DOC) was determined by CO_2 quantification using non-dispersive infrared analysis after catalytic combustion at 680°C. Manure was filtered using

acetate syringe filters (0.45 μm) and diluted 50 times using deionized water. The dissolved organic carbon was measured using a Shimadzu TOC-L analyzer.

3.5.3 Chemical oxygen demand (COD) determination

The measurement of the liquid manure chemical oxygen demand (COD) was carried out following the method suggested by the American Public Health Association (APHA), American Water Works Association (AWWA), and Water Environment Federation (WEF) for the examination of water and wastewater [112]. Filtered (acetate syringe filters 0.45 μm) and non-filtered samples were analyzed.

Liquid manure was homogenized, 1 mL of sample was taken and diluted to 20 mL. 2 mL of the resulting solution was added to high range COD vials (0-1500 mg O_2/L) and heated at 150°C for 2 hours. Later, vials were cooled to room temperature and analyzed using a Hach DR 2800 Portable Spectrophotometer. The COD was reported as mg O_2/L.

3.6 Repeatability of Experimental Measurements and Procedures

The following considerations were taken into account to ensure the experimental repeatability and data processing:

- Fresh lincomycin solutions were prepared the day prior the samples preparation. Initial concentration was measured for all the prepared solutions, and initial concentration did not deviate more than 0.5 ppm from the desired concentration in all the cases.
- Adsorption isotherms experiments were triplicated for samples at pH 6.5 and duplicated for samples at pH 10 in deionized water and synthetic and real manure. The adsorption capacity was calculated for each concentration point, and the standard deviation was reported for Y axis representing lincomycin solution concentration and adsorption capacity respectively.
- The weight of adsorbent for each sample had a maximum deviation of ±1 mg from the desired value (50 mg for 1240, NR, F400 and F300, 100 mg for SAN, and 200 mg/L for

SAD and zeolites). This deviation was corrected by the solution volume added to the Erlenmeyer flask.

- Solutions were collocated into the controlled temperature chambers the day before samples preparation, fluctuations of temperature in the chamber were less than ±0.1 K.
- A calibration curve using MECASYS Optizen POP UV-Vis spectrophotometer provided an accuracy of 3 significant digits. Hence concentration and standard deviation in the determination of equilibrium time was reported with one decimal digit accuracy in the ppm range. On the other hand, calibration curve using Thermo Scientific Ultimate 3000 HPLC provided a precision of 4 significant digits, and subsequently, concentration and standard deviation in the isotherms essays was reported with two decimal digits in the ppm range.
- The point of zero charge and oxygen content characterizations assays were duplicated, and the average value was reported. Thermo Fisher pH meter possessed a tolerance of ±0.01. Burettes had a precision of 0.1 mL.

CHAPTER 4
CHARACTERIZATION OF ADSORBENTS

The adsorbents porosity, surface area and pore size distribution (PSD), the point of zero charge (PZC), oxygen content for activated carbons and elemental composition for zeolites were characterized using the methodologies described in chapter three. The following paragraphs present the results obtained from these procedures.

4.1 Measurement of Adsorbent surface area and pore size distribution

The porosity characterization of the adsorbents used in this study was carried out by physical adsorption of nitrogen at 77 K using an Accelerated Surface Area and Porosimeter system (ASAP 2020, Micromeritics). Results obtained from the characterization are shown in Table 4.1. Activated carbons can be divided into two groups, the first group is comprised of 1240, NR, F400 and F300; and the second group consists of SAN and SAD.

The first group showed surface and micro-pore areas greater than 1000 m^2/g and 800 m^2/g respectively, hence, the majority of their structure is composed of micropores. Average pore size confirms that, in the case of these adsorbents, the corresponding values are near the limit of micropores size definition (<2 nm) [113]. The second group corresponds to activated carbons with BET surface areas less than 800 m^2/g. These activated carbons can be defined as mesoporous materials since their average pore size is greater than 40 Å [81].

Natural zeolite showed lower surface area and microporosity. However, due to the acid treatment, an increase in the surface area and a decrease in the pore size due to the removal of cations such Al, Mg, Fe and Ca from the clinoptilolite structure [60] was observed.

Table 4.1. Activated carbons porosity characterization by nitrogen adsorption at 77 K

Adsorbent	BET surface area (m^2/g)	Average pore size (A)	t-Plot micropore surface area (m^2/g)	t-Plot external surface area (m^2/g)	Micropore volume (cm^3/g)	Mesopore volume (cm^3/g)
1240	1449	27	974	475	0.404	0.988
NR	1155	23	885	270	0.375	0.655
F400	1184	22	869	315	0.370	0.647
F300	1046	23	845	201	0.358	0.598
SAN	787	44	381	406	0.167	0.876
SAD	764	45	420	344	0.182	0.856
NZ	47	72	8	39	0.003	0.084
NZH	121	46	58	63	0.030	0.139

4.2 Measurement of point of zero charge

The point of zero charge of activated carbons and natural zeolites used in this study was determined using the drift method, explained in chapter three. Figure 4.1 shows the obtained PZC diagram.

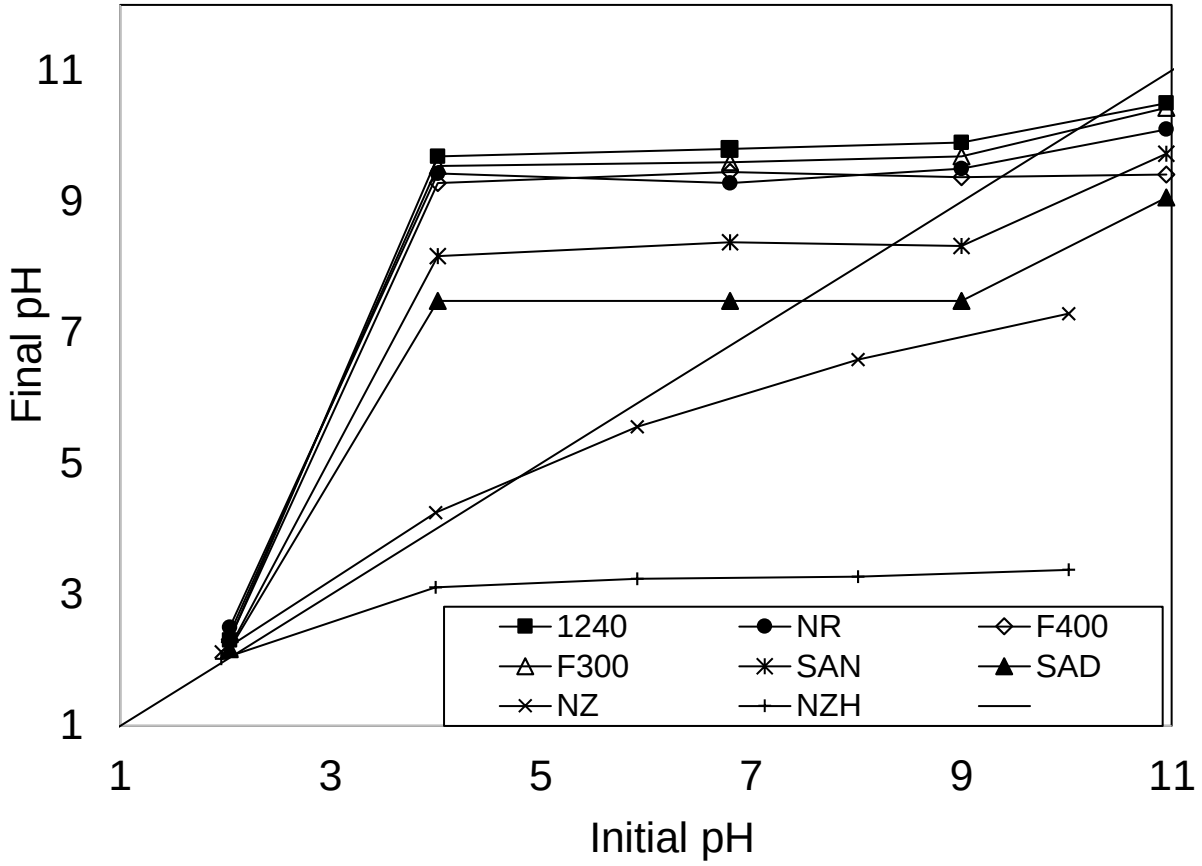

Figure 4.1. PZC determination diagram for activated carbons and zeolites by drift method

In the case of activated carbons the point of zero charge value decreased as 1240>F300>NR>F400>SAN>SAD. The PZC represents the pH value at which the total surface charge is zero [39], so below the PZC, the total charge is positive and, conversely, pH values above the PZC provides negatively charged surface [114]. The adsorption of charged species onto charged surfaces can be expected to be strongly influenced by electrostatic attraction or repulsion forces [37]. Hence, determination of PZC value is necessary to explain the electrostatic interactions that influence the adsorption process. The calculated values are presented in Table 4.2.

Table 4.2. Points of zero charge for activated carbons and zeolites used in this study determined by drift method

Adsorbent	1240	NR	F400	F300	SAN	SAD	NZ	NZH
PZC	10.3	9.7	9.4	9.0	8.3	7.5	4.9	2.1

According to the PZC values for activated carbons, SAN and SAD were neutral and 1240, NR, F400, and F300 were basic [40]. Acidity and basicity in ACs are established by the concentration of oxygen groups on the carbon surface [39]. Thus, acid properties are caused by the presence of carboxyl, phenol and lactone groups [42]. On the other hand, basic properties are due to the presence of chromene and pyrone structures [14]. Activated carbons presented in this study are mainly basic and it is expected a low concentration of carboxylic, phenolic and lactone groups. The results obtained for the quantification of acid and basic groups is presented in section 4.3.

For natural zeolite and modified natural zeolite, the point of zero charge value depends on factors such as crystallinity, Si/Al ratio and the presence of cations [115]. The PZC of natural zeolite was 4.9; this value is similar to the one obtained for a Chinese clinoptilolite by Zhang [116]. The PZC determines the charge of the zeolite surface at the experimental pH conditions [117], hence, in this study, the surface is negatively charged at pH 6.5 and 10.0 due to proton deficit [118]. At pH 6.5 lincomycin is positively charged and ion exchange is possible, conversely, at pH 10.0 lincomycin is in its neutral form and adsorption interactions are not related to ion exchange mechanism [62].

Acid modification of natural zeolite produced a decrease in the PZC value from 4.9 to 2.1 due to the alumina and other cations removal that modifies the anion framework [17,59]. Thus, hydroxyl groups bonded to the zeolite structure present weaker interactions with the framework and become available for deprotonation, increasing the acid character represented by the PZC value [118].

4.3 Measurement of oxygen content on activated carbon

The oxygen content of activated carbons was determined by Boehm's titration method, explained in chapter three. Characterization results are shown in Table 4.3.

Table 4.3. Surface chemistry analysis of activated carbons using Boehm's titration method

Adsorbent	Carboxylic groups (µeq/g)	Lactonic groups (µeq/g)	Phenolic groups (µeq/g)	Acid groups (µeq/g)	Basic groups (µeq/g)
1240	17	174	43	234	524
NR	50	199	22	271	717
F400	33	157	62	253	456
F300	100	24	10	134	400
SAN	182	16	26	224	346
SAD	240	75	31	346	239

Boehm's titration characterization results of activated carbons revealed the presence of more basic than acidic functional groups for 1240, NR, F400, F300 and SAN. On the other hand, only SAD presented greater concentration of acid than basic sites. As mentioned in section 4.2, acidity is represented by the total acid groups concentration, due to the presence of carboxyl, phenol and lactone groups [42]. On the other hand, basicity is represented by the concentration of basic groups, caused by the presence of chromene and pyrone structures [14].

Activated carbons point of zero charge is related directly to the concentration of oxygen groups. Thus, a high concentration of acid groups promotes low PZC values and, conversely, a high concentration of basic sites increases the value of PZC [39] as shown in Table 4.2.

Acidic groups such as carboxylic, lactonic and phenolic are responsible for hydrogen bonds and electron-donor complex systems intermolecular interactions [39]. On the other hand, basic groups produce hydrophobic zones where adsorption of water is avoided, and organic molecules can interact with the surface [47]. Hence, the presence of both acid and basic groups on the carbon surface plays a major role in the mechanisms that control the adsorption process [43].

4.4 Determination of composition of natural and modified zeolites

Natural zeolite was treated with acid to dissolve cations such Al, Mg, Fe and Ca from the clinoptilolite structure and increase the ratio Si/Al. X-ray fluorescence analysis was carried out to determine the composition of the samples. Results obtained are shown in

Table **4.4**.

Table 4.4. X-ray fluorescence analysis for natural and acid modified clinoptilolite

	Composition (%)									
Adsorbent	**Na_2O**	**MgO**	**Al_2O_3**	**SiO_2**	**P_2O_5**	**K_2O**	**CaO**	**TiO_2**	**MnO**	**Fe_2O_3**
NZ	0.35	0.21	8.81	61.07	0.04	2.90	0.91	0.12	0.00	1.80
NZH	0.00	0.15	7.00	66.59	0.04	0.81	0.55	0.12	0.00	1.70

Table 4.4 presents the results obtained by X-ray fluorescence analysis of natural zeolite (NZ) and modified natural zeolite (NZH). It can be noted that the ratio Si/Al increased from 6.12 in NZ to 8.46 in NZH, this variation can improve the hydrophobic character of this material, useful for the adsorption of non-polar molecules from water [119]. On the other hand, acid treatment also removed cations such as Na, Mg, K, Ca and Fe that reduce the cation-exchange capacity [17] and also modifies the zeolite cell structure [59].

The reduction in the value of the point of zero charge of clinoptilolite is attributed to the removal of cations such as Na, Mg, K, Ca, as shown in

Table 4.4, that modifies the zeolite framework and releases hydroxyl groups that can act as acid sites [17,59,118].

CHAPTER 5
ADSORPTION OF LINCOMYCIN ON ACTIVATED CARBON AND ZEOLITES IN DEIONIZED WATER

The following chapter presents the results obtained from the adsorption of lincomycin on activated carbons and zeolites in deionized water at different temperatures (280, 288, 296 and 306 K), initial pH values (6.5 and 10.0), and solution ionic strength levels (0-100 mM). First, the adsorption process was described using traditional two parameters isotherms models such as Langmuir and Freundlich models and a three parameter model (Sips model) by non-linear regressions using Origin 2017 software. The second section of this chapter deals with the effect of temperature in the adsorption capacity through the thermodynamic characterization associated to each adsorbent at neutral pH. Thermodynamic parameters of enthalpy, entropy and Gibbs energy changes were determined and discussed. Finally, since pH value affects both lincomycin and adsorbent surface charge and because electrostatic interactions can play a major role in the adsorption process, the effect of varying this parameter value was studied. Thus, adsorbents 1240, NR and F400 activated carbons that showed high adsorption capacity and NZ were tested at pH 10.0. The process was characterized by the determination of the characteristic parameters of Langmuir, Freundlich, and Sips models through non-linear regressions.

5.1 Modeling of lincomycin adsorption on selected adsorbents at different temperatures (280, 288, 296 and 306 K) in deionized water at neutral pH

First stage adsorption assays were conducted following the methodology established in chapter three. The following section explains the mechanisms that control the adsorption of

lincomycin on selected adsorbents. However, the effect of temperature on the adsorption process is discussed later through the thermodynamic characterization presented in section 5.2. Samples were analyzed by HPLC and processed using the calibration curve described in Figure 3.4.

5.1.1 Modeling of lincomycin adsorption on activated carbons at different temperatures (280, 288, 296 and 306 K) in deionized water

The complete set of adsorption isotherms of lincomycin on activated carbons at different temperatures is shown in Appendix B.

Isotherms obtained by the adsorption of lincomycin on activated carbons were fitted to Langmuir and Freundlich models. Table 5.1 shows the fitting results by Langmuir and Freundlich non-linear regressions using Origin 2017 Pro software through Levenberg–Marquardt algorithm method. The Levenberg-Marquardt algorithm method was used because it is considered a combination of the gradient descent and the Gauss-Newton methods [120]. Therefore, when the parameters are far and near the optimal values it approaches to the gradient descent and Gauss-Newton models, respectively [120].

It can be noted that temperature increase affected the uptake of lincomycin directly. Thus, the adsorption capacity was maximum, in all the cases, at 306 K. To determine if the temperature variation has statistically significant impact on the adsorption capacity, a statistical analysis was carried out. Thus, a two-factor (temperature and initial concentration) Analysis of Variance (ANOVA) with Least Significant Differences (LSD) multiple range tests (95% confidence), for means analysis, was carried out. First, it was found that for all the adsorbents, the statistical parameter P-Value was less than 0.05. Therefore, at 95.0% confidence level, it was determined that temperature is a statistically significant variable on the adsorption capacity. Statistical analysis results, regarding the ANOVA table and Multiple Range test results are presented in Appendix C. Further explanation of the temperature effect is provided in section 5.2.

Table 5.1. Parameters for Langmuir and Freundlich adsorption isotherms of lincomycin on activated carbons at different temperatures in deionized water at initial pH 6.5

Adsorbent	Temperature (K)	Freundlich model			Langmuir model		
		K_F $(mg/g)(L/mg)^{1/n}$	n	R^2	q_{max} $(mg*g^{-1})$	K_L $(L*mg^{-1})$	R^2
1240	280	124.1	6.22	0.986	241.3	0.378	0.986
	288	133.3	6.11	0.993	259.0	0.413	0.983
	296	150.5	6.53	0.992	275.4	0.548	0.978
	306	171.1	6.88	0.995	295.8	0.831	0.966
NR	280	152.6	9.23	0.981	235.2	0.781	0.993
	288	168.2	9.55	0.980	253.2	0.958	0.993
	296	179.5	9.33	0.985	269.4	1.189	0.988
	306	192.7	9.42	0.989	283.5	1.717	0.980
F400	280	127.3	6.47	0.987	239.4	0.423	0.981
	288	135.5	6.52	0.993	251.3	0.474	0.981
	296	149.1	6.83	0.997	263.8	0.630	0.973
	306	162.3	7.19	0.996	275.3	0.823	0.969
F300	280	106.7	6.14	0.988	212.6	0.319	0.995
	288	117.2	6.27	0.986	228.2	0.356	0.988
	296	129.6	6.68	0.991	238.9	0.447	0.987
	306	145.3	7.36	0.990	249.4	0.607	0.985
SAN	280	43.4	6.88	0.997	80.4	0.359	0.987
	288	47.8	7.25	0.998	85.1	0.416	0.985
	296	51.5	7.75	0.998	87.4	0.499	0.981
	306	56.5	8.61	0.998	90.7	0.595	0.989
SAD	280	25.3	7.16	0.998	45.1	0.444	0.981
	288	27.6	7.28	0.997	48.1	0.508	0.974
	296	31.0	8.16	0.996	50.5	0.653	0.977
	306	35.0	9.44	0.995	52.9	0.898	0.983

Adsorption capacity at 306 K, corresponded to 295.8 mg/g for 1240, 283.5 mg/g for NR, 275.2 mg/g for F400 and 249.4 mg/g for F300 that presented high adsorption capacity. On the other hand, SAN and SAD provided adsorption capacities of 90.7 mg/g and 52.9 mg/g, respectively. Adsorption capacities obtained in this study are higher than the ones obtained using smectite clays [34], manure-derived biochars [62], synthetic zeolites [33] and carbon nanotubes [54], in the adsorption of lincomycin from deionized water. However, the range of concentrations used in the studies mentioned before is smaller than the one utilized in this study. Therefore, it is only possible to consider these values as references since extrapolating results can lead to overestimation of the removal capacity [121].

Freundlich model represented the isotherms better than Langmuir model using the determination coefficient (R^2) as comparison parameter for 1240, F400, F300, SAN and SAD and Langmuir model described better the behavior of NR based on the same parameter value. Kim et al., [54] studied the adsorption of lincomycin on carbon nanotubes and determined that Langmuir model did not predict correctly the behavior of the process (R^2<0.7), probably, because adsorption of lincomycin is not a pure monolayer type. Thus, Freundlich model was well fitted to the experimental data (R^2>0.96). Figure 5.1. Adsorption isotherms and Freundlich model fitting for adsorption of lincomycin on activated carbons at 306 K and Figure 5.2 show the adsorption isotherms and Langmuir and Freundlich models fitting respectively, for adsorption of lincomycin on selected activated carbons at 306 K, which promoted the maximum adsorption capacity.

For all activated carbons adsorption process was nonlinear with n greater than 6, indicating that the adsorption isotherm behavior is different from the linear isotherm and suggesting a highly heterogeneous distribution of sorption energy with non-localized adsorption sites [51,63]. Besides, K_F was greater than 100 $mg^{1-n}*Ln*g^{-1}$ for 1240, NR, F400, and F300, demonstrating high adsorption affinity for these activated carbons and less than 56.5 $mg^{1-n}*Ln*g^{-1}$ for SAN and SAD.

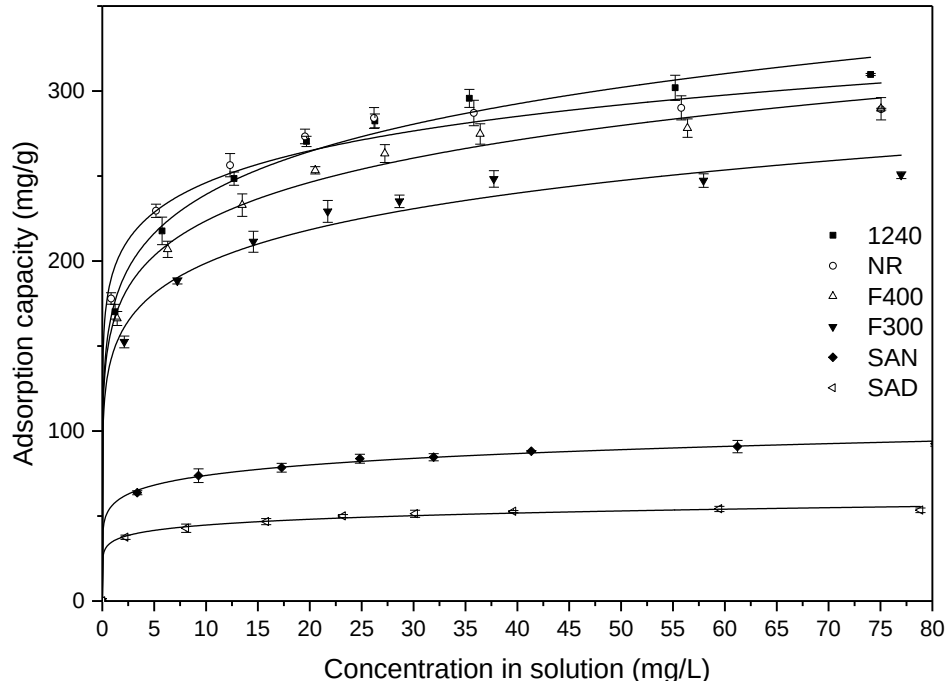

Figure 5.1. Adsorption isotherms and Freundlich model fitting for adsorption of lincomycin on activated carbons at 306 K in deionized water at initial pH 6.5

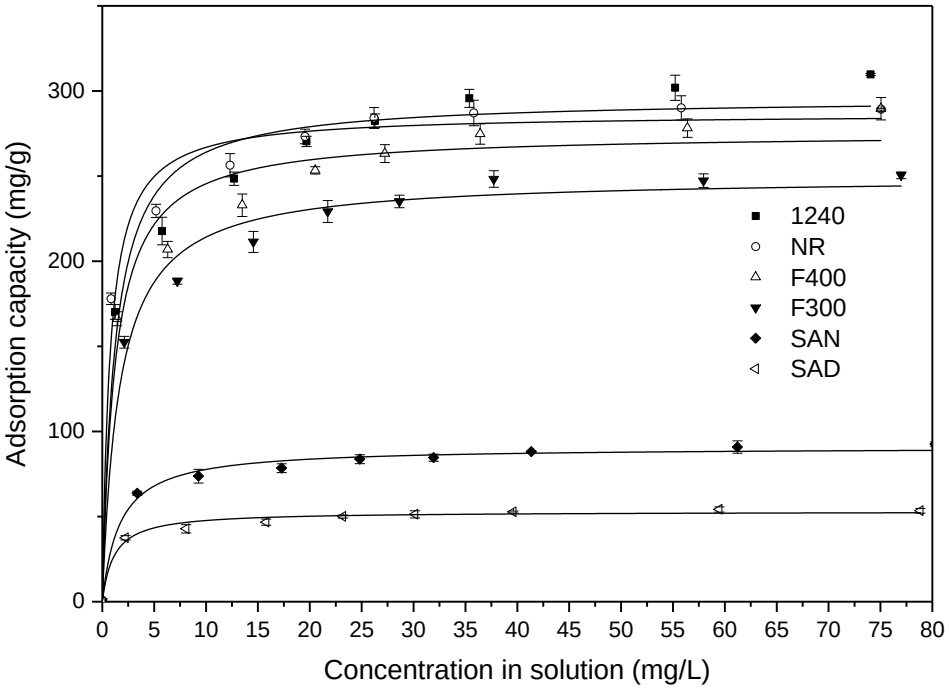

Figure 5.2. Adsorption isotherms and Langmuir model fitting for adsorption of lincomycin on activated carbons at 306 K in deionized water at initial pH 6.5

On the other hand, Langmuir model predicted the highest q_{max} parameter values at 306 K for the adsorbents in the order of 1240>NR>F400>F300>SAN>SAD. Figure 5.1 and Figure 5.2 show the fitting of data to Freundlich and Langmuir models, respectively. It can be noted that, although Freundlich model describes better the isotherms data based on the determination coefficient, it does not describe well the data in the high concentrations range and does not consider a saturation capacity [63]. Therefore, the range of application of this model is limited to low to medium concentrations. On the other hand, Langmuir model does not work properly in the low concentrations range but, it describes better the high concentrations range through its maximum adsorption capacity parameter [64]. It can be due to the assumptions used to develop this model, associated to the energetic homogeneity of the surface and a limited number of similar adsorption energy sites [37,65] are not necessarily true for activated carbons. It can be confirmed by the heterogeneity parameter value (n) determined by Freundlich model.

Based on the problems of the continuing increase in the adsorption capacity with an increase in the solution concentration predicted by Freundlich equation, Sips model provides an equation similar in form to the Freundlich equation, but it has a finite limit when the concentration is sufficiently high [63,64]. Therefore, it can predict the behavior of the process in the complete range of concentrations [63,64]. Table 5.2 shows the results obtained by non-linear regression method for Sips model fitting.

Table 5.2 shows the results obtained for fitting adsorption data to Sips model. The determination coefficient minimum value corresponded to 0.993 showing the good fitting that this model provided in the complete range of concentrations used in this study. The n value, related to the heterogeneity of the adsorption sites on the surface [63], was in all the cases greater than 1. It agrees with the results obtained by Freundlich model.

Table 5.2. Parameters for Sips adsorption isotherms of lincomycin on activated carbons at different temperatures in deionized water at initial pH 6.5

Temp. (K)	Ads.	K_S ($L*mg^{-1}$)	q_m ($mg*g^{-1}$)	n	R^2	Ads.	K_S ($L*mg^{-1}$)	q_m ($mg*g^{-1}$)	n	R^2
280	**1240**	0.299	282.0	1.75	0.995	**F300**	0.290	235.8	1.51	0.998
288		0.217	336.4	2.17	0.998		0.292	264.7	1.72	0.995
296		0.252	366.6	2.37	0.997		0.327	289.5	1.98	0.998
306		0.148	458.0	3.09	0.998		0.472	300.2	2.08	0.996
280	**NR**	0.878	247.3	1.41	0.995	**SAN**	0.107	120.1	2.94	0.998
288		1.078	266.9	1.45	0.996		0.055	144.0	3.54	0.999
296		1.269	298.4	1.83	0.997		0.003	212.3	4.96	0.998
306		1.447	338.2	2.42	0.997		0.265	129.4	3.28	0.999
280	**F400**	0.285	295.6	2.04	0.993	**SAD**	0.002	113.7	4.71	0.998
288		0.237	331.9	2.33	0.997		0.001	244.6	6.04	0.998
296		0.106	419.2	3.16	0.998		0.036	93.5	4.29	0.996
306		0.115	444.5	3.36	0.998		0.557	71.6	3.20	0.997

Besides, qm represented the adsorption capacity at saturation conditions. The results differ from the ones obtained by Langmuir model (q_{max}) due to the slow increase that experimental adsorption capacity presents with concentrations approaching the saturation plateau. Figure 5.3 shows the adsorption isotherms and Sips model fitting respectively, for adsorption of lincomycin on selected activated carbons at 306 K, which showed the maximum adsorption capacity.

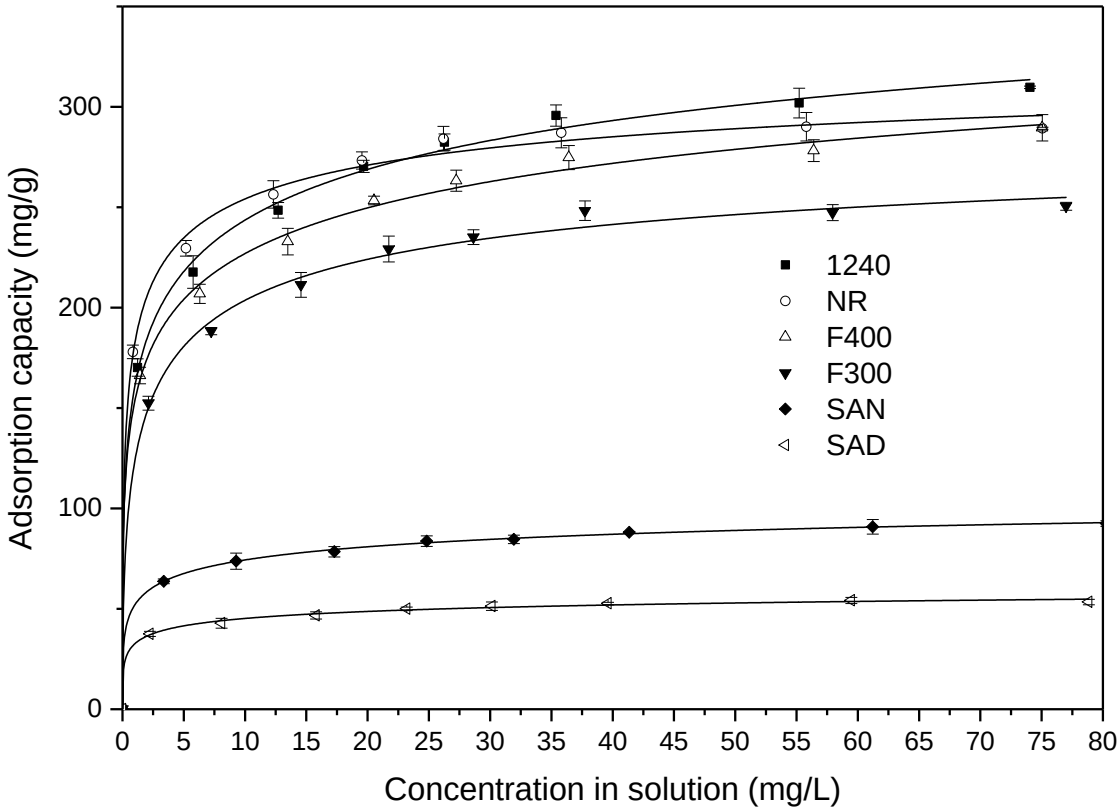

Figure 5.3. Adsorption isotherms and Sips model fitting for adsorption of lincomycin on activated carbons at 306 K in deionized water at initial pH 6.5

Adsorption capacity decreasing order was 1240=NR>F400>F300>SAN>SAD. This trend was consistent with the BET surface area presented in Table 4.1 but not proportional to the differences presented there. 1240 had a BET surface of 1449 m^2/g and NR, F400, F300 had areas of 1155, 1184 and 1046 m^2/g respectively. Therefore, 1240 adsorption capacity should be significantly greater than the other activated carbons and, shown in Figure 5.3, differences between 1240, NR and F400 are minimal. Yu, Li, Han, & Ma (2016) indicated that macro and mesopores are used for entrance and diffusion of molecules respectively; meanwhile, adsorption of contaminants occur on the surface of micropores. Therefore, adsorption capacity should be related to the micropore area. 1240, NR, F400, and F300, with the similar micropore area, provided similar adsorption capacity. These values were higher than SAN and SAD with lower micropore area. In consequence, adsorption capacity can be enhanced by increasing micropore area of the selected material. These results are confirmed by Kim et al., [54] that investigated the influence of surface area in the adsorption of lincomycin on carbon nanotubes. They determined

a positive linear correlation (R^2=0.98) between the Freundlich constant and surface area. However, it is mentioned that other properties additional to the surface area control the adsorption on carbon materials.

Since micropore area seems to be important for the adsorption process, it was necessary to analyze the accessibility to this specific group of pores. Lincomycin dimensions are 5.3*7.2*15.6 A, and the corresponding Stokes diameter is 0.58 nm [33], besides, for all the activated carbons used in this research the smallest pore that could be measured from BET porosity characterization was bigger than 0.804 nm, indicating that all the microporosity is accessible to the target molecules.

Even though micropore surface area seems to have a major role in predicting adsorption capacity it does not explain the low adsorption capacity presented by SAN and SAD and also the lower adsorption capacity presented by F300 in comparison with 1240, NR and F400 with similar micropore area. Therefore, other factors should have also played relevant roles in the adsorption of lincomycin, these parameters are discussed below.

To avoid introduction of species that affect the process characterization [40], experiments were carried out without adding any reagent to control the pH value . The pH value corresponded to around 6.5 for all the samples. At this pH value, lincomycin with a pKa of 7.8 [28], was present in the system approximately 87% as cation species and the remaining 13% as neutral species [62]. Besides, from the point of zero charge characterization results, all the activated carbons were also positively charged. Therefore, electrostatic interactions caused adsorbent-adsorbate repulsion [43] and, consequently, adsorption process must be controlled by non-electrostatic interactions like hydrophobic interactions, van der Waals forces, and hydrogen bonding [39].

The hydrophobic character in activated carbons is directly affected by the presence of oxygen surface groups [39]. Therefore, both Boehm's titration method and point of zero charge characterizations may be used as comparison parameters. The point of zero charge decreasing values were in the order of 1240>F400>NR>F300>SAN=SAD. This trend agrees with the results obtained in the adsorption process. Lincomycin is not a hydrophobic compound as shown by its high solubility in water (2930 mg/L) and octanol-water partitioning coefficient (log D=-

2.20) and, as a consequence, hydrophobic interactions between activated carbon and lincomycin are not as important as hydrogen bonds and π- π interactions [33]. However, this hydrophobic character on activated carbon surface creates "hydrophobic zones", where the adsorption of water on the carbon surface by hydrogen bonds is avoided, but the same interaction can take place between the carbon limited oxygen groups and lincomycin [62]. Although activated carbons that provided high adsorption capacity are mainly hydrophobic, Boehm's titration characterization determined the presence of carbonyl and in less quantity carboxyl groups on the activated carbon surface. These groups are probably located at the graphene layer edges [39]; therefore, hydrogen bonds play a role in the adsorption process [54].

Lincomycin molecule has hydroxyl groups bonded to the pyranose ring. These groups can interact and form hydrogen bonds with the limited number of oxygen groups on carbon surface [53,54]. Lincomycin molecule presents three hydroxyl groups associated with the same pyranose ring. However, the number of hydroxyl groups on the carbon surface is limited. Therefore, it would be expected that a single lincomycin molecule can form only a single functional group on the carbon surface [33]. Velasco & Ania (2011) reported that the incorporation of hydroxyl functionalities on the edges of the basal planes due to oxidation can improve the hydrogen bonding but reduce the hydrophobic character and, subsequently, promote competition between water and adsorbate for adsorption sites.

Other possible mechanisms are π- π bonds between the carbon basal planes and the aromatic rings in the adsorbate's structure [39,47]. This mechanism can not be used for explaining the adsorption of lincomycin on activated carbon because adsorbate molecule does not contain aromatic rings or π electrons that interact with the π electrons of aromatic rings on the carbon surface [53,62]. Hence, at this stage, it can be stated that this mechanism does not affect the adsorption process.

A third possible mechanism is electron donor-acceptor complex systems. Carbonyl groups on the surface are weak acid oxygen sites on the activated carbon surface and can be used as electron donor sites or Lewis bases [39,124]. On the other hand, lack of aromatic rings in the structure of lincomycin does not allow this type of dipole interactions [62,125].

Figure 5.4 shows the schematics of hydrogen bond interactions between lincomycin and activated carbon surface.

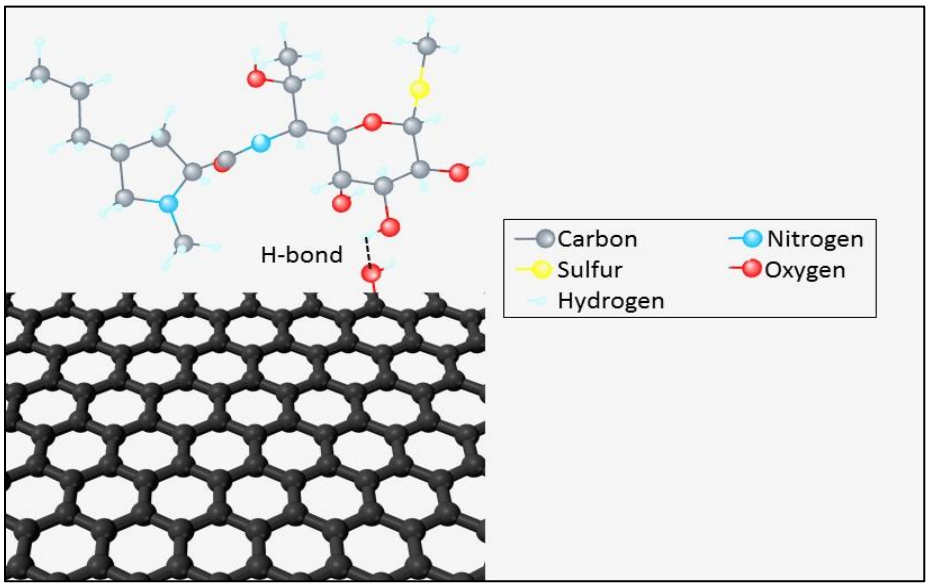

Figure 5.4. The schematics of hydrogen bond interactions between lincomycin and activated carbon surface

The introductory paragraphs about the parameters and mechanisms controlling the adsorption process stated that micropore area plays a major role in the adsorption process. However, micropore area do not explain the mechanisms controlling the process. At the initial experimental conditions, electrostatic interactions cause repulsion between adsorbent-adsorbate and other mechanisms such as hydrophobic interactions, π- π interactions, and hydrogen bonding should control the process. Therefore, it can be stated that even though hydrophobic interactions are not strong, due to the hydrophilic character of lincomycin, it can play a major role in the creation of highly hydrophobic zones where other interactions like hydrogen bonds appear between the graphene oxygen groups and hydroxyl groups in the lincomycin's pyranose ring. Besides, other mechanisms such as electron donor-acceptor interaction and π - π interactions are not possible due to the lack of aromatic rings in the lincomycin's structure. At this stage, from textural and surface characterizations it is possible to infer that hydrogen bonding is the main

mechanism controlling the adsorption process. However, thermodynamic characterization, presented in section 5.2, provides relevant information for clarifying this discussion.

5.1.2 Modeling of lincomycin adsorption on natural zeolite at different temperatures (280, 288, 296 and 306 K) in deionized water

Isotherms obtained by adsorption of lincomycin on natural zeolite and modified natural zeolite were fitted to Langmuir, Freundlich, and Sips models. Table 5.3 shows the fitting results by Langmuir and Freundlich non-linear regressions, using Origin 2017 Pro software through Levenberg–Marquardt algorithm method. Complete adsorption isotherms and models fitting the adsorption of lincomycin on zeolites are shown in Appendix B.

Characteristic parameters of Langmuir and Freundlich models are listed in Table 5.3. To verify if the temperature is a variable that causes significant differences in the adsorption capacity, the same statistical analysis used in section 5.1.1 was applied. Thus, a two-factor (temperature and initial concentration) ANOVA analysis with LSD multiple range tests (95% confidence), for means analysis, was carried out. Statistical analysis results are presented in Appendix C and showed that temperature is a statistically significant variable affecting the adsorption capacity based on the P-value (less than 0.05) and multiple range test.

Table 5.3. Parameters for Langmuir and Freundlich adsorption isotherms of lincomycin on natural zeolite at different temperatures in deionized water at initial pH 6.5

Adsorbent	Temperature (K)	Freundlich model			Langmuir model		
		K_F $(mg/g)(L/mg)^{1/n}$	n	R^2	q_{max} $(mg*g^{-1})$	K_L $(L*mg^{-1})$	R^2
NZ	280	30.1	10.47	0.994	44.5	0.711	0.998
	288	31.2	10.14	0.996	46.5	0.746	0.996
	296	33.1	10.66	0.996	48.3	0.841	0.996
	306	34.3	10.47	0.998	49.9	0.943	0.992
NZH	280	7.3	5.19	0.955	18.0	0.148	0.986
	288	7.9	5.08	0.957	19.8	0.145	0.990
	296	8.1	4.69	0.973	21.8	0.134	0.994
	306	8.6	4.72	0.970	23.0	0.138	0.990

Table 5.3 shows the fitting results for Freundlich and Langmuir models. In this case, both Langmuir and Freundlich models predicted well the adsorption data (R^2>0.955), but Langmuir model predicted the behavior of the process better than Freundlich model based on the determination coefficient (R^2>0.986) values as comparison parameter. It can be because adsorption on natural zeolites is carried out as monolayer coverage on the surface as described in Langmuir model [58,63]. Besides, due to the structure framework, the adsorption sites are homogenously distributed on the zeolite surface [65]. Li, Stockwell, Niles, Minegar and Hong, Hanlie [57] studied the adsorption of sulfadiazine sulfonamide from water on clinoptilolite and concluded that the best fitting to Langmuir model is caused by electrostatic interactions such as cation exchange. Even though Langmuir model described the data well, it was also be fitted to Sips model.

Table 5.4 shows the results obtained by non-linear regressions method for Sips model fitting.

Table 5.4. Parameters for Sips adsorption isotherms of lincomycin on natural zeolite at different temperatures in deionized water at initial pH 6.5

Adsorbent	Temperature (K)	K_S ($L*mg^{-1}$)	q_m ($mg*g^{-1}$)	n	R^2
NZ	280	0.930	46.9	1.50	0.999
	288	1.029	52.4	2.04	0.999
	296	1.204	53.0	1.88	0.999
	306	1.094	61.9	2.85	0.999
NZH	280	0.147	16.9	0.73	0.989
	288	0.140	18.4	0.69	0.994
	296	0.136	21.5	0.95	0.994
	306	0.138	22.9	0.98	0.989

Table 5.4 shows the results obtained for fitting adsorption data on zeolites to Sips model. The determination coefficient minimum value corresponded to 0.999 for NZ and 0.989 for NZH. These values showed the good fitting that this model provided in the complete range of concentrations used in this study for zeolites.

Characteristic parameter qm changed about 20% from Langmuir to Sips model due to the later model considering a slow increase until reaching the saturation plateau. The predicted adsorption capacity at 306 K was 61.9 mg/g for NZ and 22.9 mg/g for NZH. Figure 5.5 shows the adsorption isotherms and Langmuir and Sips models fitting, for adsorption of lincomycin on NZ and NZH at 306 K, which exhibited the maximum adsorption capacity.

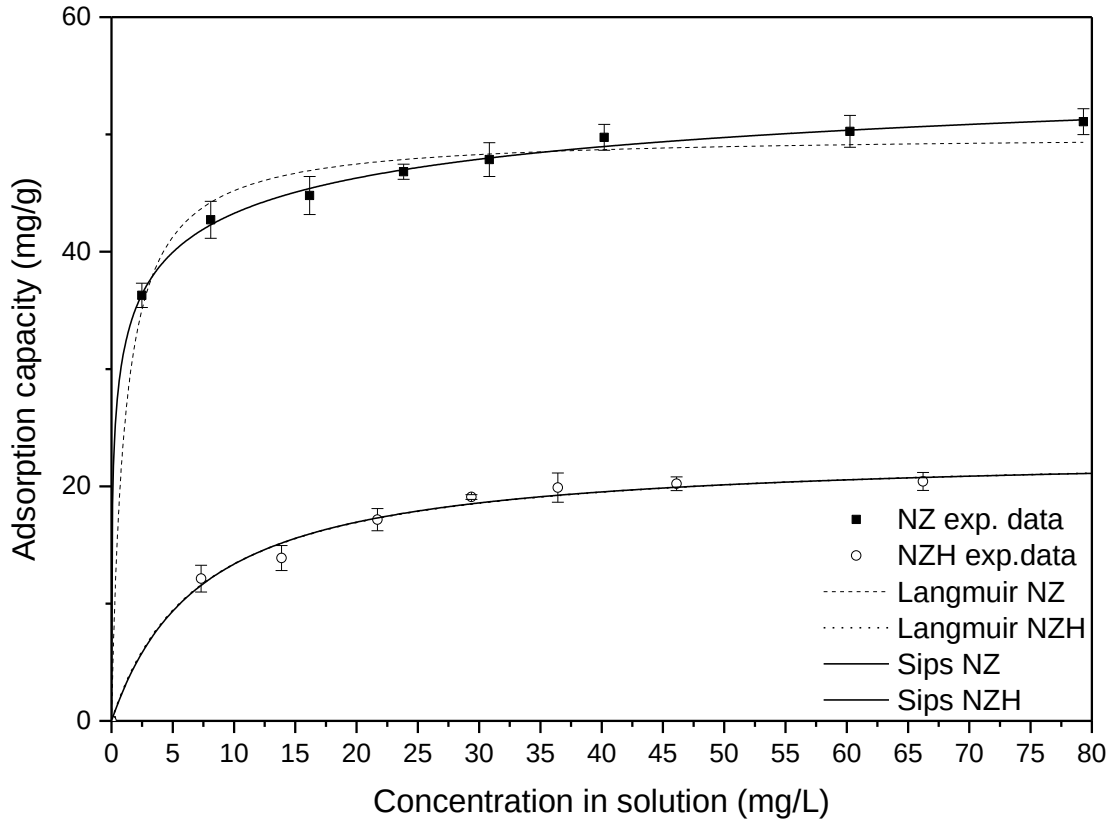

Figure 5.5. Adsorption isotherms and Langmuir and Sips model fitting for adsorption of lincomycin on natural zeolite at 306 K in deionized water at initial pH 6.5

Adsorption capacity, at 306 K, decreased from 61.9 mg/g in NZ to 22.9 mg/g in NZH because the acid treatment removed cations such as Na, Mg, K, Ca and Fe that, probably, reduced the cation-exchange capacity [17] and modified the zeolite cell structure [59]. At the current stage, experiments initial pH was around 6.5 for all the samples with lincomycin 87% as cation species and 13% as neutral species [62]. Besides, from the results obtained in the point of zero charge characterization, natural zeolite was negatively charged. Hence, electrostatic interactions caused adsorbent-adsorbate attraction [43] and, consequently, adsorption process can be influenced by these interactions.

Wang et al. [34] studied the adsorption of lincomycin on smectite zeolites and determined that significant reduction in adsorption capacity occurs between pH 7.0 and 7.5 due to the reduction of cationic lincomycin near its pka value (pH 7.8). Besides, reduction of lincomycin

adsorption was observed at pH values greater than 4 due to the decrease in the organic cation species. Hence, they concluded that the principal mechanism for adsorption of lincomycin on aluminosilicate materials as zeolite is cationic exchange. To verify that ion exchange plays a major role in the process, NaCl addition effect as ion exchanger competitor was studied [72]. Figure 5.6 shows the adsorption capacity of lincomycin on natural zeolite in the presence of three solutions at different NaCl concentrations. The initial concentration of lincomycin was 50 ppm (0.1 mM), and the temperature was 295 K.

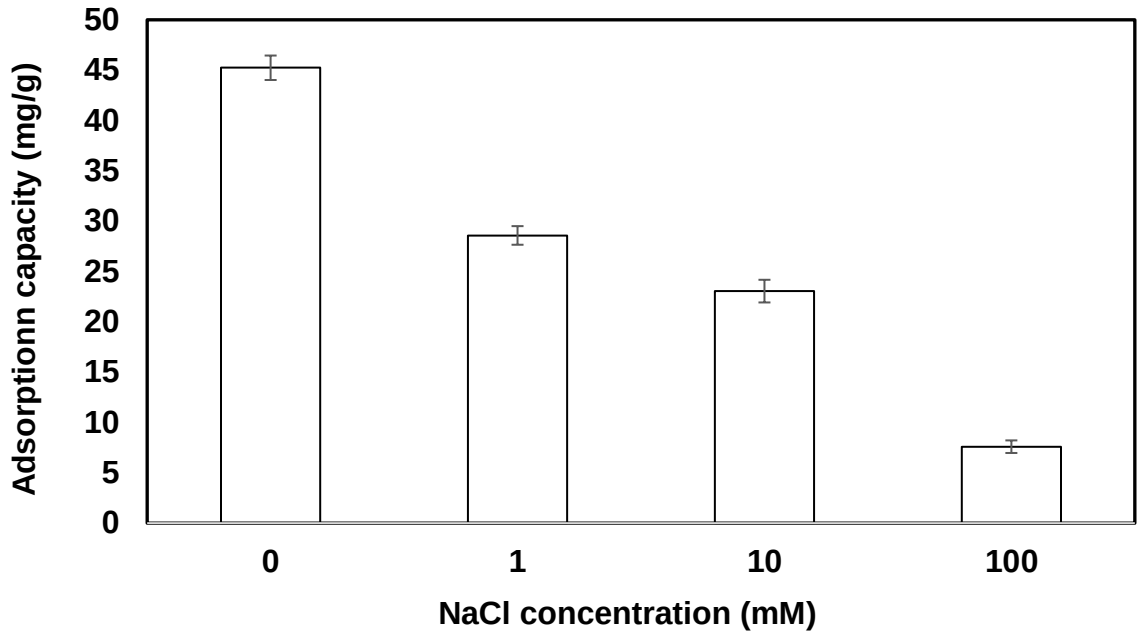

Figure 5.6. Adsorption capacity of lincomycin (Initial concentration 50 ppm) on natural zeolite in the presence of three different NaCl concentration solutions at 295 K in deionized water at initial pH 6.5

Figure 5.6 shows that the addition of NaCl causes a decrease in the adsorption of lincomycin on natural zeolite, reductions from 45.2 mg/g to 28.5, 23.5 and 7.5 mg/g for 1, 10 and 100 mM of NaCl, respectively were determined. Therefore, ion exchange is, probably, the main mechanism for adsorption of lincomycin on the natural zeolite. However, pH variation results, presented in section 6.2, can add significant information to confirm this theory.

One of the objectives of this research was applying the process to a complex matrix that could reproduce some characteristics of real liquid swine manure. The results of applying adsorption of lincomycin in synthetic manure are presented in Chapter 6. However, at this stage, it is possible to mention that one of the main components of manure is organic nitrogen in the form of ammonium [106]. Natural zeolite has been used commonly for the adsorption of this species by ionic exchange [37] and may compete with lincomycin for active sites.

Regarding the adsorption capacity of NZH, the objectives of acid treatment were, firstly, to increase the ratio Si/Al to improve the hydrophobic bonding of organic molecules to natural zeolite [17] and, secondly, to increase the surface area and micro porosity of NZ [59]. It can be calculated from data in

Table 4.4 that the ratio Si/Al rose from 6.12 in NZ to 8.46 in NZH; this variation improved the hydrophobic character of this material. However, acid treatment also removed cations from zeolite structure (

Table 4.4). As a consequence, the ion exchange properties of the material, probably, were affected [60].

On the other hand, zeolites porosity was modified by acid treatment. Thus, BET surface area increased from 47 m^2/g in NZ to 121 m^2/g in NZH, and micropore area was also increased from 8 m^2/g in NZ to 58 m^2/g in NZH as shown in Table 4.1. Activated carbons porosity characterization by nitrogen adsorption at 77 K. Kurama et al. [59] mention that the surface area increase was affected by the concentration of acid and experimental temperature due to the dissolution of alumina during the treatment. Also, Christidis, Moraetis, Keheyan, Akhalbedashvili, Kekelidze, Gevorkyan, Yeritsyan and Sargsyan [126] mention that the increase of surface and microporosity was due to the dissolution of free linkages and Si-tetrahedra, unblocking micropores.

Therefore, although acid treatment increased the surface area, microporosity, and hydrophobicity of natural zeolite, it also reduced the cation exchange capacity, producing a reduction in the adsorption capacity of lincomycin.

5.2 Thermodynamic characterization of adsorption of lincomycin on activated carbons and zeolites in deionized water.

Thermodynamic equilibrium constant for the adsorption of lincomycin on activated carbons and zeolites in deionized water was determined using the methodology proposed by Khan & Singh (1987) and corrected by Milonjić (2007) as explained in chapter two. Complete data and plots for determination of the equilibrium constant are shown in Appendix D. Gibbs free energy change was calculated using equation (2.5), and Van't Hoff plot was used for determining enthalpy and entropy changes using the slope and intercept of the best fit straight line, respectively. Complete fitting results are presented in Appendix E. Figure 5.7, and Figure 5.8 show Van't Hoff plots for different activated carbons and zeolites respectively.

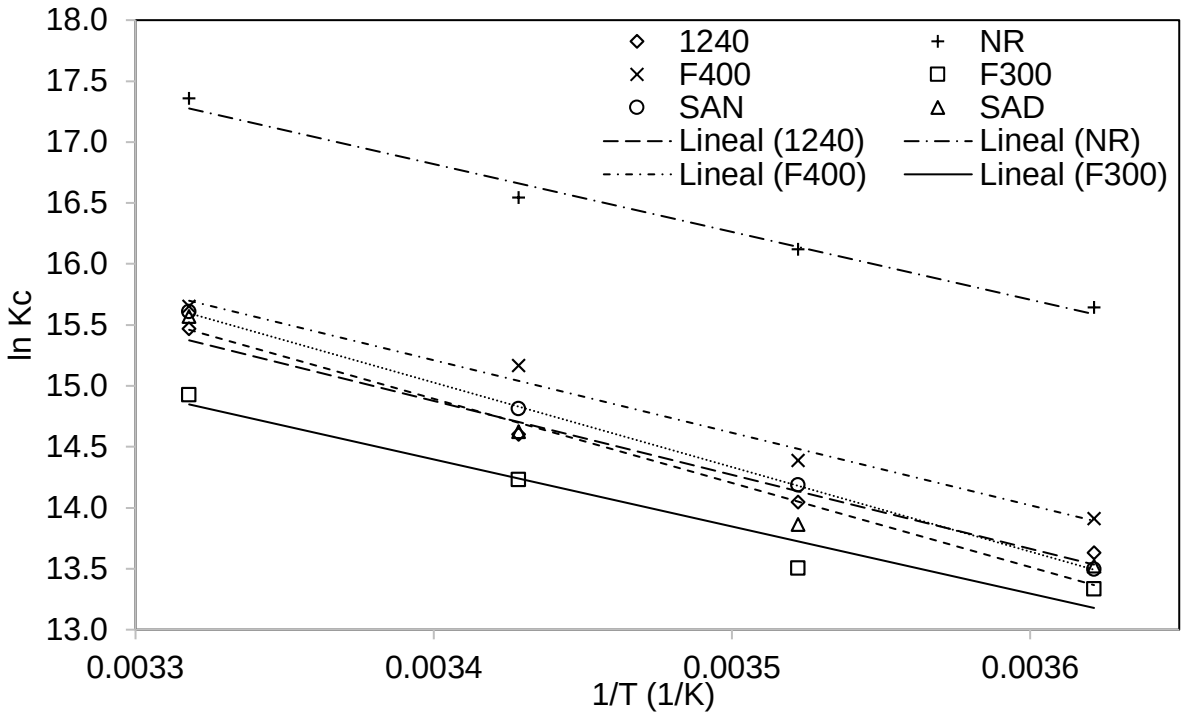

Figure 5.7. Van't Hoff plot for thermodynamic analysis of adsorption of lincomycin on activated carbons at 280-306 K in deionized water at initial pH 6.5

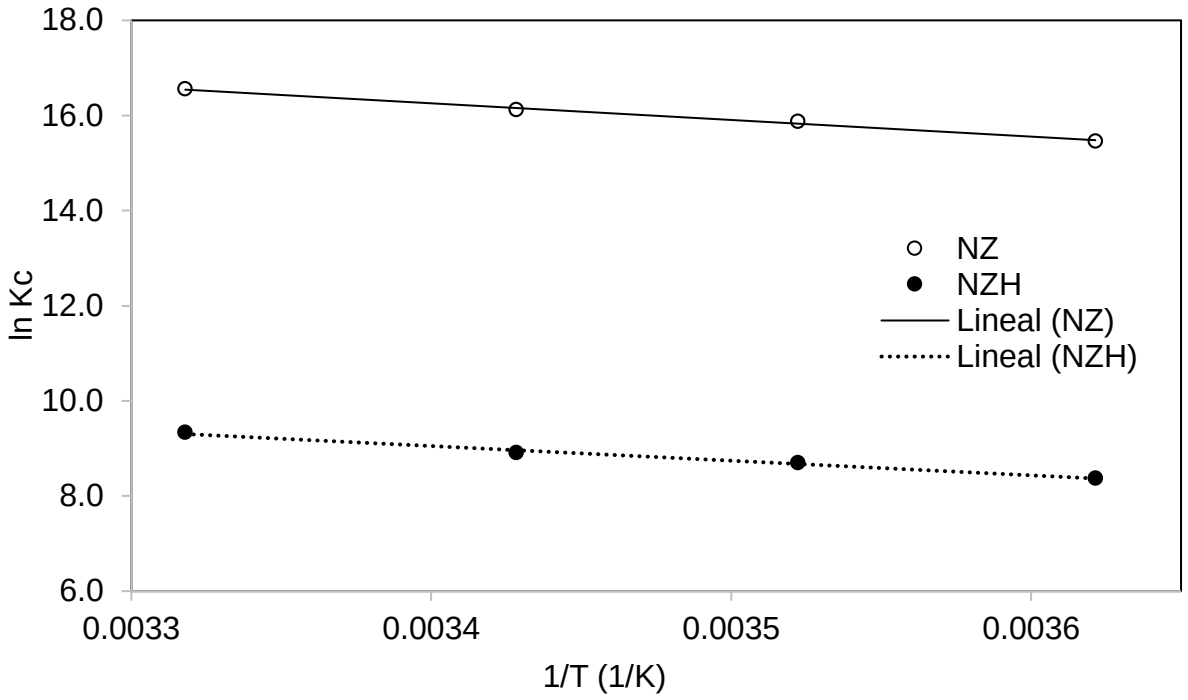

Figure 5.8. Van't Hoff plot for thermodynamic analysis of adsorption of lincomycin on zeolites at 280-306 K in deionized water at initial pH 6.5

The slope values, for each adsorbent, in Figure 5.7 and Figure 5.8 determine the enthalpy change of the process and, subsequently, provides clue about the range of the bonding strength [79]. Hence, from the figures analysis, it is possible to draw two preliminary conclusions. First, by comparison between different ACs and various zeolites, it can be noted that the slope value trend is similar for each group of adsorbents. Therefore, it is expected to obtain similar enthalpy change values for all the activated carbons, and the same behavior is expected for zeolites. Thus, it can be concluded that similar mechanisms control the adsorption process on each type of adsorbent. Second, it is possible to state that slope values for activated carbons are greater than the ones obtained for zeolites. Hence, the bonding strength for the adsorption of lincomycin on activated carbons is higher than the bonding strength on zeolites.

5.2.1 Thermodynamic characterization parameters on activated carbons at different temperatures (280, 288, 296 and 306 K) in deionized water

From the slope and intercept values shown in Figure 5.7, it was possible to determine the thermodynamic characteristic parameters for adsorption of lincomycin on activated carbons. Results of change in standard Gibbs free energy, enthalpy and entropy for each adsorbent are presented in Table 5.5.

Table 5.5. Thermodynamic parameters for the adsorption of lincomycin on activated carbons in deionized water at initial pH 6.5

Adsorbent	ΔG° (KJ/mol)				ΔH° (KJ/mol)	ΔS° (J/molK)
	280 K	288 K	296 K	306 K		
1240	-31.7	-33.6	-35.9	-39.4	50.4	293
NR	-36.4	-38.6	-40.7	-44.2	46.2	295
F400	-32.4	-34.5	-37.3	-39.8	49.5	292
F300	-31.0	-32.3	-35.0	-38.0	45.7	273
SAN	-31.4	-34.0	-36.4	-39.7	57.6	318
SAD	-31.5	-33.2	-36.0	-39.6	57.4	316

Gibbs free energy is related to the spontaneity of the process, and its value is negative for all the cases. Hence, the adsorption of lincomycin is spontaneous and thermodynamically favorable [77]. Besides, the absolute values of the Gibbs free energy change increase with increasing temperature, indicating more favorable conditions at higher temperatures, as shown in isotherms fitting results presented in Table 5.3. The enthalpy and entropy changes were positive, in consequence, the adsorption process is endothermic, and the entropy change showed increase of disorder in the system [84].

For activated carbons, adsorption enthalpy change values fall within the range between 46.2 KJ/mol for NR and 57.6 KJ/mol in the case of SAN, according to literature these values correspond to chemisorption [58,82,83] process. It has been assumed that adsorption process is by nature exothermic [85–87], it means that due to the bonding of adsorbed molecules on the adsorbent surface there is a subsequent energy release (e.g. condensation of gas molecules on the solid surface) [85]. However, this statement is only complete for physical adsorption, in the case of chemisorption, presented in this study, rupture and creation of chemical bonds take place, and some of these reactions can be of endothermic nature, providing an endothermic character to the complete process [85].

Adsorption in liquid phase involves a simultaneous process of water desorption from the surface, by breaking hydrogen bonding, and adsorption of lincomycin, through the mechanisms detailed in section 5.1. Therefore, the energy absorbed due to bond breaking must be greater than the energy released by the bond formation to obtain a global positive enthalpy change [84,85]. This phenomenon can be explained by the positive entropy change, detailed in Table 5.5, because in lincomycin adsorption, the adsorbate molecule must replace at least two molecules of water to justify the increase in the global degrees of freedom and subsequent entropy increase [84]. Hence, two (or more) hydrogen bonds, where water molecules were adsorbed, are broken and one bond, due to the lincomycin's adsorption, is created, this theory explains positive values of both the enthalpy and entropy changes. Endothermic adsorption on activated carbons has been widely reported in the recent years [86,89,90,127]. Pouretedal and Sadegh [127] justified their positive entropy change due to adsorption of organic molecules onto the surface of the solid implying that a chemical reaction is taking place and, hence, protonation or hydrogen bonding occurs.

Previously, in section 5.1, it was speculated that the mechanisms occurring on the carbon surface could be π - π interaction, hydrogen bonding and/or electron donor-acceptor systems. Thus, physisorption is characterized by weak dispersion forces like π- π interactions and chemisorption by the formation of hydrogen bonds and electron donor–acceptor complex systems [39]. Kim et al., [54] speculated that the adsorption of lincomycin on carbonaceous materials is controlled by H-bonding. However, no thermodynamic evidence was provided. As

mentioned in section 5.1, and from the thermodynamic evidence presented in section 5.2 it can be stated that the mechanism controlling the process is hydrogen bonding.

5.2.2 Thermodynamic characterization on zeolites at different temperatures (280, 288, 296 and 306 K) in deionized water

From the slope and intercept of Van't Hoff plot for zeolites, presented in Figure 5.8, the thermodynamic characteristic parameters were determined. Results for the thermodynamic parameters of the adsorption of lincomycin on zeolites are presented in Table 5.6.

Table 5.6. Thermodynamic parameters for the adsorption of lincomycin on natural and modified zeolite

Adsorbent	ΔG° (KJ/mol)				ΔH° (KJ/mol)	ΔS° (J/molK)
	280 K	288 K	296 K	306 K		
NZ	-22.6	-23.2	-23.8	-24.5	29.1	232
NZH	-21.0	-21.2	-22.4	-23.3	25.6	161

Adsorption on zeolites was spontaneous and thermodynamically favorable due to the Gibbs energy free change values [77], the enthalpy and entropy changes were positive. Subsequently, the adsorption process was endothermic, and system disorder was increased [72].

Adsorption enthalpy change values, shown in Table 5.6, were 29.1 KJ/mol for NZ and 25.6 for NZH. These values, according to literature, do not correspond to physical or chemical adsorption but other mechanisms such as ion exchange [79,83,128,129]. Several documents have reported endothermic ion exchange as the mechanism controlling the adsorption process on aluminosilicate materials [58]. Ötker and Akmehmet-Balcioğlu [58] studied the adsorption of enrofloxacin on natural zeolite and determined that adsorption was endothermic, they indicated that the process can be controlled by either ionic interactions or hydrogen bonding that present low enthalpy change values. Lin, Zhan, and Zhu [83] applied adsorption for the removal of

Cu(II) on surfactant modified zeolite. They reported that the endothermic ion exchange was caused due to the affinity of the charged surface and Cu(II) ions. Besides, the positive entropy variation was caused by increasing disorder at the solid/liquid interface. Otker [58] and Lin [83] presented thermodynamic results following the methodology used in this study. However, a different approach to confirm the existence of endothermic ion exchange was provided by Nowara, Burhenne and Spiteller [130]. They studied the thermodynamics of the adsorption of enrofloxacin on clays by microcalorimetric measured exchange enthalpies. They determined enthalpy change values between 19.5 KJ/mol and 42.2 KJ/mol on kaolinite, illite, vermiculite and montmorillonite. These values were attributed to a dipole or ionic binding interactions. In section 5.1.2, it was mentioned that ion exchange is the mechanism controlling the adsorption of lincomycin on zeolites. Due to the thermodynamic characterization and binding strength, it can be confirmed that that ion exchange is the main mechanism controlling the process.

5.3 Effect of the pH value and ionic strength on the adsorption capacity

5.3.1 Modeling of lincomycin adsorption on activated carbons at pH 10 at 306 K in deionized water

At initial pH 10, the isotherms obtained in the adsorption of lincomycin on activated carbons 1240, NR and F400 were fitted to Langmuir, Freundlich, and Sips models. Table 5.7 shows the fitting results obtained by non-linear regressions using Origin 2017 Pro software.

The complete set of adsorption isotherms of lincomycin on activated carbons at different temperatures is shown in Appendix B and the results obtained from fitting data to the selected models are listed in Table 5.7.

Table 5.7. Parameters for Langmuir, Freundlich, and Sips adsorption isotherms of lincomycin on activated carbons in deionized water at initial pH 10.0

Ads.	Temp. (K)	Freundlich			Langmuir			Sips			
		K_F*	n	R^2	q_{max}*	K_L*	R^2	K_S*	q_m*	n	R^2
1240	280	333.3	11.69	0.991	453.1	1.95	0.989	2.81	506.1	2.15	0.997
	288	345.0	11.47	0.993	466.5	2.63	0.987	3.28	541.1	2.51	0.998
	296	354.0	11.35	0.995	478.8	2.74	0.985	3.08	574.6	2.79	0.999
	306	370.3	12.18	0.993	485.2	4.69	0.983	5.27	577.2	2.92	0.998
NR	280	210.5	7.69	0.978	339.5	1.16	0.976	0.88	393.9	1.94	0.994
	288	227.3	8.32	0.978	348.3	1.74	0.971	1.24	409.7	2.14	0.992
	296	234.1	8.18	0.981	355.9	2.33	0.957	1.02	451.7	2.55	0.992
	306	248.9	8.63	0.983	367.8	3.02	0.962	1.48	456.4	2.56	0.995
F400	280	242.9	6.82	0.970	412.1	1.11	0.967	0.74	483.8	1.88	0.992
	288	263.5	6.96	0.977	435.2	1.48	0.967	0.86	522.6	2.05	0.997
	296	284.8	7.31	0.973	450.0	2.21	0.952	1.09	550.9	2.21	0.995
	306	310.9	8.00	0.974	465.6	3.74	0.958	1.98	554.6	2.26	0.997

* Units: K_F $(mg/g)(L/mg)^{1/n}$, q_{max} $(mg*g^{-1})$, K_L $(L*mg^{-1})$, K_S $(L*mg^{-1})$, q_m $(mg*g^{-1})$

It can be noted that, at pH 10.0, an increase in temperature enhanced the adsorption capacity. Therefore, the adsorption capacity was maximum at 306 K for 1240, NR and F400 activated carbons. Two factors (temperature and initial concentration) Analysis of Variance (ANOVA) with Least Significant Differences (LSD) multiple range tests (95% confidence), for means analysis, was carried out to study the effect of temperature on the lincomycin's uptake. It was determined that temperature is a statistically significant variable on the adsorption capacity based on the P-Value (less than 0.05) and the multiple range test. Complete results are presented in Appendix C.

Table 5.7 shows that fitting results, based on the determination coefficient (R^2) as comparison parameter, were in the order Sips>Freundlich>Langmuir. It was discussed, in section 5.1.1, that Langmuir model did not predict adsorption data correctly due to the heterogeneous distribution of adsorption sites on the AC surface [14,34]. Thus, even though Freundlich equation is a semi-empirical model, it provides good fitting results and has been widely used for modeling the adsorption of organic compounds on carbonaceous materials with heterogeneous surfaces [51,63,131]. Although fitting results were improved, Sips or so-called Langmuir-Freundlich model was applied and showed the best results with determination coefficients greater than 0.992 for all the activated carbons [63,64].

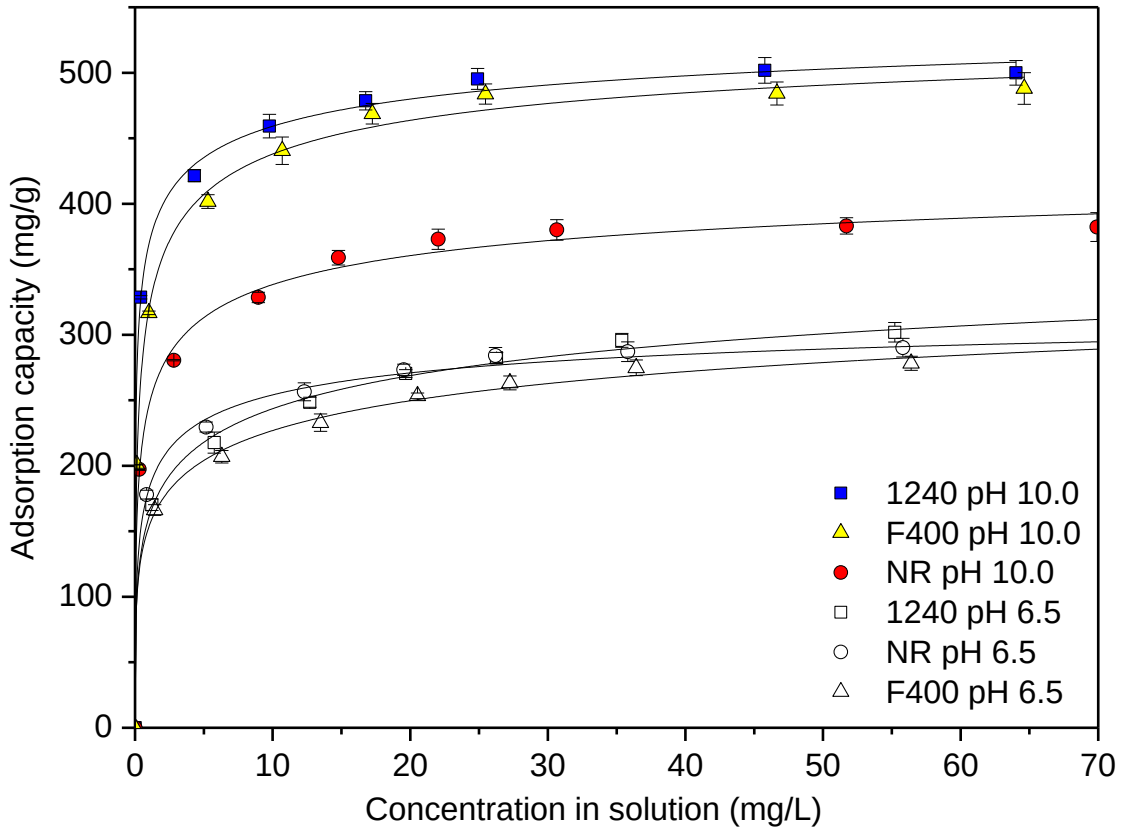

Figure 5.9. Adsorption isotherms, at pH 6.5 and pH 10.0 in deionized water, and Sips model fitting for adsorption of lincomycin on activated carbons at 306 K

Adsorption capacity was maximum at 306 K. At this temperature, Sips model predicted uptakes of 577.2 mg/L, 554.6 mg/L and 456.4 mg/L for 1240, F400 and NR respectively. These values are higher than the ones obtained at pH 6.5. In this case adsorption capacities, predicted by Sips model, were 458.0 mg/L, 444.5 mg/L and 338.2 mg/L for 1240, F400 and NR respectively. Therefore, pH plays a major role in the adsorption process. Figure 5.9 shows the adsorption isotherms, at pH 6.5 and pH 10.0, and Sips model fitting, for adsorption of lincomycin at 306 K.

As mentioned in section 5.1.1, at pH 6.5 both activated carbon surface and lincomycin were positively charged, producing repulsive electrostatic interactions [39]. Bautista-Toledo, Ferro-García, Rivera-Utrilla, Moreno-Castilla, and Fernández, [40] studied the removal of bisphenol A on activated carbon. They determined that, at pH values above the pKa, both activated carbon and bisphenol-A were negatively charged and electrostatic repulsions took place decreasing the adsorption capacity as the pH increases.

At pH 10.0, lincomycin with a pka of 7.8 [28], was only present in its neutral form [62]. Hence, electrostatic interactions should be negligible [40]. Therefore, non-electrostatic interactions must control the process [39]. Rivera-Utrilla, Prados-Joya, Sánchez-Polo, Ferro-García and Bautista-Toledo [42] studied the adsorption of nitroimidazole antibiotics by adsorption on activated carbon. They found that the adsorption capacity was not affected at pH values above the pKa of nitroimidazoles when the adsorbate was in its neutral form. Therefore, they concluded that electrostatic interactions do not affect the adsorption capacity. However, at pH values below the pKa, the adsorption capacity was reduced due to electrostatic repulsion.

In section 5.1.1, hydrogen bonding was determined as the main mechanism controlling the adsorption of lincomycin on activated carbons. Therefore, the presence of oxygen groups on the carbon surface is necessary to promote the formation of these bonds [62]. At pH 10, the electrostatic repulsion taking place at pH 6.5 was avoided [51]. As a consequence, the formation of hydrogen bonds was favored and, subsequently, the adsorption capacity increased as shown in Figure 5.9.

To study the influence of the electrostatic interactions in the adsorption of lincomycin on activated carbons, the effect of the ionic strength of the solution was studied. Thus, NaCl, with

different concentrations, was added to 50 ppm lincomycin solutions with 50 mg/L of activated carbons 1240, NR and F400 at pH 6.5 and pH 10.0. The obtained adsorption capacities are shown in Figure 5.10.

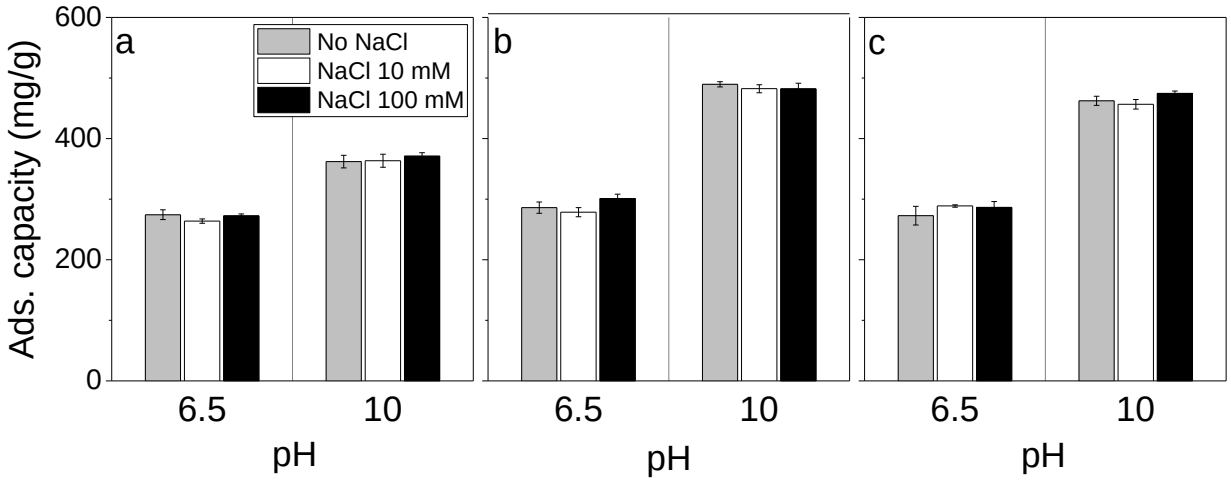

Figure 5.10. Adsorption capacity of lincomycin on activated carbons in the presence of NaCl 10 mM and 100 mM in deionized water at initial pH values of 6.5 and 10.0
a) 1240 b) NR c) F400

It can be noted, in Figure 5.10, that the addition of NaCl did not affect the adsorption capacity at the two pH levels. Thus, the presence of ionic species in the solution did not change the adsorption capacity of the three different activated carbons used in this stage of research.

The results obtained confirm that the mechanisms controlling the adsorption process are not of electrostatic nature [42]. Similar observations were made by Liu and colleagues [62], who studied the adsorption of lincomycin on biochars and determined that, at acid pH values, electrostatic interactions played a major role in the process with significant reductions in the adsorption capacity when NaCl was added. However, at pH 10, above the pKa, these interactions were negligible, and no significant changes in the adsorption capacity were observed due to the absence of charged lincomycin molecules.

Moreover, the addition of NaCl increased the adsorption capacity slightly for F400 activated carbon at pH 6.5. This behavior may be explained by the so-called screening effect

[40]. It occurs when NaCl molecules bind to the carbon surface reducing its net charge and decreasing the electrostatic repulsions. As a consequence, the adsorption capacity of the material was increased under the experimental conditions [40].

In conclusion, at pH 10, electrostatic interactions did not contribute to the adsorption capacity. However, at pH 6.5, electrostatic repulsion took place in the adsorption on activated carbons. Thus, pH of the solution determines the fraction of positively charged lincomycin and, subsequently, affects the adsorption capacity directly due to electrostatic interactions. In contrast, the presence of NaCl did not affect the adsorption capacity because the mechanisms controlling the adsorption process are not of electrostatic nature.

5.3.2 Modeling of lincomycin adsorption on natural zeolite and modified natural zeolite at pH value of 10.0 at 306 K in deionized water

The adsorption of lincomycin on natural zeolite at pH 10.0 was studied. The adsorption capacity at this pH value, at different temperatures ranging from 280 K and 306 K, was negligible because the mechanism controlling the adsorption on zeolites, as determined in section 5.1.2, is a cationic exchange. Therefore, as shown in Figure 1.2, at pH 10 lincomycin cationic species are not present [34] and, subsequently, the ion exchange did not occur.

This behavior was also reported by Wang and colleagues [34] that studied the adsorption of lincomycin on smectite clays and determined that the main mechanism was cationic exchange. They studied the effect of varying the pH values and confirmed that the adsorption capacity decreased at pH values greater than 7.0. They proposed that the adsorption variation is directly related to the reduction of cationic lincomycin available in the solution at values near the pKa.

Regarding the adsorbate charge and its influence on the adsorption on natural zeolite, Li et al. [57] studied the uptake of sulfadiazine sulfonamide on clinoptilolite. Sulfadiazine sulfonamide has three ionic forms, so cation, zwitterion, and anion species were present in solution depending on the pH value. They established that the adsorption capacity on clinoptilolite was minimum when working with the zwitterion form of the target compound because the electrostatic interactions were weak, and the cationic exchange did not occur.

5.3.3 Thermodynamic characterization of adsorption of lincomycin on activated carbons and zeolites in deionized water at pH 10

Thermodynamic characterization, at this stage, was conducted only for activated carbons using the same methodology discussed in section 2.6. Figure 5.11 shows the Van't Hoff plot for different activated carbons at pH 6.5 and pH 10.0.

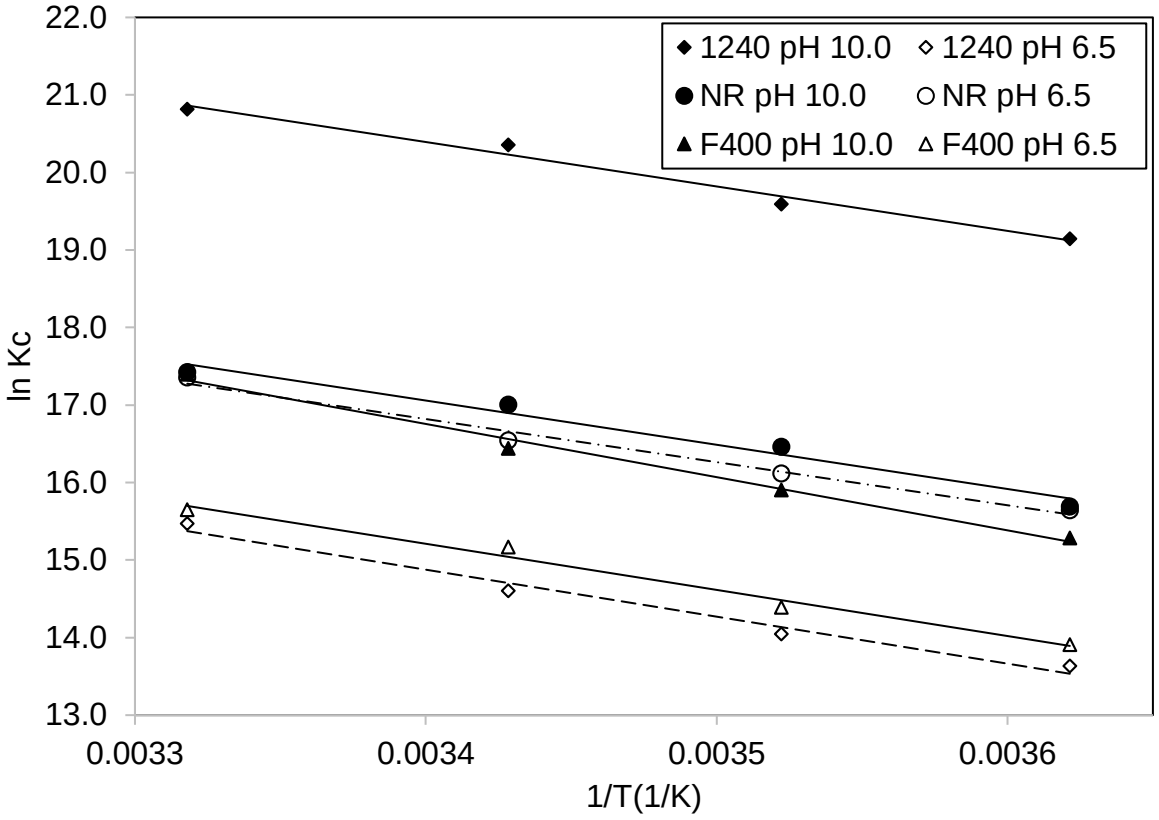

Figure 5.11. Van't Hoff plot for thermodynamic analysis of adsorption of lincomycin on activated carbons at 280-306 K in deionized water at initial pH 10.0

The slope of the lines, in Figure 5.11, determines the enthalpy change of the process for each adsorbent and, subsequently, provides an idea of the bonding strength [79]. It can be noted that the slopes for 1240, NR, and F400 obtained at pH 10 are similar to the ones obtained at pH

6.5. Consequently, the strength of bonding was not affected by the pH variation even when the adsorption capacity was increased as shown in Section 5.3.1. In consequence, similar mechanisms seem to be controlling the adsorption process at the different pH values.

From the slopes and intercept values determined in Figure 5.11, it was possible to calculate the thermodynamic characteristic parameters for adsorption of lincomycin on activated carbons at pH 10.0.

Table 5.8. Thermodynamic parameters for the adsorption of lincomycin on activated carbons in deionized water at pH 6.5 and pH 10.0

Adsorbent	**pH**	**ΔG° (KJ/mol)**				**ΔH° (KJ/mol)**	**ΔS° (J/molK)**
		280 K	**288 K**	**296 K**	**306 K**		
1240	**6.5**	-31.7	-33.6	-35.9	-39.4	50.4	293
	10.0	-44.6	-46.9	-50.1	-53.0	47.7	329
NR	**6.5**	-36.4	-38.6	-40.7	-44.2	46.2	295
	10.0	-36.5	-39.4	-41.9	-44.3	47.4	301
F400	**6.5**	-32.4	-34.5	-37.3	-39.8	49.5	292
	10.0	-35.6	-38.1	-40.5	-44.3	57.1	330

Thermodynamic characterization results for both pH tested levels are shown in Table 5.8. The negative free Gibbs energy changes, with values ranging from -35.6 to -53.0 KJ/mol, suggestthat the adsorption of lincomycin is spontaneous and thermodynamically favorable [77]. Besides, at pH 10.0, the endothermic character found at pH 6.5, is almost constant based on the enthalpy change values that fall within the range between 47.4 KJ/mol for NR and 57.1 KJ/mol for F400. From these values, it is also possible to conclude that chemisorption is also controlling the process at a pH value above the pKa [58,82,83].

Besides, Table 5.8 shows that the entropy changes at pH 10.0 are greater than at pH 6.5 for the three selected adsorbents. Thus, at pH 6.5 entropy change values range from 292 to 295 J/mol*K, and, at pH 10.0 values fall within 301 and 330 J/mol*K. This behavior can be explained because as stated in section 5.2.1, the adsorption of lincomycin on activated carbons is entropy-driven. It means that the release of water molecules from the surface and attachment of lincomycin by hydrogen bonding produces a positive entropy change [84]. It is believed that at pH 10, the number of water molecules that are replaced by lincomycin molecules is increased, with a subsequent increase in the entropy change values [132], from pH 6.5 to pH 10, as shown in Table 5.8.

CHAPTER 6
ADSORPTION OF LINCOMYCIN ON ACTIVATED CARBON IN SYNTHETIC AND REAL LIQUID SWINE MANURE

The final objective of this research was to study the behavior of the best performing adsorbents in the adsorption of lincomycin from a synthetic formulation of swine manure and real liquid swine manure.

The first section of this chapter presents the results obtained from the adsorption of lincomycin on activated carbons and zeolites in synthetic liquid swine manure at 280, 288, 296 and 306 K. The composition used for the preparation of the synthetic manure is presented in Chapter 3. The obtained data was fitted to isotherms models such as Langmuir, Freundlich, and Sips by non-linear regressions.

The second part of this chapter presents the adsorption of lincomycin from real liquid swine manure obtained from Prairie Swine Centre. In this case adsorption experiments were carried using manure fortified with lincomycin (90 ppm). Adsorption isotherms at room temperature were constructed, and data was simulated by the SEBCM presented in section 2.5.3.

6.1 Adsorption of lincomycin from synthetic liquid swine manure

Isotherms obtained in the adsorption of lincomycin, from synthetic manure, on activated carbons 1240, NR and F400 were fitted to Langmuir, Freundlich, and Sips models. Table 6.1 shows the fitting results obtained by non-linear regressions using Origin 2017 Pro software through Levenberg–Marquardt algorithm method.

Table 6.1. Parameters for Langmuir, Freundlich, and Sips adsorption isotherms of lincomycin in synthetic manure on activated carbons at different temperatures

Ads.	Temp. (K)	Freundlich			Langmuir			Sips			
		K_F*	n	R^2	q_{max}*	K_L*	R^2	K_S*	q_m*	n	R^2
1240	280	185.4	4.76	0.971	423.7	0.36	0.989	0.29	470.2	1.39	0.994
	288	206.5	4.95	0.961	424.2	0.41	0.990	0.36	481.8	1.24	0.992
	296	241.3	5.56	0.960	470.1	0.67	0.989	0.57	506.7	1.35	0.994
	306	267.2	5.99	0.940	493.1	0.82	0.983	0.76	510.6	1.19	0.982
NR	280	160.1	6.54	0.990	288.8	0.62	0.984	0.40	353.5	2.02	0.999
	288	182.2	7.09	0.991	308.6	0.87	0.980	0.52	384.9	2.22	0.999
	296	199.3	7.41	0.986	324.7	1.18	0.979	0.78	389.7	2.09	0.999
	306	226.1	8.29	0.996	336.4	3.59	0.952	0.25	544.6	3.87	0.999
F400	280	170.4	4.27	0.979	438.7	0.26	0.976	0.14	552.7	1.70	0.993
	288	184.9	4.40	0.978	458.7	0.29	0.977	0.16	567.8	1.70	0.994
	296	211.4	4.89	0.983	459.6	0.45	0.962	0.17	622.1	2.10	0.996
	306	228.6	5.00	0.981	483.3	0.52	0.970	0.24	621.4	1.92	0.997

* Units: K_F $(mg/g)(L/mg)^{1/n}$, q_{max} $(mg*g^{-1})$, K_L $(L*mg^{-1})$, K_S $(L*mg^{-1})$, q_m $(mg*g^{-1})$

The complete set of adsorption isotherms of lincomycin on activated carbons at different temperatures is shown in Appendix B and the results obtained from fitting data to the selected two parameters models are listed in Table 6.1.

Table 6.1 shows the modeling results. Based on the determination coefficient (R^2), the order of quality of fit is: Sips>Freundlich>Langmuir. This is similar to the results obtained at pH 6.5 and pH 10 in deionized water. Thus, Sips model provided determination coefficients greater than 0.982 for all the activated carbons. Figure 6.1 shows the adsorption isotherms and Sips

model fitting, for adsorption of lincomycin in synthetic manure on selected activated carbons at 306 K.

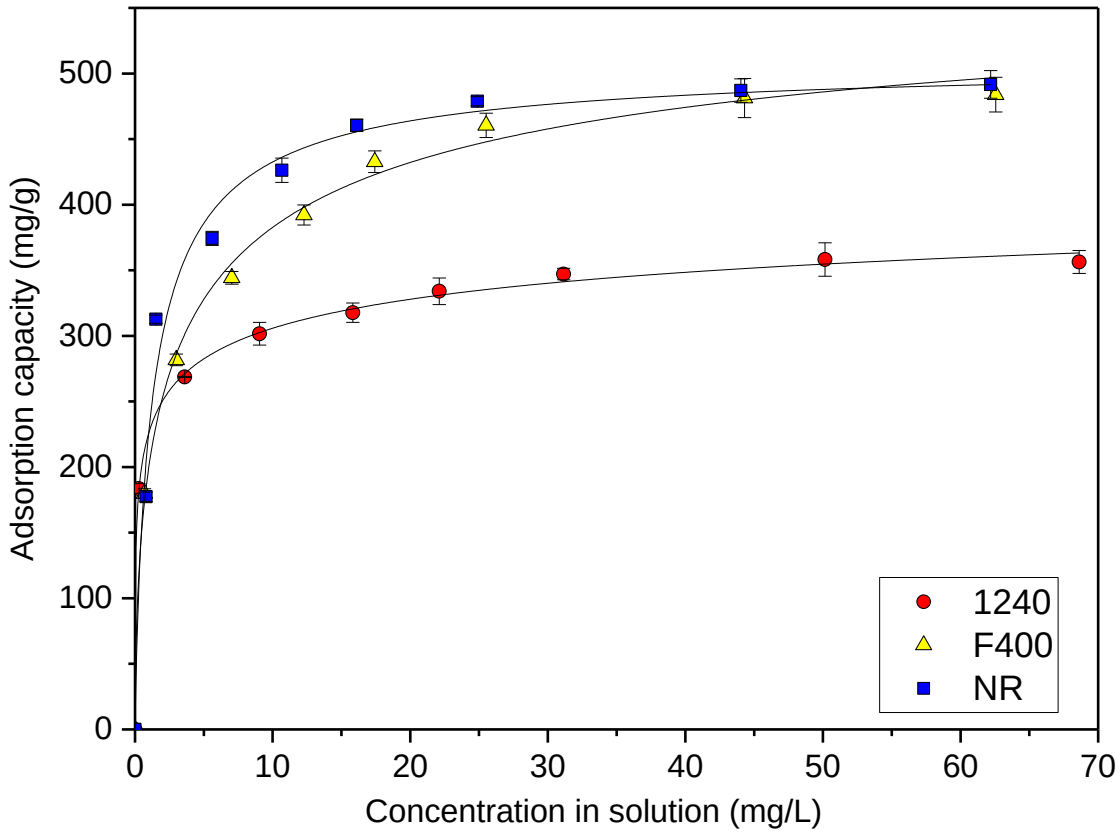

Figure 6.1. Adsorption isotherms and Sips model fitting for adsorption of lincomycin, in synthetic manure, on activated carbons and zeolites at 306 K

The temperature increase affected positively the uptake of lincomycin. Thus, the adsorption capacity was maximum, in all the cases, at 306 K. At this temperature, the adsorption capacity corresponded to 493.1 mg/L for 1240, 336.4 mg/L for NR and 483.3 mg/L for F400 based on Langmuir model. These values were comparable to the ones obtained in deionized water at pH 10 (485.2 mg/L for 1240, 367.8 mg/L for NR and 465.6 mg/L for F400) and higher than the values obtained at pH 6.5 (295.8 mg/L for 1240, 283.5 mg/L for NR and 275.3 mg/L for F400).

The addition of the components of synthetic manure did not affect the adsorption capacity of activated carbons significantly, in comparison with the capacities obtained in

deionized water. This can be explained by the low affinity of activated carbon to the selected synthetic manure components and the experimental pH value.

First, the pH of synthetic manure is around 8.4. This value is higher than the lincomycin pKa [9] and, therefore, electrostatic repulsions are not affecting the adsorption process. Besides, at this pH value, the activated carbons are near their points of zero charge and, subsequently, are weakly positively charged. Therefore, weak electrostatic interactions take place [39].

Second, the other components of synthetic manure are not competing with lincomycin for the adsorption sites. For example, one of the main compounds in real manure is organic nitrogen, especially found as ammonia [106]. Long et al. [133] studied the adsorption of ammonia in aqueous solutions on activated carbon (Surface area=1050 m^2/g and PZC=9.2) and determined an adsorption capacity of 17.2 mg/g using Langmuir model. Besides, it was determined that the process was carried out by physical bonding. The activated carbon used by Long and colleagues is similar to the activated carbons used in this study based surface characteristics and surface area. Therefore, it would be expected that the adsorption capacities of ammonia on the selected activated carbons in this study are similar to the ones reported by Long and colleagues. Consequently, as shown in the experimental results, the adsorption of organic nitrogen by physisorption do not interfere with the chemical adsorption of lincomycin on the selected activated carbons.

Other components in the synthetic manure matrix such as phosphates, sulfates, and acetates may affect the adsorption capacity. However, the adsorption of these compounds from aqueous matrices is carried out by electrostatic interactions and ion exchange [134]. Therefore, biosorption [135] and adsorption on metal oxides [136–140] and clays [141] have been applied for their removal. On the other hand, activated carbons have been only effective when surface treatments that improve the material electrostatic characteristics, are applied [142]. For non-treated activated carbons, like the ones used in this study, the mechanisms controlling the process are mainly non-electrostatic, related to the bonding between oxygen groups on the surface of the material and functional groups in the molecule structure [39]. Due to the absence of molecules competing with lincomycin for the active sites, the adsorption capacity, as shown in the results, was not affected.

6.2 Adsorption of lincomycin from real liquid swine manure

The real liquid manure sample obtained from Prairie Swine Centre was characterized, Table 6.2 shows the results obtained for relevant parameters.

Table 6.2. Liquid swine manure characterization results

Parameter	Value	Units
Dissolved organic carbon (DOC)	4056	mg/L
Chemical oxygen demand (COD)	8160	mg O_2/L
Total solids (TS)	13957	mg/L
Dissolved solids (DS)	9760	mg/L
pH	7.83	-

Although the effect of the presence of the main components of swine manure was studied in Section 6.1, the real liquid manure contains other organic compounds that, potentially, can compete with lincomycin in the adsorption on activated carbon [143].

Table 6.2 shows the liquid manure characterization results. Due to the complex composition of real manure, the DOC and COD concentrations are much higher than the values found in wastewater treatment plant effluents [75], groundwater [144], river water [145], lake water [146], and other similar matrices [69,121,147]. Moreover, the high concentration of solids may decrease the adsorption capacity by pore blocking [75]. The pH of manure was neutral, and its value was near the lincomycin pKa value [9]. Therefore, electrostatic interactions are negligible in the system [9].

To quantify the removal of lincomycin from a competitive system such as real manure, the activated carbon dose was increased at this stage of research. Therefore, Table 6.3 shows the results obtained for the adsorption of lincomycin, from real liquid swine manure, carried out at

different concentrations of activated carbon in preconditioned swine manure (deposited and centrifuged at 3000 rpm for 15 min).

Table 6.3. Final concentration (ppm) and removal of lincomycin (%) from real manure solution at different activated carbon concentrations

	Activated carbon dose (g/L)							
	1	**2.5**	**5**	**10**	**1**	**2.5**	**5**	**10**
Adsorbent	**Final concentration (ppm)**				**Removal (%)***			
1240	30.1	**	**	**	66.7	**	**	**
NR	39.2	6.8	**	**	56.5	92.4	**	**
F400	55.3	**	**	**	38.5	**	**	**

*Lincomycin initial concentration was 90 ppm
**Below the detection limit

Table 6.3 shows the final concentration of lincomycin in real manure solution at different concentrations of various activated carbons. It can be noted that doses greater than 5 g/L removed the target compound to concentrations below the detection limit of HPLC analysis. Besides, activated carbon 1240 exhibited the best results removing the lincomycin completely with doses greater than 2.5 g/L. From the results obtained in this stage, two activated carbons such as 1240 and F400 were selected for constructing the adsorption isotherms at room temperature (296 K) of lincomycin in real manure. Obtained isotherms and linear fitting are shown in

Figure 6.2.

For 1240 and F400 activated carbons, the adsorption capacity decreased significantly from the values obtained in deionized water in the pure component adsorption system. This behavior can be attributed to the presence of dissolved solids (DS) and natural organic matter (NOM) in the real liquid swine manure [37]. It is known that the presence of NOM, represented as the dissolved organic carbon (DOC), in wastewater reduces the number of available

adsorption sites for micropollutants, such as lincomycin, by competition for adsorption sites [75]. Besides, the high concentration of DS can decrease the adsorption capacity by pore blocking [75].

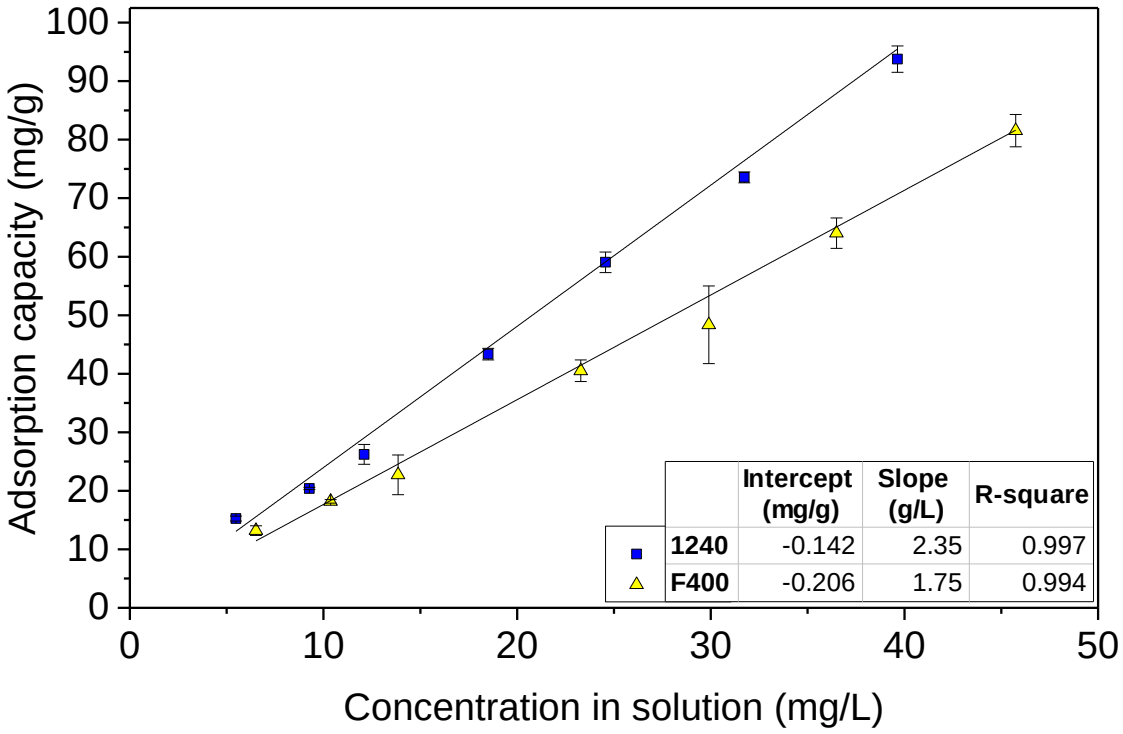

Figure 6.2. Adsorption isotherms for the adsorption of lincomycin from real liquid manure on activated carbons at 296 K
(Box: Linear regression fitting parameters and determination coefficient)

The adsorption isotherms shape varied significantly from the isotherms observed in deionized water. In pure component systems, the uptake of lincomycin usually has a maximum adsorption capacity. However, in real manure in the same range of lincomycin concentrations (5-90 ppm), the adsorption isotherms are linear. It means that, at constant activated carbon dose, an increase in the lincomycin concentration in liquid phase produces a linear increase in the uptake of lincomycin [65]. This behavior has been reported for the adsorption of micro-pollutants from slurry water matrices with high NOM concentration [37,75,76]. In the present study, the concentration of DOC (4056 mg/L) is 40 times greater than the maximum concentration of lincomycin (100 ppm).

As explained in section 2.5.3, the adsorption of lincomycin from real manure on activated carbons is a multicomponent adsorption system where NOM competes with lincomycin for active adsorption sites. Besides, due to the high concentration of DOC, the adsorption isotherms of lincomycin follow the behavior of the linear isotherm. As a consequence, the adsorption capacity of lincomycin does not depend on the initial micro pollutant concentration [76]. Therefore, the SEBCM, presented in section 2.5.3, was applied for simulating the adsorption of lincomycin in real manure [69]. The adsorption isotherms and SEBCM fitting for adsorption of lincomycin in real manure for different activated carbon doses are presented in Figure 6.3.

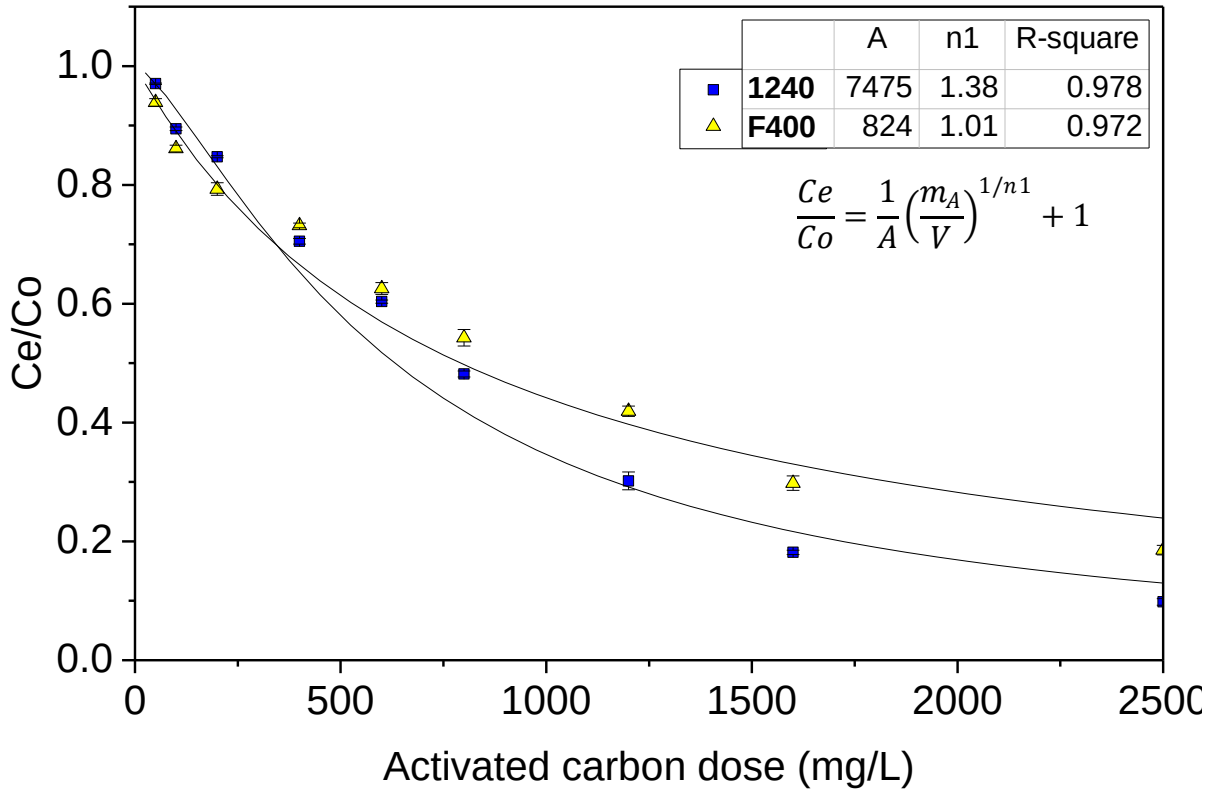

Figure 6.3. Adsorption isotherms and SEBCM fitting at 296 K for the adsorption of lincomycin from real liquid manure at different activated carbons doses
(Box: EBMC adsorption model characteristic parameters and determination coefficient)

Figure 6.3 shows the adsorption isotherms and SEBCM fitting for the adsorption of lincomycin from real liquid manure. This model predicts the adsorption capacity of a micro-

pollutant based on the activated carbon dose [69]. The application of the SEBCM has been carried out for wastewater treatment plant effluents [75], groundwater [144], river water [145], lake water [146], and other similar matrices [69,121,147]. In these studies, the micro-pollutant concentration is in the range from 50 to 200 μg/L, and the concentration of DOC is around 5 mg/L. Thus, the ratio between the concentration of DOC and the micro-pollutant is in the range from 25 to 100. In this research, the ratio between the concentration of DOC and lincomycin is around 45 (COD = 4056 mg/L, lincomycin = 90 ppm). Hence, the application of SEBCM is suitable for this system, as shown in the determination coefficient of the isotherm fitting.

To compare the efficiency of each activated carbon, two removal zones are identified in Figure 6.3. On the one hand, for removal values, less than 30% (C/Co = 0.70), activated carbon F400 was more efficient. On the contrary, for removal values greater than 30%, activated carbon 1240 provided higher adsorption capacity using the same adsorbent dose. Both 1240 and F400 activated carbons are materials with basic point of zero charge (PZC_{1240} = 10.3, PZC_{F400} = 9.4). As a consequence, their surface properties, such as oxygen content and concentration of surface functional groups, are similar [39]. Therefore, the difference in the adsorption capacity can be attributed to the higher micropore area that activated carbon 1240 presents. For example, Kim et al., [54] that investigated the influence of surface area in the adsorption of lincomycin on carbon nanotubes determined a positive linear correlation (R^2=0.98) between the Freundlich constant and surface area. In this study, activated carbon 1240 provided the highest adsorption capacity removing lincomycin from both, deionized water and real swine manure.

CHAPTER 7
GENERAL CONCLUSIONS AND RECOMMENDATIONS FOR FUTURE WORKS

In the present study, the effectiveness of adsorption technology for removal of lincomycin using activated carbons and natural zeolite was investigated. The effect of parameters such as temperature, pH and ionic strength on the adsorption capacity was analyzed. Finally, the efficiency of the process applied to synthetic and real manure matrices was evaluated.

General Conclusions

The adsorption equilibrium data of lincomycin on activated carbons and natural zeolites was modeled using established two-parameter isotherm models such as Langmuir and Freundlich models and a three parameter model such as Sips model. Sips model provided a better fit for adsorption data. It was concluded that activated carbons with a high point of zero charge provided higher adsorption capacity. Besides, the uptake of lincomycin was enhanced by increasing the activated carbon micropore area.

The effect of the temperature on the adsorption capacity was studied through the thermodynamic characterization. Parameters such as Gibbs free energy, enthalpy, and entropy changes were determined through the partition coefficient method. It was concluded that the adsorption process was endothermic and spontaneous. Hence, higher temperatures improved the adsorption capacity.

The effect of pH and ionic strength on the adsorption capacity was studied. It was concluded that solution pH values higher than the lincomycin's pKa improved the adsorption capacity on activated carbons. On the other hand, pH values below the pKa were beneficial for the adsorption on the natural zeolite. At pH 6.5, the best results obtained in this research provided adsorption capacities of 296 mg/g for activated carbons and 50 mg/g for natural zeolite. Adsorption on activated carbon was, probably, controlled by hydrogen bonding between hydroxyl groups in lincomycin's structure and oxygen groups on the carbon. Besides, acid treatment of natural zeolite removed cations and the adsorption capacity was significantly decreased. At pH 10.0, the adsorption capacity was 485 mg/g for 1240 activated carbon, and negligible adsorption was observed for natural zeolite. Also, the presence of NaCl did not affect the adsorption capacity on activated carbons because the mechanisms controlling the adsorption process were not of electrostatic nature. On the other hand, for natural zeolite, adding NaCl decreased the adsorption capacity because the cationic exchange between positively charged lincomycin and cations on zeolite surface was affected.

The efficiency of the process in the adsorption of lincomycin from synthetic manure was evaluated. The adsorption capacity corresponded to 493.1 mg/L for 1240, 336.4 mg/L for NR and 483.3 mg/L for F400 based on Langmuir model at 306 K. These values were similar to the ones found at pH 10 in deionized water but greater than the ones determined at pH 6.5. It was concluded that the synthetic manure pH value, greater than the lincomycin pKa, produced the unaltered adsorption capacity because electrostatic repulsions did not take place.

For real manure, the adsorption capacity decreased significantly from the values obtained in deionized water in the pure component adsorption system. It was concluded that the presence of dissolved solids (DS) and natural organic matter (NOM) in the real liquid swine manure affected the adsorption capacity. Therefore, different doses of activated carbon between 50 mg/L and 2500 mg/L were tested and the simplified equivalent background component model (SEBCM) was used for simulating the adsorption process. The application of this model allowed the prediction of the adsorption capacity of a micro-pollutant based on the activated carbon dose.

From the reviewed published literature, the present research constitutes the first study that applies adsorption technology for the removal of lincomycin from real liquid swine manure.

The application of adsorption technology is a feasible alternative for the removal of lincomycin from swine manure.

Recommendations for future works

The results obtained in the present study opens opportunities for additional research related to the application of adsorption technology for removing antibiotics from real manure. The following recommendations can be mentioned.

Alternative adsorbents should be used. Even though activated carbons provided good adsorption capacity, materials such as biochar or bio sorbents are cheaper and can be synthesized from organic residues. Besides, the selective adsorption of antibiotics could be carried out identifying specific functional groups in the selected adsorbate.

A pre-treatment for the removal of solids present in real manure should be designed. The presence of solids in the real liquid swine manure can cause pore blocking and reduce the number of available adsorption sites.

The range of micro-pollutant concentration should be adjusted to real conditions. The range of concentration of antibiotic used in this study was in the order of mg/L. However, in swine manure, the concentration of antibiotics falls in the range of µg/L. The use of mass spectrometry coupled to liquid chromatography would allow the quantification of antibiotics in this range of concentrations.

To completely characterize the adsorption of antibiotics on activated carbons, it is necessary to evaluate the kinetics of the process. The adsorption rate added to the equilibrium information can be used for designing continuous adsorption systems. Besides, desorption studies should be carried out to clarify the adsorption mechanisms. Finally, the breakthrough curves of the process should be constructed to analyze the adsorbent saturation applied in real matrices.

The application of other multicomponent adsorption models in the removal of antibiotics from real matrices should be carried out. Mathematical models such as EBCM and the tracer model (TRM) will allow the complete understanding of the process in complex matrices like real manure.

REFERENCES

[1] R. Rosal, A. Rodriguez, J.A. Perdigon-Melon, A. Petre, E. Garcia-Calvo, M.J. Gomez, A. Aguera, A.R. Fernandez-Alba, Occurrence of emerging pollutants in urban wastewater and their removal through biological treatment followed by ozonation, Water Res. 44 (2010) 578–588. doi:10.1016/j.watres.2009.07.004.

[2] N. Vieno, T. Tuhkanen, L. Kronberg, Removal of pharmaceuticals in drinking water treatment: effect of chemical coagulation., Environ. Technol. 27 (2006) 183–192. doi:10.1080/09593332708618632.

[3] K. Kumar, S. C. Gupta, Y. Chander, A.K. Singh, Antibiotic Use in Agriculture and Its Impact on the Terrestrial Environment, Adv. Agron. 87 (2005) 1–54. doi:10.1016/S0065-2113(05)87001-4.

[4] L. Du, W. Liu, Occurrence, fate, and ecotoxicity of antibiotics in agro-ecosystems. A review, Agron. Sustain. Dev. 32 (2012) 309–327. doi:10.1007/s13593-011-0062-9.

[5] P.H.A. of Canada, Canadian Antimicrobial Resistance Surveillance System Report 2016, 2016. http://healthycanadians.gc.ca/publications/drugs-products-medicaments-produits/antibiotic-resistance-antibiotique/antimicrobial-surveillance-antimicrobioresistance-eng.php#a3-3.

[6] S.L. Kuchta, A.J. Cessna, Lincomycin and spectinomycin concentrations in liquid swine manure and their persistence during simulated manure storage, Arch. Environ. Contam. Toxicol. 57 (2009) 1–10. doi:10.1007/s00244-008-9229-z.

[7] S.L. Kuchta, A.J. Cessna, J.A. Elliott, K.M. Peru, J. V Headley, Transport of lincomycin to surface and ground water from manure-amended cropland., J. Environ. Qual. 38 (2009) 1719–1727. doi:10.2134/jeq2008.0365.

[8] R. Andreozzi, M. Canterino, R. Lo Giudice, R. Marotta, G. Pinto, A. Pollio, Lincomycin solar photodegradation, algal toxicity and removal from wastewaters by means of ozonation, Water Res. 40 (2006) 630–638. doi:10.1016/j.watres.2005.11.023.

[9] C.P. Wang, B.J. Teppen, S.A. Boyd, H. Li, Sorption of Lincomycin at Low Concentrations from Water by Soils, Soil Sci. Soc. Am. J. 76 (2012) 1222–1228. doi:10.2136/sssaj2011.0408.

[10] S.T. Glassmeyer, J.A. Shoemaker, Effects of chlorination on the persistence of pharmaceuticals in the environment, Bull. Environ. Contam. Toxicol. 74 (2005) 24–31. doi:10.1007/s00128-004-0543-5.

[11] Z. Qiang, C. Adams, R. Surampalli, Determination of Ozonation Rate Constants for Lincomycin and Spectinomycin, Ozone Sci. Eng. 26 (2004) 525–537. doi:10.1080/01919510490885334.

[12] F. Zaviska, P. Drogui, A. Grasmick, A. Azais, M. Héran, Nanofiltration membrane bioreactor for removing pharmaceutical compounds, J. Memb. Sci. 429 (2013) 121–129. doi:10.1016/j.memsci.2012.11.022.

[13] J. Rivera-Utrilla, M. Sánchez-Polo, M.Á. Ferro-García, G. Prados-Joya, R. Ocampo-Pérez, Pharmaceuticals as emerging contaminants and their removal from water. A review, Chemosphere. 93 (2013) 1268–1287. doi:10.1016/j.chemosphere.2013.07.059.

[14] E.K. Putra, R. Pranowo, J. Sunarso, N. Indraswati, S. Ismadji, Performance of activated carbon and bentonite for adsorption of amoxicillin from wastewater: Mechanisms, isotherms and kinetics, Water Res. 43 (2009) 2419–2430. doi:10.1016/j.watres.2009.02.039.

[15] V. Homem, L. Santos, Degradation and removal methods of antibiotics from aqueous matrices - A review, J. Environ. Manage. 92 (2011) 2304–2347. doi:10.1016/j.jenvman.2011.05.023.

[16] R. Crisafully, M.A.L. Milhome, R.M. Cavalcante, E.R. Silveira, D. De Keukeleire, R.F. Nascimento, Removal of some polycyclic aromatic hydrocarbons from petrochemical wastewater using low-cost adsorbents of natural origin, Bioresour. Technol. 99 (2008) 4515–4519. doi:10.1016/j.biortech.2007.08.041.

[17] S. Wang, Y. Peng, Natural zeolites as effective adsorbents in water and wastewater treatment, Chem. Eng. J. 156 (2010) 11–24. doi:10.1016/j.cej.2009.10.029.

[18] D. Krajisnik, A. Dakovic, M. Milojevic, A. Malenovic, M. Kragovic, D.B. Bogdanovic, V. Dondur, J. Milic, Properties of diclofenac sodium sorption onto natural zeolite modified with cetylpyridinium chloride, Colloids Surfaces B Biointerfaces. 83 (2011) 165–172. doi:10.1016/j.colsurfb.2010.11.024.

[19] a S. Shadrikov, a D. Petukhov, Natural Zeolite-Clinoptilolite Characteristics, Вісник Національного Університету. (2014) 162–167.

[20] R.E. Apreutesei, C. Catrinescu, C. Teodosiu, Surfactant-modified natural zeolites for environmental applications in water purification, Environ. Eng. Manag. J. 7 (2008) 149–161. http://www.scopus.com/inward/record.url?eid=2-s2.0-47849122205&partnerID=40&md5=1bfbf6633c7058ee47d7ce39f392ff8c.

[21] K. Ikehata, M. Gamal El-Din, Degradation of Aqueous Pharmaceuticals by Ozonation and Advanced Oxidation Processes: A Review, Ozone Sci. Eng. 27 (2006) 83–114. doi:10.1080/01919510600985937.

[22] K. Kümmerer, Drugs in the environment: Emission of drugs, diagnostic aids and disinfectants into wastewater by hospitals in relation to other sources - A review, Chemosphere. 45 (2001) 957–969. doi:10.1016/S0045-6535(01)00144-8.

[23] V.K. Sharma, N. Johnson, L. Cizmas, T.J. McDonald, H. Kim, A review of the influence of treatment strategies on antibiotic resistant bacteria and antibiotic resistance genes, Chemosphere. 150 (2016) 702–714. doi:10.1016/j.chemosphere.2015.12.084.

[24] A. Tello, B. Austin, T.C. Telfer, Selective pressure of antibiotic pollution on bacteria of importance to public health, Environ. Health Perspect. 120 (2012) 1100–1106. doi:10.1289/ehp.1104650.

[25] A.J. Alanis, Resistance to antibiotics: Are we in the post-antibiotic era?, Arch. Med. Res. 36 (2005) 697–705. doi:10.1016/j.arcmed.2005.06.009.

[26] F. Baquero, J.L. Martínez, R. Cantón, Antibiotics and antibiotic resistance in water environments, Curr. Opin. Biotechnol. 19 (2008) 260–265. doi:10.1016/j.copbio.2008.05.006.

[27] WHO, Antimicrobial resistance., Bull. World Health Organ. 61 (2014) 383–94. doi:10.1007/s13312-014-0374-3.

[28] C.F. Williams, J.E. Watson, S.D. Nelson, C.W. Walker, Sorption/Desorption of Lincomycin from Three Arid-Region Soils, J. Environ. Qual. 42 (2014) 1460–1465. doi:10.2134/jeq2013.04.0138.

[29] R. Andreozzi, M. Canterino, R. Lo Giudice, R. Marotta, G. Pinto, A. Pollio, Lincomycin solar photodegradation, algal toxicity and removal from wastewaters by means of ozonation., Water Res. 40 (2006) 630–8. doi:10.1016/j.watres.2005.11.023.

[30] D.W. Kolpin, M.T. Meyer, Pharmaceuticals , Hormones , and Other Organic Wastewater Contaminants in U . S . Streams , 1999 - 2000 : A National Reconnaissance, Environ. Sci. Technol. 36 (2002) 1202–1211. doi:10.1021/es011055j.

[31] L. Lissemore, C. Hao, P. Yang, P.K. Sibley, S. Mabury, K.R. Solomon, An exposure assessment for selected pharmaceuticals within a watershed in Southern Ontario, Chemosphere. 64 (2006) 717–729. doi:10.1016/j.chemosphere.2005.11.015.

[32] A.J. Watkinson, E.J. Murby, S.D. Costanzo, Removal of antibiotics in conventional and advanced wastewater treatment: Implications for environmental discharge and wastewater recycling, Water Res. 41 (2007) 4164–4176. doi:10.1016/j.watres.2007.04.005.

[33] D.J. de Ridder, Adsorption of organic micropollutants onto activated carbon and zeolites, 2012.

[34] C. Wang, Y. Ding, B.J. Teppen, S.A. Boyd, C. Song, H. Li, Role of interlayer hydration in lincomycin sorption by smectite clays, Environ. Sci. Technol. 43 (2009) 6171–6176. doi:10.1021/es900760m.

[35] C.E. Dewey, B.D. Cox, B.E. Straw, E.J. Bush, S. Hurd, Use of antimicrobials in swine feeds in the United States, Swine Heal. Prod. 7 (1999) 19–25.

[36] S.L. Kuchta, Lincomycin and Spectinomycin : persistence in liquid hog manure and their transport from manure-amended soil, (2008). http://ecommons.usask.ca/handle/10388/etd-02292008-125535.

[37] E. Worch, Adsorption Technology in Water Treatment: Fundamentals, Processes, and

Modeling, 2012. doi:10.1515/9783110240238.

[38] J. Liu, S.A. Carr, Removal of Estrogenic Compounds from Aqueous Solutions Using Zeolites, Water Environ. Res. 85 (2013) 2157–2163. doi:10.2175/106143013X13736496909356.

[39] C. Moreno-Castilla, Adsorption of organic molecules from aqueous solutions on carbon materials, Carbon N. Y. 42 (2004) 83–94. doi:10.1016/j.carbon.2003.09.022.

[40] I. Bautista-Toledo, M.A. Ferro-García, J. Rivera-Utrilla, C. Moreno-Castilla, F.J.V. Fernández, Bisphenol A removal from water by activated carbon. Effects of carbon characteristics and solution chemistry, Environ. Sci. Technol. 39 (2005) 6246–6250. doi:10.1021/es0481169.

[41] L.R. Radovic, I.F. Silva, J.I. Ume, J. a. Menéndez, C.A.L.Y. Leon, a. W. Scaroni, An experimental and theoretical study of the adsorption of aromatics possessing electron-withdrawing and electron-donating functional groups by chemically modified activated carbons, Carbon N. Y. 35 (1997) 1339–1348. doi:10.1016/S0008-6223(97)00072-9.

[42] J. Rivera-Utrilla, G. Prados-Joya, M. Sánchez-Polo, M.A. Ferro-García, I. Bautista-Toledo, Removal of nitroimidazole antibiotics from aqueous solution by adsorption/bioadsorption on activated carbon, J. Hazard. Mater. 170 (2009) 298–305. doi:10.1016/j.jhazmat.2009.04.096.

[43] A.P. Terzyk, Molecular properties and intermolecular forces - Factors balancing the effect of carbon surface chemistry in adsorption of organics from dilute aqueous solutions, J. Colloid Interface Sci. 275 (2004) 9–29. doi:10.1016/j.jcis.2004.02.011.

[44] D.H. Carrales-Alvarado, R. Ocampo-Pérez, R. Leyva-Ramos, J. Rivera-Utrilla, Removal of the antibiotic metronidazole by adsorption on various carbon materials from aqueous phase, J. Colloid Interface Sci. 436 (2014) 276–285. doi:10.1016/j.jcis.2014.08.023.

[45] M. Bjelopavlic, G. Newcombe, R. Hayes, Adsorption of NOM onto Activated Carbon: Effect of Surface Charge, Ionic Strength, and Pore Volume Distribution., J. Colloid Interface Sci. 210 (1999) 271–280. doi:10.1006/jcis.1998.5975.

[46] J.D. Méndez-Díaz, G. Prados-Joya, J. Rivera-Utrilla, R. Leyva-Ramos, M. Sánchez-Polo, M.A. Ferro-García, N.A. Medellín-Castillo, Kinetic study of the adsorption of nitroimidazole antibiotics on activated carbons in aqueous phase, J. Colloid Interface Sci. 345 (2010) 481–490. doi:10.1016/j.jcis.2010.01.089.

[47] H. Peng, B. Pan, M. Wu, Y. Liu, D. Zhang, B. Xing, Adsorption of ofloxacin and norfloxacin on carbon nanotubes: Hydrophobicity- and structure-controlled process, J. Hazard. Mater. 233–234 (2012) 89–96. doi:10.1016/j.jhazmat.2012.06.058.

[48] B. Peng, L. Chen, C. Que, K. Yang, F. Deng, X. Deng, G. Shi, G. Xu, M. Wu, Adsorption of Antibiotics on Graphene and Biochar in Aqueous Solutions Induced by π-π Interactions, Sci. Rep. 6 (2016) 31920. doi:10.1038/srep31920.

[49] J.A. Mattson, H.B. Mark, M.D. Malbin, W.J. Weber, J.C. Crittenden, Surface chemistry of active carbon: Specific adsorption of phenols, J. Colloid Interface Sci. 31 (1969) 116–130. doi:10.1016/0021-9797(69)90089-7.

[50] Z. Jeirani, C.H. Niu, J. Soltan, Adsorption of emerging pollutants on activated carbon, Rev. Chem. Eng. 0 (2016). doi:10.1515/revce-2016-0027.

[51] H. Li, D. Zhang, X. Han, B. Xing, Adsorption of antibiotic ciprofloxacin on carbon nanotubes: PH dependence and thermodynamics, Chemosphere. 95 (2014) 150–155. doi:10.1016/j.chemosphere.2013.08.053.

[52] F. Salvador, M.D. Merchán, Study of the desorption of phenol and phenolic compounds from activated carbon by liquid-phase temperature-programmed desorption, Carbon N. Y. 34 (1996) 1543–1551. doi:10.1016/S0008-6223(96)00105-4.

[53] J. Xu, L. Wang, Y. Zhu, Decontamination of bisphenol A from aqueous solution by graphene adsorption, Langmuir. 28 (2012) 8418–8425. doi:10.1021/la301476p.

[54] H. Kim, Y.S. Hwang, V.K. Sharma, Adsorption of antibiotics and iopromide onto single-walled and multi-walled carbon nanotubes, Chem. Eng. J. 255 (2014) 23–27. doi:10.1016/j.cej.2014.06.035.

[55] B. Bogdanov, D. Georgiev, K. Angelova, I. Markovska, Y. Hristov, International Science conference 4, Int. Sci. Conf. 4th - 5th June 2009, Stara Zagor. Bulg. “Economics Soc. Dev. Base Knowledge.” VII (2009) 1–5.

[56] K. Margeta, N. Zabukovec Logar, M. Šiljeg, A. Farkas, Natural Zeolites in Water Treatment – How Effective is Their Use, Water Treat. (2013). doi:10.5772/50738.

[57] Z. Li, C. Stockwell, J. Niles, S. Minegar, H. Hong, Uptake of sulfadiazine sulfonamide from water by clinoptilolite, Appl. Environ. Soil Sci. 2013 (2013). doi:10.1155/2013/648697.

[58] H.M. Ötker, I. Akmehmet-Balcioğlu, Adsorption and degradation of enrofloxacin, a veterinary antibiotic on natural zeolite, J. Hazard. Mater. 122 (2005) 251–258. doi:10.1016/j.jhazmat.2005.03.005.

[59] H. Kurama, A. Zimmer, W. Reschetilowski, Chemical modification effect on the sorption capacities of natural clinoptilolite, Chem. Eng. Technol. 25 (2002) 301–305. doi:10.1002/1521-4125(200203)25:3<301::AID-CEAT301>3.0.CO;2-#.

[60] F. Cakicioglu-Ozkan, S. Ulku, The effect of HCl treatment on water vapor adsorption characteristics of clinoptilolite rich natural zeolite, Microporous Mesoporous Mater. 77 (2005) 47–53. doi:10.1016/j.micromeso.2004.08.013.

[61] C. Li, Y. Dong, D. Wu, L. Peng, H. Kong, Surfactant modified zeolite as adsorbent for removal of humic acid from water, Appl. Clay Sci. 52 (2011) 353–357. doi:10.1016/j.clay.2011.03.015.

[62] C.-H. Liu, Y.-H. Chuang, H. Li, B.J. Teppen, S. a. Boyd, J.M. Gonzalez, C.T. Johnston, J. Lehmann, W. Zhang, Sorption of Lincomycin by Manure-Derived Biochars from Water, J. Environ. Qual. 45 (2016) 519. doi:10.2134/jeq2015.06.0320.

[63] D.D. Do, Adsorption Analysis: Equilibria and Kinetics, 1998. doi:10.1142/9781860943829.

[64] G. Limousin, J.P. Gaudet, L. Charlet, S. Szenknect, V. Barthès, M. Krimissa, Sorption isotherms: A review on physical bases, modeling and measurement, Appl. Geochemistry. 22 (2007) 249–275. doi:10.1016/j.apgeochem.2006.09.010.

[65] K.Y. Foo, B.H. Hameed, Insights into the modeling of adsorption isotherm systems, Chem. Eng. J. 156 (2010) 2–10. doi:10.1016/j.cej.2009.09.013.

[66] Z. Aksu, Ö. Tunç, Application of biosorption for penicillin G removal: Comparison with activated carbon, Process Biochem. 40 (2005) 831–847. doi:10.1016/j.procbio.2004.02.014.

[67] S.H. Kim, H.K. Shon, H.H. Ngo, Adsorption characteristics of antibiotics trimethoprim on powdered and granular activated carbon, J. Ind. Eng. Chem. 16 (2010) 344–349. doi:10.1016/j.jiec.2009.09.061.

[68] O. Hamdaoui, E. Naffrechoux, Modeling of adsorption isotherms of phenol and chlorophenols onto granular activated carbon. Part II. Models with more than two parameters, J. Hazard. Mater. 147 (2007) 401–411. doi:10.1016/j.jhazmat.2007.01.023.

[69] E. Worch, Competitive adsorption of micropollutants and NOM onto activated carbon: Comparison of different model approaches, J. Water Supply Res. Technol. - AQUA. 59 (2010) 285–297. doi:10.2166/aqua.2010.065.

[70] S. Qi, L. Schideman, B.J. Marin, V.L. Snoeyink, Simplification of the IAST for activated carbon adsorption of trace organic compounds from natural water, 41 (2007) 440–448. doi:10.1016/j.watres.2006.10.018.

[71] H.S. Fogler, Elements of chemical reaction engineering., 1999. doi:10.1016/0009-2509(87)80130-6.

[72] Y. Liu, C. Dong, H. Wei, W. Yuan, K. Li, Adsorption of levofloxacin onto an iron-pillared montmorillonite (clay mineral): Kinetics, equilibrium and mechanism, Appl. Clay Sci. 118 (2015) 301–307. doi:10.1016/j.clay.2015.10.010.

[73] H. Hindarso, S. Ismadji, F. Wicaksana, Mudjijati, N. Indraswati, Adsorption of Benzene and Toluene from Aqueous Solution onto Granular Activated Carbon, J. Chem. Eng. Data. 46 (2001) 788–791. doi:10.1021/je000176g.

[74] O.A. Attallah, M.A. Al-Ghobashy, M. Nebsen, M.Y. Salem, Adsorptive Removal of Fluoroquinolones from Water by Pectin-Functionalized Magnetic Nanoparticles: Process Optimization Using a Spectrofluorimetric Assay, ACS Sustain. Chem. Eng. 5 (2017) 133–145. doi:10.1021/acssuschemeng.6b01003.

[75] F. Bonvin, L. Jost, L. Randin, E. Bonvin, T. Kohn, Super-fine powdered activated carbon (SPAC) for efficient removal of micropollutants from wastewater treatment plant effluent, Water Res. 90 (2016) 90–99. doi:10.1016/j.watres.2015.12.001.

[76] V.L. Snoeyink, P. Roche, M. Jose, A. Recherche, C. Ge, Predicting the Capacity of Powdered Activated Carbon for Trace Organic Compounds in Natural Waters, 32 (1998) 1694–1698.

[77] H.N. Tran, S.J. You, H.P. Chao, Thermodynamic parameters of cadmium adsorption onto orange peel calculated from various methods: A comparison study, J. Environ. Chem. Eng. 4 (2016) 2671–2682. doi:10.1016/j.jece.2016.05.009.

[78] E. Çalışkan, S. Göktürk, Adsorption Characteristics of Sulfamethoxazole and Metronidazole on Activated Carbon, Sep. Sci. Technol. 45 (2010) 244–255. doi:10.1080/01496390903409419.

[79] Y. Liu, Is the free energy change of adsorption correctly calculated?, J. Chem. Eng. Data. 54 (2009) 1981–1985. doi:10.1021/je800661q.

[80] Y. Sag, T. Kutsal, Determination of the biosorption activation energies of heavy metal ions on Zoogloea ramigera and Rhizopus arrhizus, Process Biochem. 35 (2000) 801–807. doi:10.1016/S0032-9592(99)00154-5.

[81] B. Belhamdi, Z. Merzougui, M. Trari, A. Addoun, A kinetic , equilibrium and thermodynamic study of l -phenylalanine adsorption using activated carbon based on agricultural waste (date stones), Rev. Mex. Trastor. Aliment. 14 (2016) 354–366. doi:10.1016/j.jart.2016.08.004.

[82] J.M. Chern, C.Y. Wu, C. Jia-Ming, W. Chia-Yuan, Desorption of dye from activated carbon beds:effects of temperature, pH and alchol, Water Res. 35 (2001) 4159–4165. doi:10.1016/S0043-1354(01)00127-0.

[83] J. Lin, Y. Zhan, Z. Zhu, Adsorption characteristics of copper (II) ions from aqueous solution onto humic acid-immobilized surfactant-modified zeolite, Colloids Surfaces A Physicochem. Eng. Asp. 384 (2011) 9–16. doi:10.1016/j.colsurfa.2011.02.044.

[84] P. Saha, S. Chowdhury, Insight Into Adsorption Thermodynamics, in: Thermodynamics, InTech, Berlin, Heidelberg, 2011: p. 440. doi:10.5772/13474.

[85] J.M. Thomas, The existence of endothermic adsorption, J. Chem. Educ. 38 (1961) 138. doi:10.1021/ed038p138.

[86] C. Michailof, G.G. Stavropoulos, C. Panayiotou, Enhanced adsorption of phenolic compounds, commonly encountered in olive mill wastewaters, on olive husk derived activated carbons, Bioresour. Technol. 99 (2008) 6400–6408. doi:10.1016/j.biortech.2007.11.057.

[87] M.B. Ahmed, J.L. Zhou, H.H. Ngo, W. Guo, Veterinary antibiotics in the aquatic and terrestrial environment, Sci. Total Environ. 532 (2015) 112–126.

doi:10.1016/j.scitotenv.2015.05.130.

[88] W.S.W. Ngah, S. Fatinathan, Adsorption characterization of Pb(II) and Cu(II) ions onto chitosan-tripolyphosphate beads: Kinetic, equilibrium and thermodynamic studies, J. Environ. Manage. 91 (2010) 958–969. doi:10.1016/j.jenvman.2009.12.003.

[89] J.F. García-Araya, F.J. Beltrán, P. Álvarez, F.J. Masa, Activated carbon adsorption of some phenolic compounds present in agroindustrial wastewater, Adsorption. 9 (2003) 107–115. doi:10.1023/A:1024228708675.

[90] Z. Aksu, E. Kabasakal, Batch adsorption of 2,4-dichlorophenoxy-acetic acid (2,4-D) from aqueous solution by granular activated carbon, Sep. Purif. Technol. 35 (2004) 223–240. doi:10.1016/S1383-5866(03)00144-8.

[91] Y.S. Ho, A.E. Ofomaja, Biosorption thermodynamics of cadmium on coconut copra meal as biosorbent, Biochem. Eng. J. 30 (2006) 117–123. doi:10.1016/j.bej.2006.02.012.

[92] K. Vijayaraghavan, Y.S. Yun, Biosorption of C.I. Reactive Black 5 from aqueous solution using acid-treated biomass of brown seaweed Laminaria sp., Dye. Pigment. 76 (2008) 726–732. doi:10.1016/j.dyepig.2007.01.013.

[93] E.F.S. Vieira, A.R. Cestari, C. d S. Oliveira, P.S. de Lima, L.E. Almeida, Thermodynamics of pyrimethamine and sulfadiazine binding to a chitosan derivative, Thermochim. Acta. 459 (2007) 9–11. doi:10.1016/j.tca.2007.03.014.

[94] M. Mouflih, A. Aklil, S. Sebti, Removal of lead from aqueous solutions by activated phosphate, J. Hazard. Mater. 119 (2005) 183–188. doi:10.1016/j.jhazmat.2004.12.005.

[95] M. Erdem, A. Ozverdi, Kinetics and thermodynamics of Cd(II) adsorption onto pyrite and synthetic iron sulphide, Sep. Purif. Technol. 51 (2006) 240–246. doi:10.1016/j.seppur.2006.02.004.

[96] C.H. Weng, C.Z. Tsai, S.H. Chu, Y.C. Sharma, Adsorption characteristics of copper(II) onto spent activated clay, Sep. Purif. Technol. 54 (2007) 187–197. doi:10.1016/j.seppur.2006.09.009.

[97] Ş. Kubilay, R. Gürkan, A. Savran, T. Şahan, Removal of Cu(II), Zn(II) and Co(II) ions from aqueous solutions by adsorption onto natural bentonite, Adsorption. 13 (2007) 41–51. doi:10.1007/s10450-007-9003-y.

[98] S.K. Milonjić, A consideration of the correct calculation of thermodynamic parameters of adsorption, J. Serbian Chem. Soc. 72 (2007) 1363–1367. doi:10.2298/JSC0712363M.

[99] S. Salvestrini, V. Leone, P. Iovino, S. Canzano, S. Capasso, Considerations about the correct evaluation of sorption thermodynamic parameters from equilibrium isotherms, J. Chem. Thermodyn. 68 (2014) 310–316. doi:10.1016/j.jct.2013.09.013.

[100] X. Zhou, X. Zhou, the Unit Problem in the Thermodynamic Calculation of Adsorption Using the Langmuir Equation, Chem. Eng. Commun. 201 (2014) 1459–1467.

doi:10.1080/00986445.2013.818541.

[101] A.A. Khan, R.P. Singh, Adsorption thermodynamics of carbofuran on Sn (IV) arsenosilicate in H+, Na+ and Ca2+ forms, Colloids and Surfaces. 24 (1987) 33–42. doi:10.1016/0166-6622(87)80259-7.

[102] V.C. Srivastava, I.D. Mall, I.M. Mishra, Adsorption thermodynamics and isosteric heat of adsorption of toxic metal ions onto bagasse fly ash (BFA) and rice husk ash (RHA), Chem. Eng. J. 132 (2007) 267–278. doi:10.1016/j.cej.2007.01.007.

[103] J. Zhou, Y. Cheng, J. Yu, G. Liu, Hierarchically porous calcined lithium/aluminum layered double hydroxides: Facile synthesis and enhanced adsorption towards fluoride in water, J. Mater. Chem. 21 (2011) 19353. doi:10.1039/c1jm13645c.

[104] M.F. Sawalha, J.R. Peralta-Videa, J. Romero-González, J.L. Gardea-Torresdey, Biosorption of Cd(II), Cr(III), and Cr(VI) by saltbush (Atriplex canescens) biomass: Thermodynamic and isotherm studies, J. Colloid Interface Sci. 300 (2006) 100–104. doi:10.1016/j.jcis.2006.03.029.

[105] S.A. Khan, Riaz-ur-Rehman, M.A. Khan, Adsorption of chromium (III), chromium (VI) and silver (I) on bentonite, Waste Manag. 15 (1995) 271–282. doi:10.1016/0956-053X(95)00025-U.

[106] K. Raby, A.A. Ramirez, M. Heitz, Elimination of nitrogen present in swine manure using a high-efficiency biotrickling filter., Environ. Technol. 34 (2016) 813–24. doi:10.1080/09593330.2012.720615.

[107] A.M. Redding, F.S. Cannon, S.A. Snyder, B.J. Vanderford, A QSAR-like analysis of the adsorption of endocrine disrupting compounds, pharmaceuticals, and personal care products on modified activated carbons, Water Res. 43 (2009) 3849–3861. doi:10.1016/j.watres.2009.05.026.

[108] S. Lowell, J.E. Shields, M.A. Thomas, M. Thommes, Characterization of Porous Solids and Powders: Surface Area, Pore Size and Density, 2004. doi:10.1007/978-1-4020-2303-3.

[109] S.A. Dastgheib, T. Karanfil, W. Cheng, Tailoring activated carbons for enhanced removal of natural organic matter from natural waters, Carbon N. Y. 42 (2004) 547–557. doi:10.1016/j.carbon.2003.12.062.

[110] S.L. Goertzen, K.D. Theriault, A.M. Oickle, A.C. Tarasuk, H.A. Andreas, Standardization of the Boehm titration. Part I. CO2 expulsion and endpoint determination, Carbon N. Y. 48 (2010) 1252–1261. doi:10.1016/j.carbon.2009.11.050.

[111] L.M.L. Nollet, Handbook of Water Analysis, 2007. doi:10.1038/006104a0.

[112] APHA/AWWA/WEF, Standard Methods for the Examination of Water and Wastewater, Stand. Methods. (2012) 541. doi:ISBN 9780875532356.

[113] P. Saha, S. Chowdhury, S. Gupta, I. Kumar, Insight into adsorption equilibrium, kinetics and thermodynamics of Malachite Green onto clayey soil of Indian origin, Chem. Eng. J. 165 (2010) 874–882. doi:10.1016/j.cej.2010.10.048.

[114] W. Liu, J. Zhang, C. Zhang, L. Ren, Sorption of norfloxacin by lotus stalk-based activated carbon and iron-doped activated alumina: Mechanisms, isotherms and kinetics, Chem. Eng. J. 171 (2011) 431–438. doi:10.1016/j.cej.2011.03.099.

[115] P. Chutia, S. Kato, T. Kojima, S. Satokawa, Arsenic adsorption from aqueous solution on synthetic zeolites, J. Hazard. Mater. 162 (2009) 440–447. doi:10.1016/j.jhazmat.2008.05.061.

[116] Y. Zhang, E. Bi, Effect of dissolved organic matter on ammonium sorption kinetics and equilibrium to Chinese clinoptilolite, Environ. Technol. 33 (2012) 2395–2403. doi:10.1080/09593330.2012.670268.

[117] M. Kragović, A. Daković, Ž. Sekulić, M. Trgo, M. Ugrina, J. Perić, G.D. Gatta, Removal of lead from aqueous solutions by using the natural and Fe(III)-modified zeolite, Appl. Surf. Sci. 258 (2012) 3667–3673. doi:10.1016/j.apsusc.2011.12.002.

[118] H. Valdés, R.F. Tardón, C.A. Zaror, Role of surface hydroxyl groups of acid-treated natural zeolite on the heterogeneous catalytic ozonation of methylene blue contaminated waters, Chem. Eng. J. 211–212 (2012) 388–395. doi:10.1016/j.cej.2012.09.069.

[119] I. Braschi, S. Blasioli, L. Gigli, C.E. Gessa, A. Alberti, A. Martucci, Removal of sulfonamide antibiotics from water: Evidence of adsorption into an organophilic zeolite Y by its structural modifications, J. Hazard. Mater. 178 (2010) 218–225. doi:10.1016/j.jhazmat.2010.01.066.

[120] H.P. Gavin, The Levenberg-Marquardt method for nonlinear least squares curve-fitting problems, (2017) 1–19. doi:10.1080/10426914.2014.941480.

[121] Z. Yu, S. Peldszus, P.M. Huck, Adsorption characteristics of selected pharmaceuticals and an endocrine disrupting compound-Naproxen, carbamazepine and nonylphenol-on activated carbon, Water Res. 42 (2008) 2873–2882. doi:10.1016/j.watres.2008.02.020.

[122] F. Yu, Y. Li, S. Han, J. Ma, Adsorptive removal of antibiotics from aqueous solution using carbon materials, Chemosphere. 153 (2016) 365–385. doi:10.1016/j.chemosphere.2016.03.083.

[123] L.F. Velasco, C.O. Ania, Understanding phenol adsorption mechanisms on activated carbons, Adsorption. 17 (2011) 247–254. doi:10.1007/s10450-011-9322-x.

[124] Y. Al-Degs, M.A.M. Khraisheh, S.J. Allen, M.N. Ahmad, Effect of carbon surface chemistry on the removal of reactive dyes from textile effluent, Water Res. 34 (2000) 927–935. doi:10.1016/S0043-1354(99)00200-6.

[125] H. Guedidi, L. Reinert, J.-M. Lévêque, Y. Soneda, N. Bellakhal, L. Duclaux, The effects of the surface oxidation of activated carbon, the solution pH and the temperature on

adsorption of ibuprofen, Carbon N. Y. 54 (2013) 432–443. doi:10.1016/j.carbon.2012.11.059.

[126] G.E. Christidis, D. Moraetis, E. Keheyan, L. Akhalbedashvili, N. Kekelidze, R. Gevorkyan, H. Yeritsyan, H. Sargsyan, Chemical and thermal modification of natural HEU-type zeolitic materials from Armenia, Georgia and Greece, Appl. Clay Sci. 24 (2003) 79–91. doi:10.1016/S0169-1317(03)00150-9.

[127] H.R. Pouretedal, N. Sadegh, Effective removal of Amoxicillin, Cephalexin, Tetracycline and Penicillin G from aqueous solutions using activated carbon nanoparticles prepared from vine wood, J. Water Process Eng. 1 (2014) 64–73. doi:10.1016/j.jwpe.2014.03.006.

[128] H. Chen, G. Dai, J. Zhao, A. Zhong, J. Wu, H. Yan, Removal of copper(II) ions by a biosorbent-Cinnamomum camphora leaves powder, J. Hazard. Mater. 177 (2010) 228–236. doi:10.1016/j.jhazmat.2009.12.022.

[129] Y. Chao, W. Zhu, F. Chen, P. Wang, Z. Da, X. Wu, H. Ji, S. Yan, H. Li, Commercial Diatomite for Adsorption of Tetracycline Antibiotic from Aqueous Solution, Sep. Sci. Technol. 49 (2014) 2221–2227. doi:10.1080/01496395.2014.914954.

[130] A. Nowara, J. Burhenne, M. Spiteller, Binding of fluoroquinolone carboxylic acid derivatives to clay minerals, J. Agric. Food Chem. 45 (1997) 1459–1463. doi:10.1021/jf960215l.

[131] Y.K. Lan, T.C. Chen, H.J. Tsai, H.C. Wu, J.H. Lin, I.K. Lin, J.F. Lee, C.S. Chen, Adsorption Behavior and Mechanism of Antibiotic Sulfamethoxazole on Carboxylic-Functionalized Carbon Nanofibers-Encapsulated Ni Magnetic Nanoparticles, Langmuir. 32 (2016) 9530–9539. doi:10.1021/acs.langmuir.6b02904.

[132] P. Somasundaran, S. Shrotri, L. Huang, Thermodynamics of adsorption of surfactants at solid-liquid interface, Pure Appl. Chem. 70 (1998) 621–626. doi:10.1351/pac199870030621.

[133] X. Long, H. Cheng, Z. Xin, W. Xiao, W. Li, W. Yuan, Adsorption of ammonia on activated carbon from aqueous solutions, Environ. Prog. 27 (2008) 225–233. doi:10.1002/ep.10252.

[134] L. Zhang, Y. Gao, Y. Xu, J. Liu, Different performances and mechanisms of phosphate adsorption onto metal oxides and metal hydroxides: A comparative study, J. Chem. Technol. Biotechnol. 91 (2016) 1232–1239. doi:10.1002/jctb.4710.

[135] K. Riahi, B. Ben Thayer, A. Ben Mammou, A. Ben Ammar, M.H. Jaafoura, Biosorption characteristics of phosphates from aqueous solution onto Phoenix dactylifera L. date palm fibers, J. Hazard. Mater. 170 (2009) 511–519. doi:10.1016/j.jhazmat.2009.05.004.

[136] X. Zhang, W. Guo, H.H. Ngo, H. Wen, N. Li, W. Wu, Performance evaluation of powdered activated carbon for removing 28 types of antibiotics from water, J. Environ. Manage. 172 (2016) 193–200. doi:10.1016/j.jenvman.2016.02.038.

[137] J.S. Geelhoed, T. Hiemstra, W.H. Van Riemsdijk, Phosphate and sulfate adsorption on goethite: Single anion and competitive adsorption, Geochim. Cosmochim. Acta. 61 (1997) 2389–2396. doi:10.1016/S0016-7037(97)00096-3.

[138] M. Özacar, Adsorption of phosphate from aqueous solution onto alunite, Chemosphere. 51 (2003) 321–327. doi:10.1016/S0045-6535(02)00847-0.

[139] R. Rietra, T. Hiemstra, van Riemsdijk WH, Sulfate Adsorption on Goethite., J. Colloid Interface Sci. 218 (1999) 511–521. doi:10.1006/jcis.1999.6408.

[140] A. Halajnia, S. Oustan, N. Najafi, A.R. Khataee, A. Lakzian, Adsorption-desorption characteristics of nitrate, phosphate and sulfate on Mg-Al layered double hydroxide, Appl. Clay Sci. 80–81 (2013) 305–312. doi:10.1016/j.clay.2013.05.002.

[141] J. Hrenovic, M. Rozic, T. Ivankovic, A. Farkas, Biosorption of phosphate from synthetic wastewater by biosolids, Cent. Eur. J. Biol. 4 (2009) 397–403. doi:10.2478/s11535-009-0030-4.

[142] Z.L. Shi, F.M. Liu, S.H. Yao, Adsorptive removal of phosphate from aqueous solutions using activated carbon loaded with Fe(III) oxide, Xinxing Tan Cailiao/New Carbon Mater. 26 (2011) 299–306. doi:10.1016/S1872-5805(11)60083-8.

[143] S. Fukahori, T. Fujiwara, N. Funamizu, K. Matsukawa, R. Ito, Adsorptive removal of sulfonamide antibiotics in livestock urine using the high-silica zeolite HSZ-385, Water Sci. Technol. 67 (2013) 319–325. doi:10.2166/wst.2012.513.

[144] S. Qi, S.S. Adham, V.L. Snoeyink, B.W. Lykins, Prediction and Verification of Atrazine Adsorption by PAC, J. Environ. Eng. 120 (1994) 202–218. doi:10.1061/(ASCE)0733-9372(1994)120:1(202).

[145] G. Newcombe, J. Morrison, C. Hepplewhite, Simultaneous adsorption of MIB and NOM onto activated carbon. I. Characterisation of the system and NOM adsorption, Carbon N. Y. 40 (2002) 2135–2146. doi:10.1016/S0008-6223(02)00097-0.

[146] M.R. Graham, R.S. Summers, M.R. Simpson, B.W. Macleod, Modeling Equilibrium Adsorption of 2- Methylisoborneol and Geosmin in Natural Waters, Water Res. 34 (2000) 2291–2300.

[147] F. Zietzschmann, G. Aschermann, M. Jekel, Comparing and modeling organic micro-pollutant adsorption onto powdered activated carbon in different drinking waters and WWTP effluents, Water Res. 102 (2016) 190–201. doi:10.1016/j.watres.2016.06.041.

APPENDIX A. Equilibrium time determination and statistical analysis

The experiments were carried out at 280 K and using 50 ppm lincomycin solutions. 3 Erlenmeyer flasks of each adsorbent, containing 5, 10 or 20 mg of adsorbent (depending on the adsorbent as detailed in Table 3.3) and 100 mL of 50 ppm lincomycin solution were stirred at 130 rpm. Later, lincomycin concentration was measured every day, until 12 days by UV spectrometry using a MECASYS Optizen POP UV-Vis spectrophotometer at a detection wavelength of 200 nm. Results are presented in Table A.1.

Table A.1. Final concentration of lincomycin in solution at 1 day of stirring (130 rpm, Initial lincomycin concentration 50 ppm, temperature 280 K) at different concentration of adsorbents

Adsorbent	ABSORBANCE			Average	CONCENTRATION (ppm)			Average (ppm)	Standard deviation (ppm)
	Sample 1	Sample 2	Sample 3		Sample 1	Sample 2	Sample 3		
C1240	0.875	0.870	0.867	0.871	47.8	47.5	47.4	47.6	0.1
NR	0.845	0.882	0.882	0.870	46.2	48.2	48.2	47.5	0.9
F400	0.832	0.841	0.876	0.850	45.5	46.0	47.9	46.4	1.1
F300	0.835	0.859	0.820	0.838	45.6	46.9	44.8	45.8	0.8
SAN	0.853	0.845	0.816	0.838	46.6	46.2	44.6	45.8	0.7
SAD	0.771	0.761	0.725	0.752	42.1	41.6	39.6	41.1	1.1
NZ	0.765	0.755	0.741	0.754	41.8	41.3	40.5	41.2	0.3
NZH	0.865	0.859	0.897	0.874	47.3	46.9	49.0	47.7	0.8

Table A.2. Final concentration of lincomycin in solution at 2 days of stirring (130 rpm, Initial lincomycin concentration 50 ppm, temperature 280 K) at different concentration of adsorbents

Adsorbent	ABSORBANCE			Average	CONCENTRATION (ppm)			Average (ppm)	Standard deviation (ppm)
	Sample 1	Sample 2	Sample 3		Sample 1	Sample 2	Sample 3		
C1240	0.779	0.788	0.810	0.871	42.6	43.1	44.2	43.3	0.5
NR	0.809	0.805	0.831	0.870	44.2	44.0	45.4	44.5	0.4
F400	0.799	0.774	0.802	0.850	43.7	42.3	43.8	43.3	0.5
F300	0.809	0.781	0.818	0.838	44.2	42.7	44.7	43.9	0.8
SAN	0.782	0.821	0.789	0.838	42.7	44.9	43.1	43.6	0.9
SAD	0.761	0.765	0.717	0.752	41.6	41.8	39.2	40.8	1.4
NZ	0.746	0.742	0.776	0.754	40.8	40.5	42.4	41.2	0.7
NZH	0.849	0.852	0.882	0.874	46.4	46.6	48.2	47.0	0.6

Table A.3. Final concentration of lincomycin in solution at 3 days of stirring (130 rpm, Initial lincomycin concentration 50 ppm, temperature 280 K) at different concentration of adsorbents

Adsorbent	ABSORBANCE			Average	CONCENTRATION (ppm)			Average (ppm)	Standard deviation (ppm)
	Sample 1	Sample 2	Sample 3		Sample 1	Sample 2	Sample 3		
C1240	0.758	0.742	0.790	0.871	41.4	40.5	43.2	41.7	1.2
NR	0.775	0.782	0.812	0.870	42.3	42.7	44.3	43.1	0.7
F400	0.745	0.781	0.802	0.850	40.7	42.7	43.8	42.4	1.7
F300	0.761	0.779	0.807	0.838	41.6	42.6	44.1	42.8	1.1
SAN	0.797	0.768	0.812	0.838	43.6	42.0	44.3	43.3	1.0
SAD	0.725	0.731	0.765	0.752	39.6	39.9	41.8	40.4	0.9
NZ	0.748	0.738	0.780	0.754	40.9	40.3	42.6	41.3	0.9
NZH	0.854	0.859	0.888	0.874	46.7	46.9	48.5	47.4	0.7

Table A.4. Final concentration of lincomycin in solution at 4 days of stirring (130 rpm, Initial lincomycin concentration 50 ppm, temperature 280 K) at different concentration of adsorbents

Adsorbent	ABSORBANCE			Average	CONCENTRATION (ppm)			Average (ppm)	Standard deviation (ppm)
	Sample 1	Sample 2	Sample 3		Sample 1	Sample 2	Sample 3		
C1240	0.738	0.739	0.754	0.871	40.3	40.4	41.2	40.6	0.2
NR	0.749	0.768	0.753	0.870	40.9	42.0	41.2	41.4	0.2
F400	0.725	0.739	0.776	0.850	39.6	40.4	42.4	40.8	1.4
F300	0.758	0.765	0.723	0.838	41.4	41.8	39.5	40.9	1.0
SAN	0.795	0.771	0.797	0.838	43.4	42.1	43.6	43.0	0.4
SAD	0.728	0.749	0.738	0.752	39.8	40.9	40.3	40.3	0.2
NZ	0.747	0.776	0.758	0.754	40.8	42.4	41.4	41.5	0.4
NZH	0.856	0.851	0.891	0.874	46.8	46.5	48.7	47.3	0.9

Table A.5. Final concentration of lincomycin in solution at 5 days of stirring (130 rpm, Initial lincomycin concentration 50 ppm, temperature 280 K) at different concentration of adsorbents

Adsorbent	ABSORBANCE			Average	CONCENTRATION (ppm)			Average (ppm)	Standard deviation (ppm)
	Sample 1	Sample 2	Sample 3		Sample 1	Sample 2	Sample 3		
C1240	0.735	0.734	0.711	0.871	40.2	40.1	38.8	39.7	0.4
NR	0.744	0.765	0.712	0.870	40.7	41.8	38.9	40.4	1.4
F400	0.715	0.731	0.713	0.850	39.1	39.9	38.9	39.3	0.2
F300	0.75	0.758	0.731	0.838	41.0	41.4	40.0	40.8	0.4
SAN	0.765	0.763	0.823	0.838	41.8	41.7	45.0	42.8	2.3
SAD	0.721	0.745	0.748	0.752	39.4	40.7	40.9	40.3	0.4
NZ	0.772	0.761	0.735	0.754	42.2	41.6	40.2	41.3	0.7
NZH	0.853	0.857	0.881	0.874	46.6	46.8	48.1	47.2	0.4

Table A.6. Final concentration of lincomycin in solution at 6 days of stirring (130 rpm, Initial lincomycin concentration 50 ppm, temperature 280 K) at different concentration of adsorbents

Adsorbent	ABSORBANCE			Average	CONCENTRATION (ppm)			Average (ppm)	Standard deviation (ppm)
	Sample 1	Sample 2	Sample 3		Sample 1	Sample 2	Sample 3		
C1240	0.705	0.712	0.718	0.871	38.5	38.9	39.2	38.9	0.1
NR	0.712	0.736	0.711	0.870	38.9	40.2	38.8	39.3	0.4
F400	0.701	0.697	0.719	0.850	38.3	38.1	39.3	38.6	0.3
F300	0.741	0.752	0.710	0.838	40.5	41.1	38.8	40.1	1.0
SAN	0.768	0.761	0.806	0.838	42.0	41.6	44.1	42.5	1.2
SAD	0.723	0.742	0.751	0.752	39.5	40.5	41.0	40.4	0.4
NZ	0.775	0.762	0.725	0.754	42.3	41.6	39.6	41.2	1.3
NZH	0.854	0.861	0.883	0.874	46.7	47.0	48.2	47.3	0.5

Table A.7. Final concentration of lincomycin in solution at 7 days of stirring (130 rpm, Initial lincomycin concentration 50 ppm, temperature 280 K) at different concentration of adsorbents

Adsorbent	ABSORBANCE			Average	CONCENTRATION (ppm)			Average (ppm)	Standard deviation (ppm)
	Sample 1	Sample 2	Sample 3		Sample 1	Sample 2	Sample 3		
C1240	0.68	0.682	0.697	0.871	37.2	37.3	38.1	37.5	0.2
NR	0.675	0.681	0.711	0.870	36.9	37.2	38.9	37.6	0.7
F400	0.692	0.678	0.705	0.850	37.8	37.0	38.5	37.8	0.4
F300	0.731	0.735	0.690	0.838	39.9	40.2	37.7	39.3	1.2
SAN	0.769	0.761	0.797	0.838	42.0	41.6	43.5	42.4	0.7
SAD	0.731	0.738	0.746	0.752	39.9	40.3	40.8	40.3	0.1
NZ	0.772	0.755	0.743	0.754	42.2	41.3	40.6	41.3	0.4
NZH	0.851	0.867	0.891	0.874	46.5	47.4	48.7	47.5	0.8

Table A.8. Final concentration of lincomycin in solution at 8 days of stirring (130 rpm, Initial lincomycin concentration 50 ppm, temperature 280 K) at different concentration of adsorbents

Adsorbent	ABSORBANCE			Average	CONCENTRATION (ppm)			Average (ppm)	Standard deviation (ppm)
	Sample 1	Sample 2	Sample 3		Sample 1	Sample 2	Sample 3		
C1240	0.681	0.675	0.676	0.871	37.2	36.9	36.9	37.0	0.1
NR	0.674	0.683	0.676	0.870	36.8	37.3	36.9	37.0	0.1
F400	0.696	0.676	0.673	0.850	38.0	36.9	36.8	37.2	0.3
F300	0.705	0.718	0.683	0.838	38.5	39.2	37.3	38.4	0.6
SAN	0.765	0.763	0.797	0.838	41.8	41.7	43.6	42.3	0.7
SAD	0.735	0.735	0.749	0.752	40.2	40.2	40.9	40.4	0.1
NZ	0.774	0.753	0.734	0.754	42.3	41.1	40.1	41.2	0.8
NZH	0.848	0.867	0.899	0.874	46.3	47.4	49.1	47.6	1.3

Table A.9. Final concentration of lincomycin in solution at 9 days of stirring (130 rpm, Initial lincomycin concentration 50 ppm, temperature 280 K) at different concentration of adsorbents

Adsorbent	ABSORBANCE			Average	CONCENTRATION (ppm)			Average (ppm)	Standard deviation (ppm)
	Sample 1	Sample 2	Sample 3		Sample 1	Sample 2	Sample 3		
C1240	0.678	0.674	0.671	0.871	37.0	36.8	36.7	36.8	0.1
NR	0.672	0.679	0.654	0.870	36.7	37.1	35.7	36.5	0.3
F400	0.688	0.679	0.666	0.850	37.6	37.1	36.4	37.0	0.2
F300	0.712	0.715	0.674	0.838	38.9	39.1	36.8	38.3	1.0
SAN	0.761	0.763	0.802	0.838	41.6	41.7	43.8	42.4	1.1
SAD	0.735	0.741	0.736	0.752	40.2	40.5	40.2	40.3	0.1
NZ	0.771	0.748	0.749	0.754	42.1	40.9	40.9	41.3	0.3
NZH	0.847	0.869	0.884	0.874	46.3	47.5	48.3	47.3	0.7

Table A.10. Final concentration of lincomycin in solution at 10 days of stirring (130 rpm, Initial lincomycin concentration 50 ppm, temperature 280 K) at different concentration of adsorbents

Adsorbent	ABSORBANCE			Average	CONCENTRATION (ppm)			Average (ppm)	Standard deviation (ppm)
	Sample 1	Sample 2	Sample 3		Sample 1	Sample 2	Sample 3		
C1240	0.676	0.672	0.680	0.871	36.9	36.7	37.2	36.9	0.1
NR	0.681	0.675	0.690	0.870	37.2	36.9	37.7	37.3	0.1
F400	0.692	0.693	0.619	0.850	37.8	37.9	33.8	36.5	3.6
F300	0.702	0.719	0.678	0.838	38.4	39.3	37.0	38.2	0.9
SAN	0.758	0.762	0.803	0.838	41.4	41.6	43.9	42.3	1.2
SAD	0.731	0.734	0.749	0.752	39.9	40.1	40.9	40.3	0.2
NZ	0.771	0.748	0.745	0.754	42.1	40.9	40.7	41.2	0.4
NZH	0.839	0.868	0.885	0.874	45.8	47.4	48.4	47.2	1.1

Table A.11. Final concentration of lincomycin in solution at 11 days of stirring (130 rpm, Initial lincomycin concentration 50 ppm, temperature 280 K) at different concentration of adsorbents

Adsorbent	ABSORBANCE			Average	CONCENTRATION (ppm)			Average (ppm)	Standard deviation (ppm)
	Sample 1	Sample 2	Sample 3		Sample 1	Sample 2	Sample 3		
C1240	0.679	0.669	0.690	0.871	37.1	36.6	37.7	37.1	0.2
NR	0.675	0.679	0.693	0.870	36.9	37.1	37.9	37.3	0.2
F400	0.688	0.69	0.677	0.850	37.6	37.7	37.0	37.4	0.1
F300	0.703	0.715	0.687	0.838	38.4	39.1	37.6	38.3	0.4
SAN	0.761	0.758	0.800	0.838	41.6	41.4	43.7	42.2	1.1
SAD	0.721	0.731	0.761	0.752	39.4	39.9	41.6	40.3	0.9
NZ	0.777	0.748	0.736	0.754	42.5	40.9	40.2	41.2	0.9
NZH	0.845	0.865	0.887	0.874	46.2	47.3	48.5	47.3	0.9

Table A.12. Final concentration of lincomycin in solution at 12 days of stirring (130 rpm, Initial lincomycin concentration 50 ppm, temperature 280 K) at different concentration of adsorbents

Adsorbent	ABSORBANCE			Average	CONCENTRATION (ppm)			Average (ppm)	Standard deviation (ppm)
	Sample 1	Sample 2	Sample 3		Sample 1	Sample 2	Sample 3		
C1240	0.681	0.665	0.692	0.871	37.2	36.3	37.8	37.1	0.4
NR	0.664	0.671	0.712	0.870	36.3	36.7	38.9	37.3	1.4
F400	0.675	0.671	0.709	0.850	36.9	36.7	38.8	37.4	0.9
F300	0.707	0.713	0.685	0.838	38.6	39.0	37.5	38.3	0.4
SAN	0.761	0.769	0.784	0.838	41.6	42.0	42.8	42.1	0.3
SAD	0.731	0.728	0.754	0.752	39.9	39.8	41.2	40.3	0.4
NZ	0.771	0.725	0.763	0.754	42.1	39.6	41.7	41.1	1.2
NZH	0.845	0.867	0.877	0.874	46.2	47.4	47.9	47.2	0.5

Later, a single factor ANOVA analysis with LSD multiple range tests (95% confidence), for means analysis, was carried out, using Statgraphics Centurion XVI software. It was used for determining the statistically significant differences between the treatment times, and the minimum time from which no significant differences were detected, was selected as the adsorption equilibrium time. The criteria for selecting this equilibrium time was based on the p-value obtained in this analysis. If this value is greater than 0.05 comparing the concentration in two consecutive days, no statistical significant differences are detected. Results are presented in Table A.13

Table A.13. Equilibrium time determined by LSD multiple range test (95% confidence) using Statgraphics Centurion XVI software

Adsorbent	Adsorbent code	Equilibrium time (days)
Cabot Norit	C1240	7
Norit Row	NR	7
Filtrasorb 400	F400	5
Filtrasorb 300	F300	4
Sigma Aldrich Norit	SAN	2
Sigma Aldrich Darco	SAD	1
Natural zeolite	NZ	1
Modified natural zeolite	NZH	1

APPENDIX B. Adsorption isotherms of lincomycin on activated carbons and natural zeolite at different temperatures and pH values

Isotherms obtained by the adsorption of lincomycin on activated carbons and zeolites at different temperatures and pH values are presented below. Sips model was used for predicting the adsorption equilibrium data since this model provided the most accurate fitting. The complete set of adsorption isotherms of lincomycin on activated carbons and zeolites is presented below.

Adsorption isotherms of lincomycin in deionized water on activated carbon and natural zeolites at pH 6.5

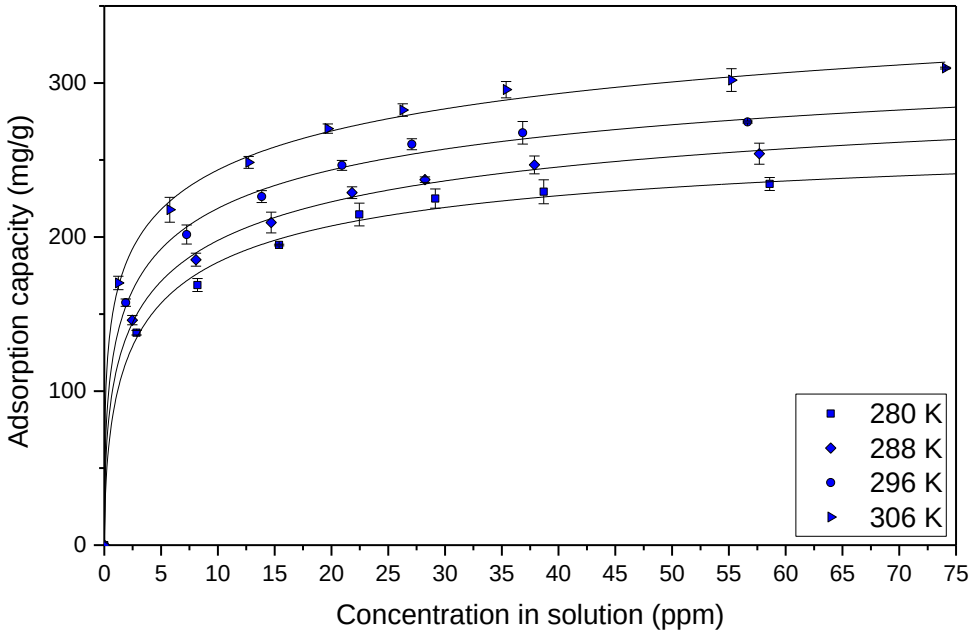

Figure B.1. Adsorption isotherms and Sips model fitting for adsorption of lincomycin on activated carbon 1240 at different temperatures and intial pH 6.5

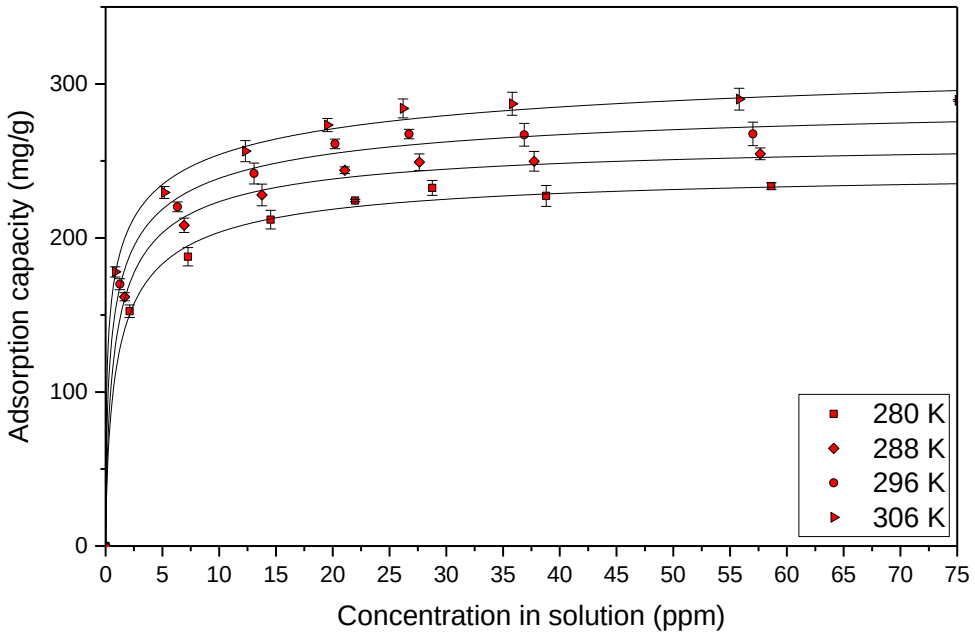

Figure B.2. Adsorption isotherms and Sips model fitting for adsorption of lincomycin on activated carbon NR at different temperatures and initial pH 6.5

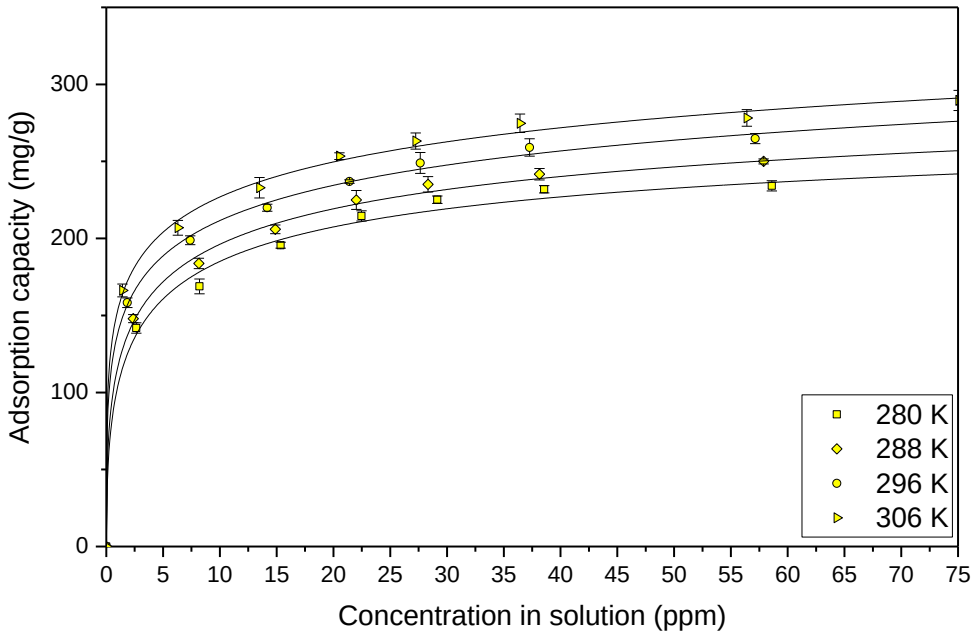

Figure B.3. Adsorption isotherms and Sips model fitting for adsorption of lincomycin on activated carbon F400 at different temperatures and initial pH 6.5

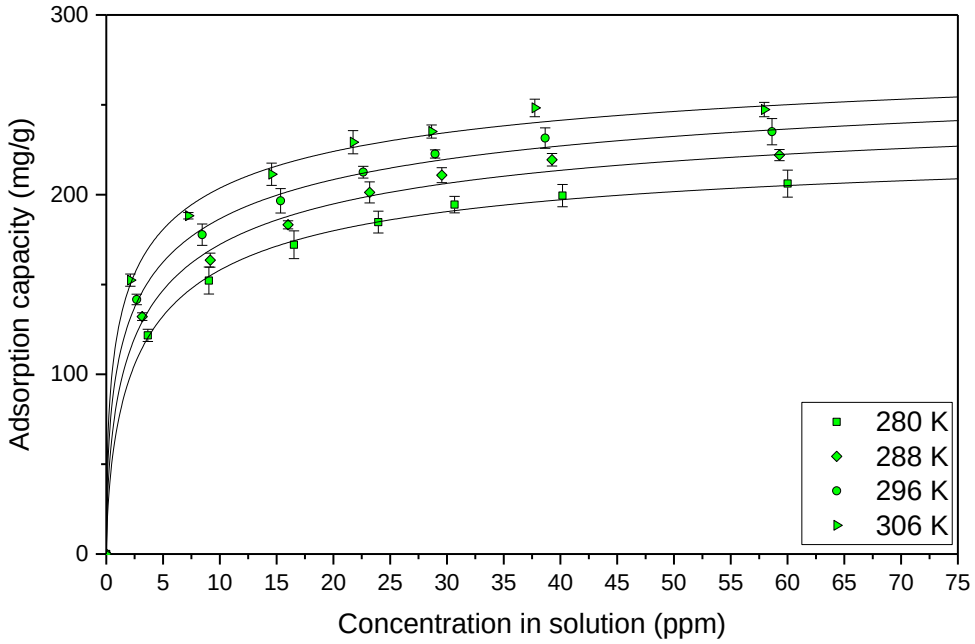

Figure B.4. Adsorption isotherms and Sips model fitting for adsorption of lincomycin on activated carbon F300 at different temperatures and initial pH 6.5

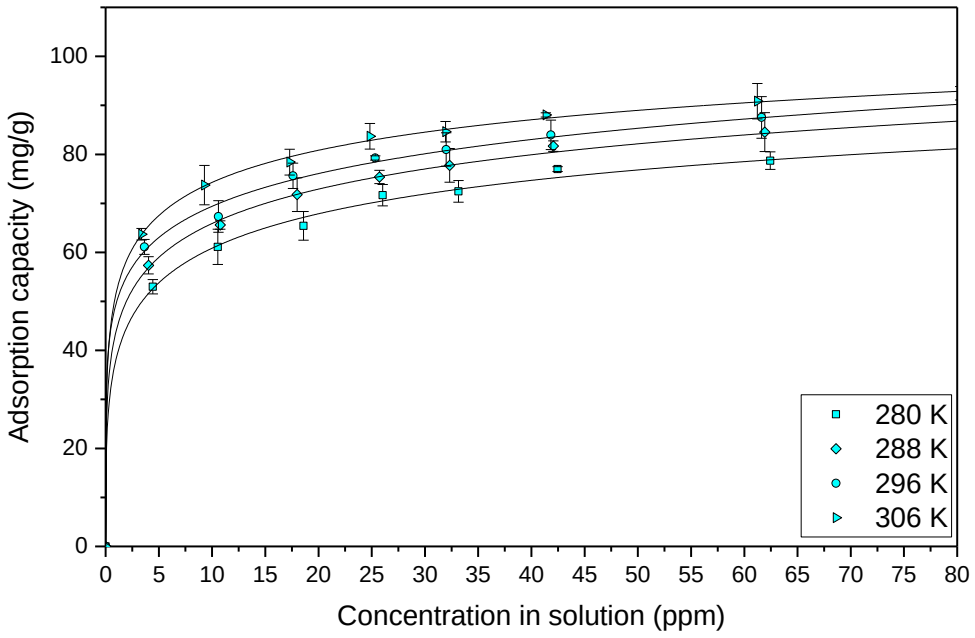

Figure B.5. Adsorption isotherms and Sips model fitting for adsorption of lincomycin on activated carbon SAN at different temperatures and initial pH 6.5

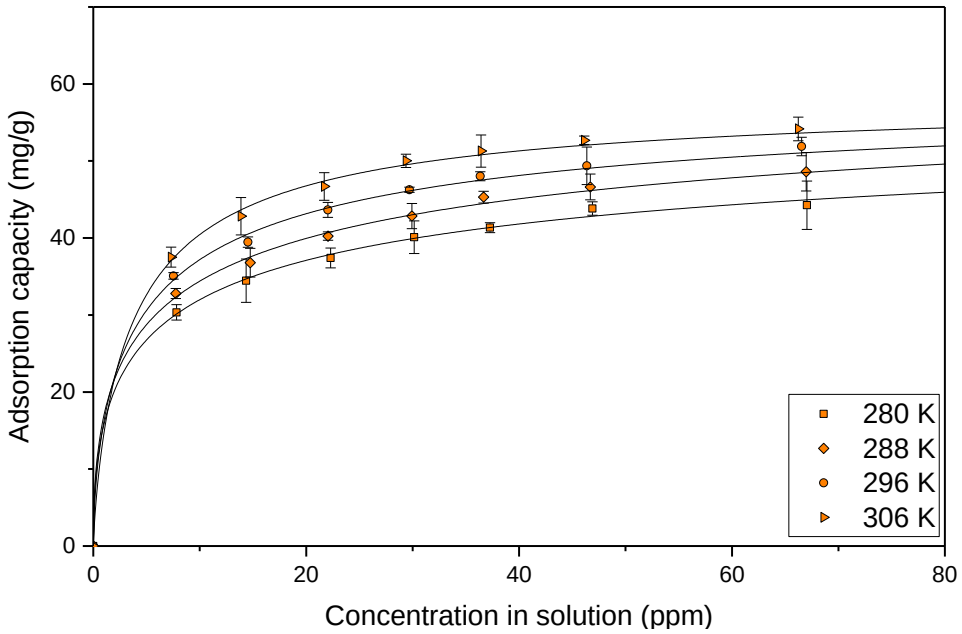

Figure B.6. Adsorption isotherms and Sips model fitting for adsorption of lincomycin on activated carbon SAD at different temperatures and initial pH 6.5

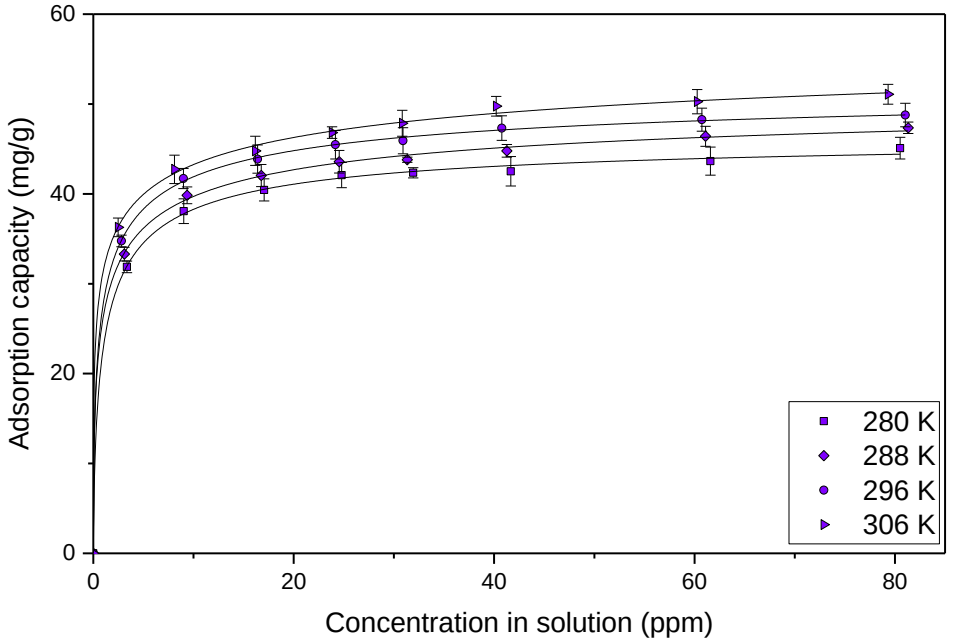

Figure B.7. Adsorption isotherms and Sips model fitting for adsorption of lincomycin on natural zeolite at different temperatures and initial pH 6.5

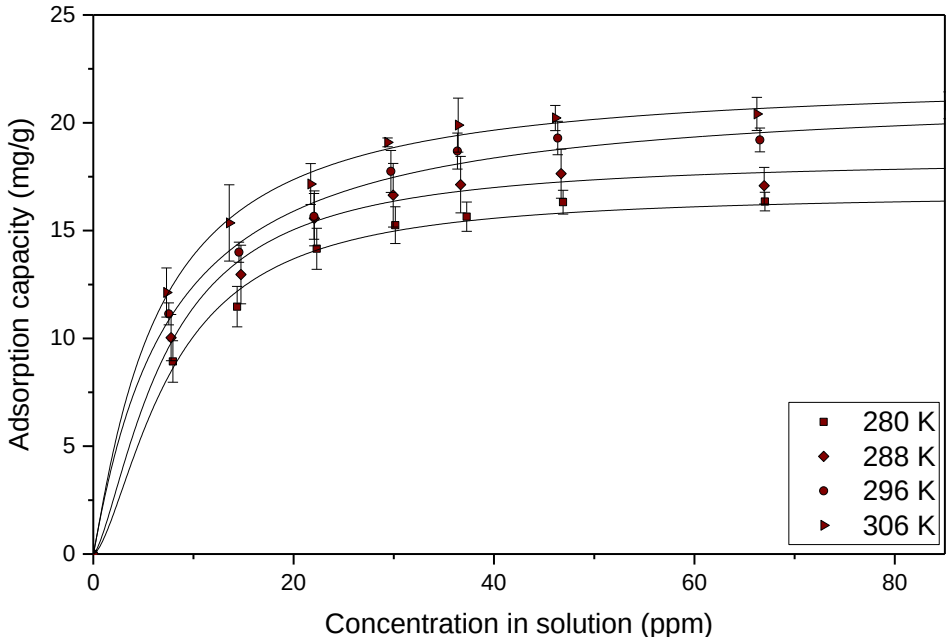

Figure B.8. Adsorption isotherms and Sips model fitting for adsorption of lincomycin on modified natural zeolite at different temperatures and initial pH 6.5

Adsorption isotherms of lincomycin in deionized water on activated carbon at pH 10.0

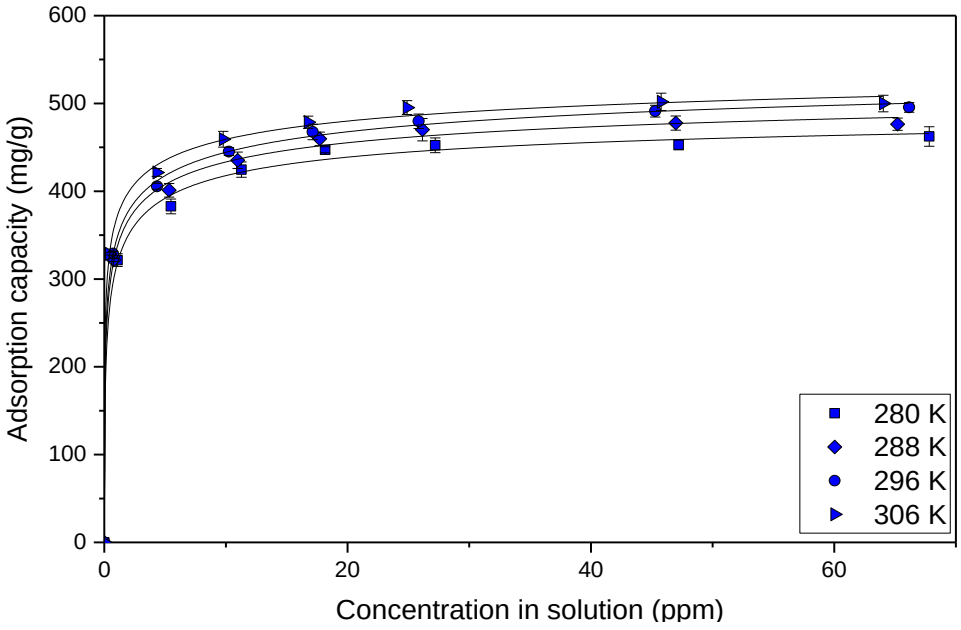

Figure B.9. Adsorption isotherms and Sips model fitting for adsorption of lincomycin on activated carbon 1240 at different temperatures and initial pH 10.0

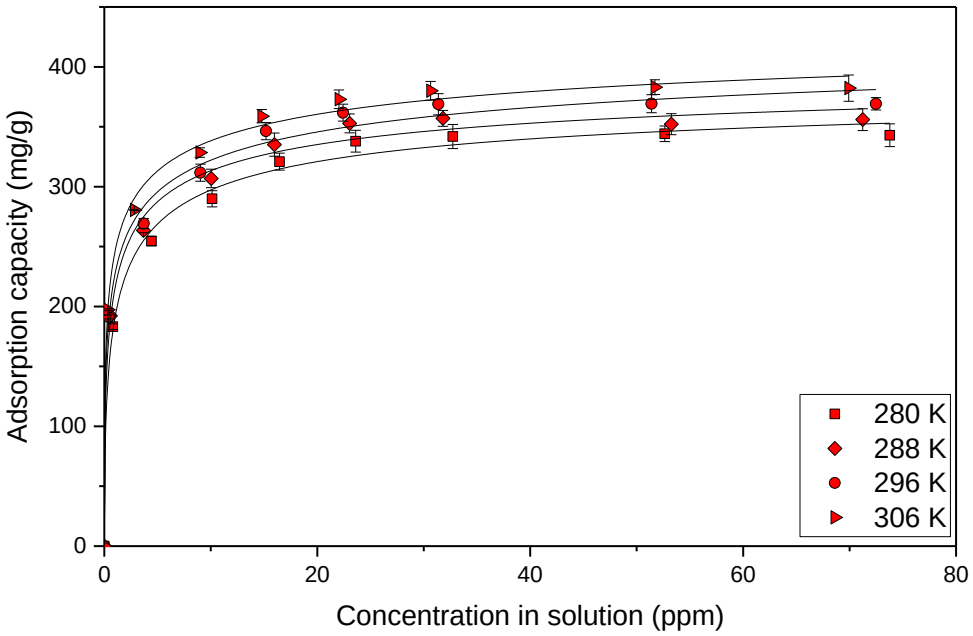

Figure B.10. Adsorption isotherms and Sips model fitting for adsorption of lincomycin on activated carbon NR at different temperatures and initial pH 10.0

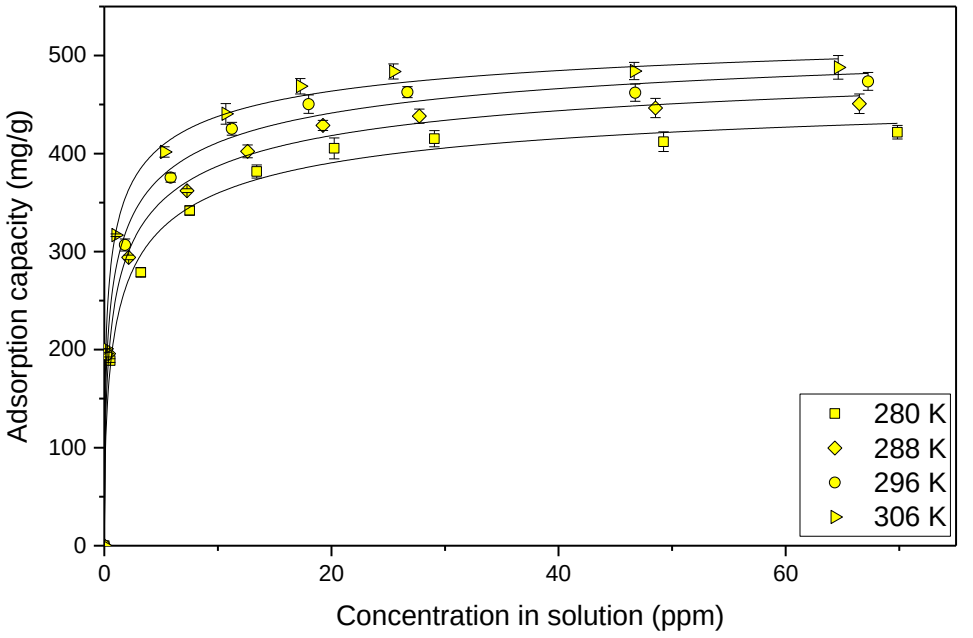

Figure B.11. Adsorption isotherms and Sips model fitting for adsorption of lincomycin on activated carbon F400 at different temperatures and initial pH 10.0

Adsorption isotherms of lincomycin in synthetic manure on activated carbons

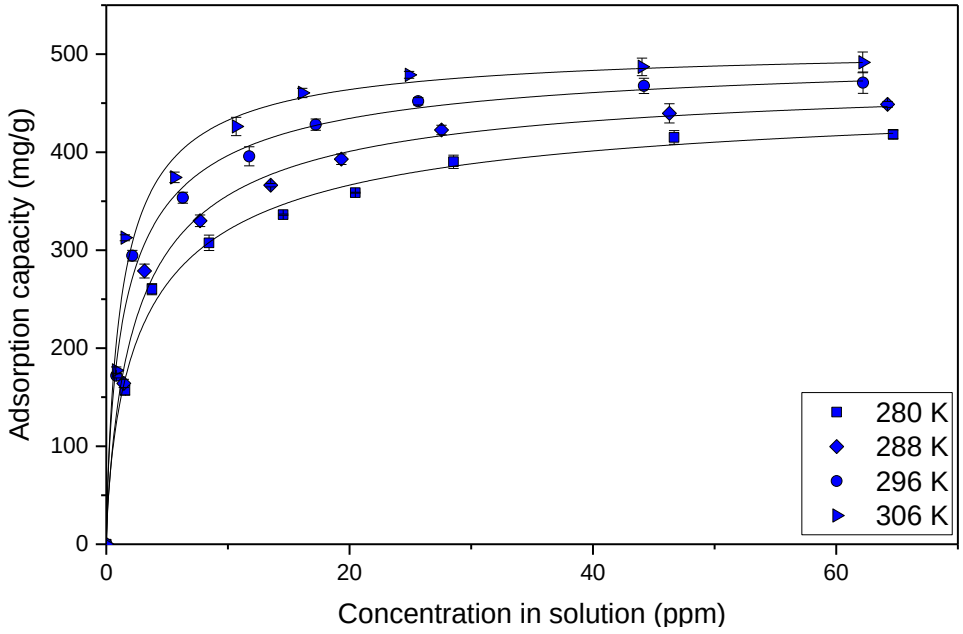

Figure B.12. Adsorption isotherms and Sips model fitting for adsorption of lincomycin in synthetic manure on activated carbon 1240 at different temperatures

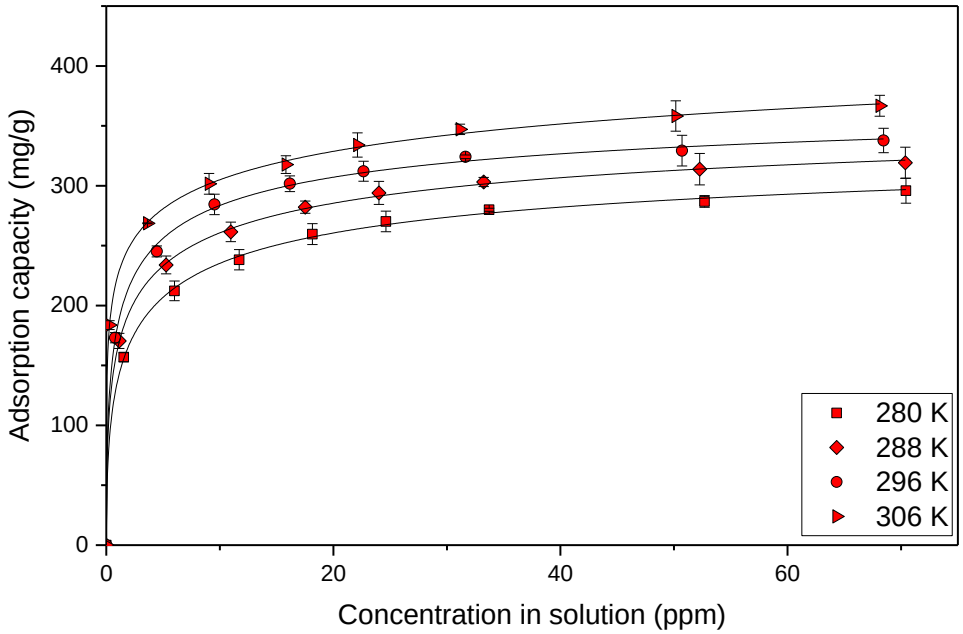

Figure B.13. Adsorption isotherms and Sips model fitting for adsorption of lincomycin in synthetic manure on activated carbon NR at different temperatures

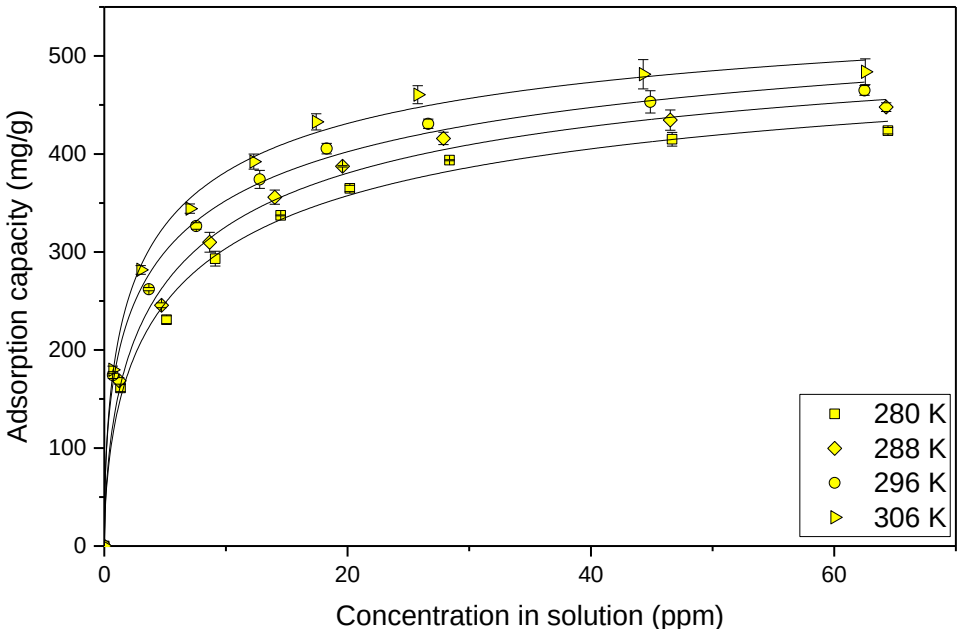

Figure B.14. Adsorption isotherms and Sips model fitting for adsorption of lincomycin in synthetic manure on activated carbon F400 at different temperatures

APPENDIX C. Statistical analysis of the influence of the temperature and different adsorbents in the adsorption capacity

To determine if the temperature variation origins statistically significant differences in the adsorption capacity, a statistical analysis was carried out. Thus, a two-factor (temperature and initial concentration) Analysis of Variance (ANOVA) with Least Significant Differences (LSD) multiple range tests (95% confidence), for means analysis, was carried out. Statgraphics Centurion software was used for performing this analysis. Table C.1 shows the p-Value, obtained from the ANOVA analysis related to the temperature variation, for different adsorbents at pH values 6.5 and 10.0.

Table C.1. p-Value for different adsorbents obtained from the ANOVA analysis performed for the influence of the temperature (280-306 K) on the adsorption capacity.

pH	Adsorbent	P-Value	pH	Adsorbent	P-Value
6.5	1240	0.0000	10.0	1240	0.0000
	NR	0.0000		NR	0.0000
	F400	0.0000		F400	0.0000
	F300	0.0000		F300	-
	SAN	0.0000		SAN	-
	SAD	0.0000		SAD	-
	NZ	0.0000		NZ	-
	NZH	0.0000		NZH	-

*P-values lower than 0.05 represent that statistical significant differences in the adsorption capacity values are caused by the temperature variation

From the results shown in Table C.1, it was found that for all the adsorbents, the statistical parameter p-Value was less than 0.05. Therefore, at 95.0% confidence level, it was determined that temperature is a statistically significant variable on the adsorption capacity.

APPENDIX D. Determination of the thermodynamic equilibrium constants at different temperatures and pH values in the adsorption of lincomycin on activated carbons and zeolites

Thermodynamic equilibrium constant for the adsorption of lincomycin on activated carbons and zeolites in deionized water was determined using the methodology proposed by Khan & Singh (1987) explained in chapter two. The distribution coefficient can be determined by plotting $\ln(qe/Ce)$ vs qe and extrapolating qe to zero. Besides, the correction proposed by Milonjic [98] was used for converting the distribution coefficient into the thermodynamic equilibrium constant in this study. Equation (2.8) describes this correction. The following Figures present the plots $\ln(qe/Ce)$ vs qe for different adsorbents, temperatures and pH values.

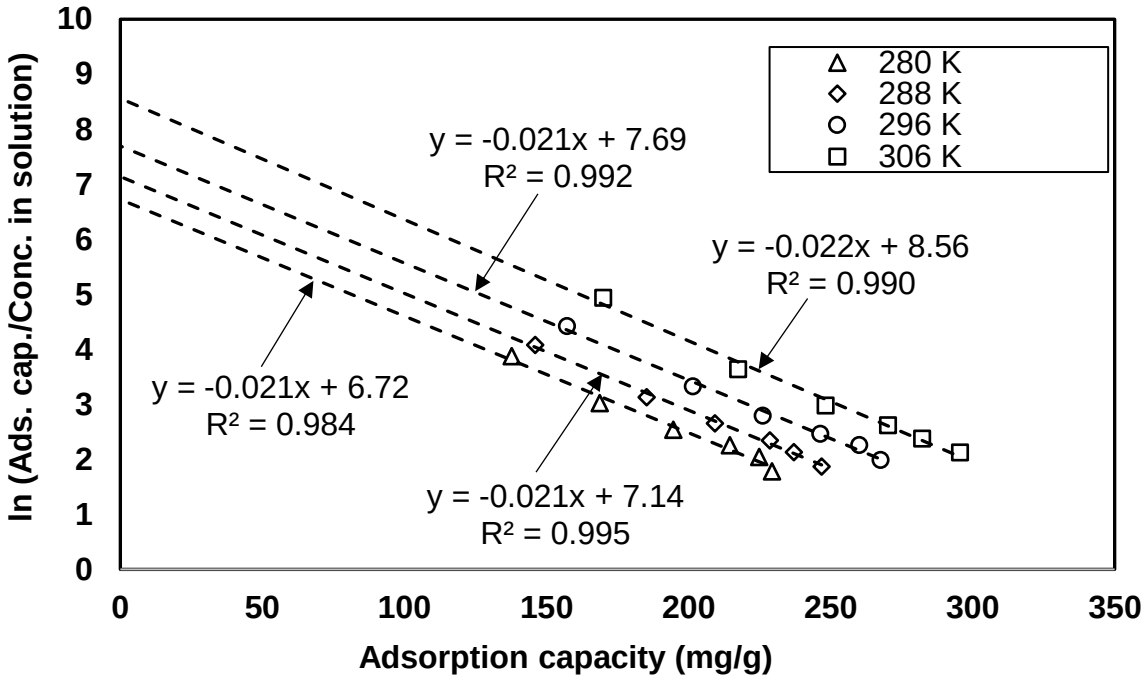

Figure D.1. Ln (adsorption capacity/concentration in solution) vs adsorption capacity plot for the adsorption of lincomycin on 1240 activated carbon at different temperatures and pH 6.5

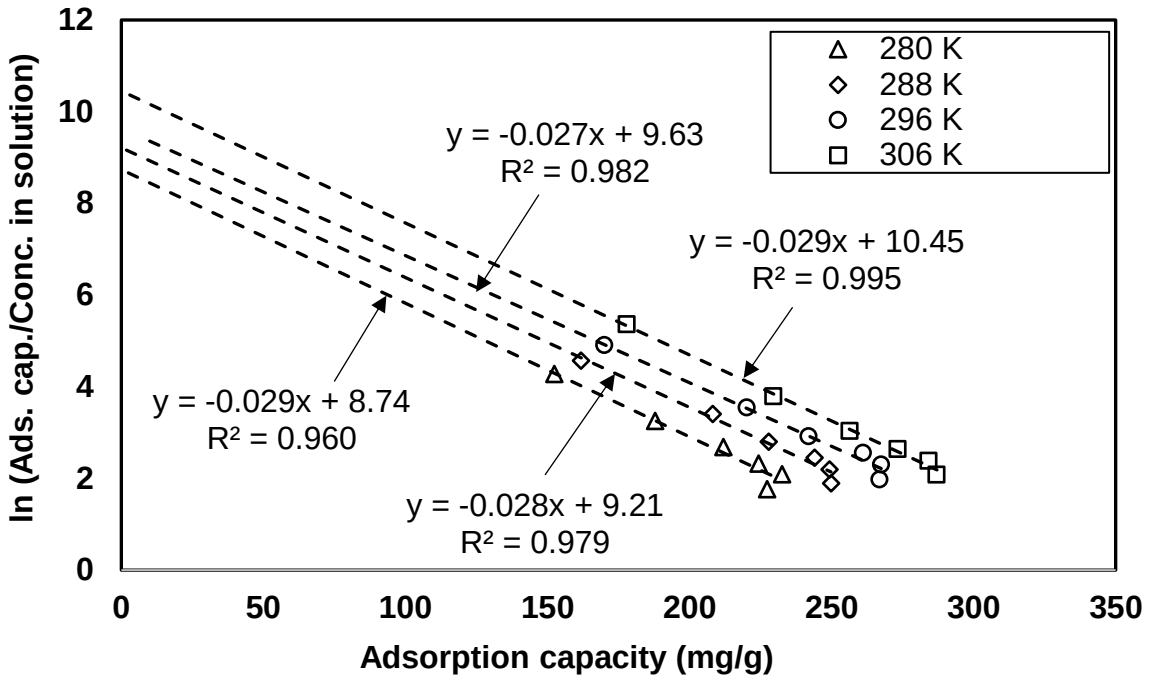

Figure D.2. Ln (adsorption capacity/concentration in solution) vs adsorption capacity plot for the adsorption of lincomycin on NR activated carbon at different temperatures and pH 6.5

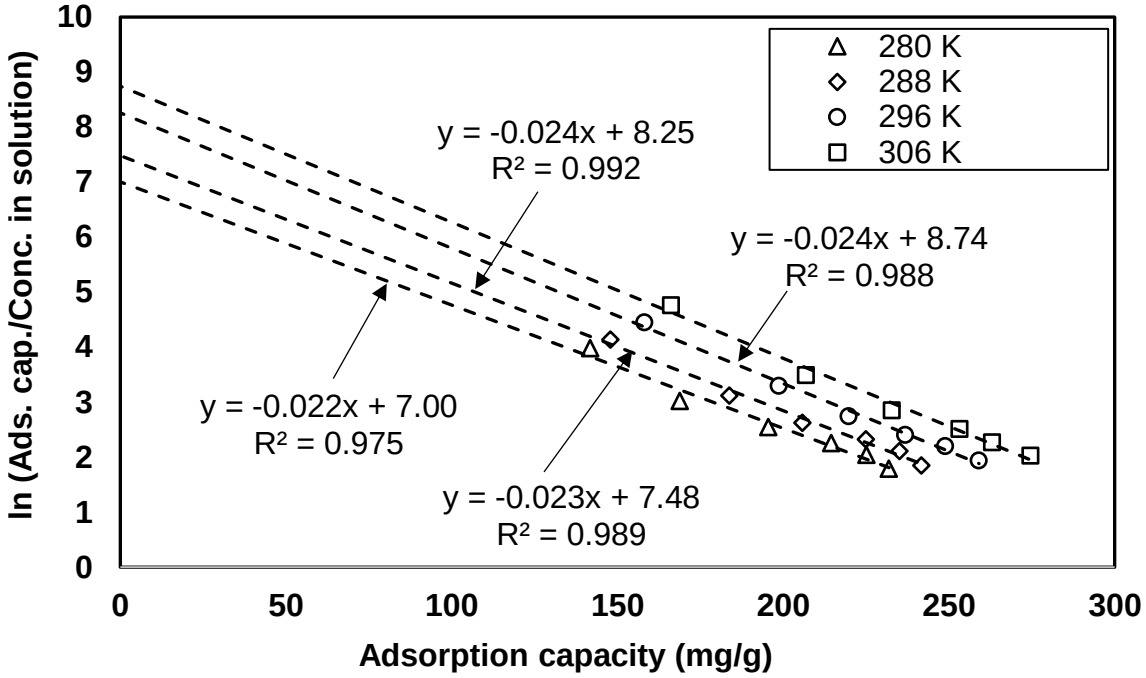

Figure D.3. Ln (adsorption capacity/concentration in solution) vs adsorption capacity plot for the adsorption of lincomycin on F400 activated carbon at different temperatures and pH 6.5

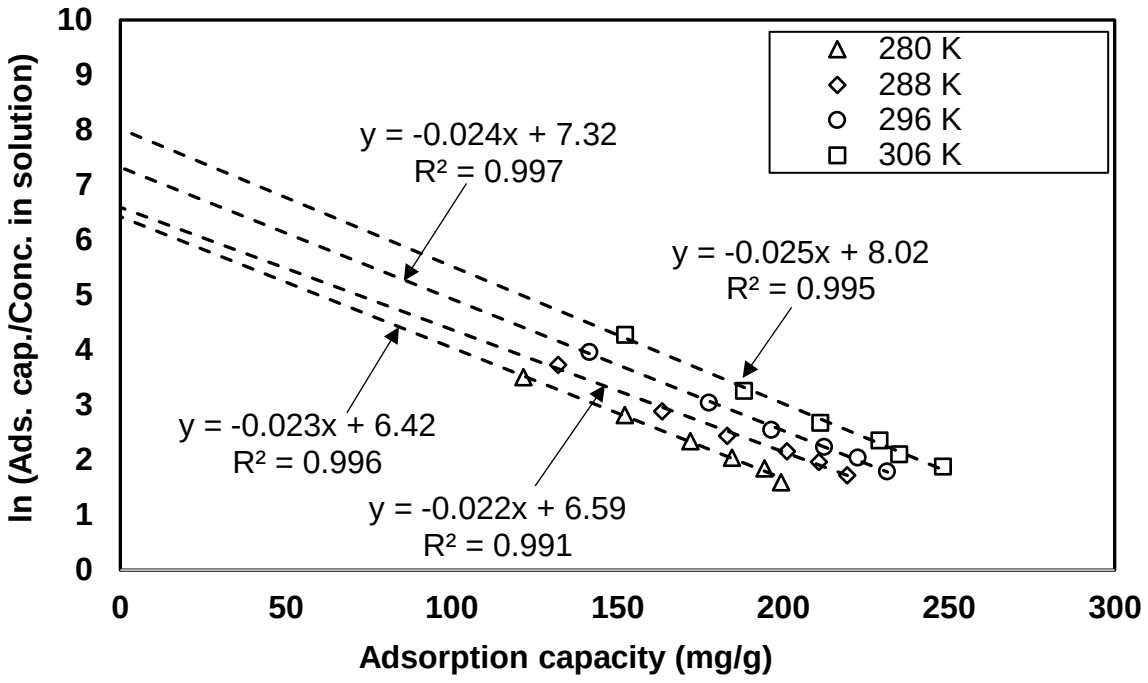

Figure D.4. Ln (adsorption capacity/concentration in solution) vs adsorption capacity plot for the adsorption of lincomycin on F300 activated carbon at different temperatures and pH 6.5

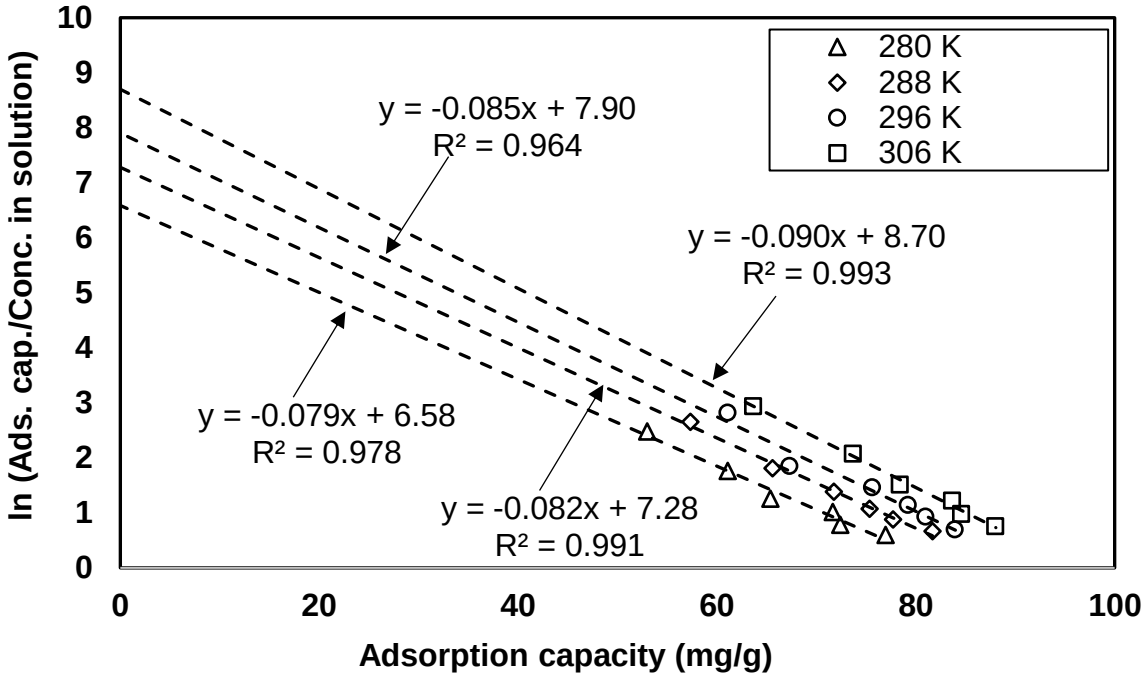

Figure D.5. Ln (adsorption capacity/concentration in solution) vs adsorption capacity plot for the adsorption of lincomycin on SAN activated carbon at different temperatures and pH 6.5

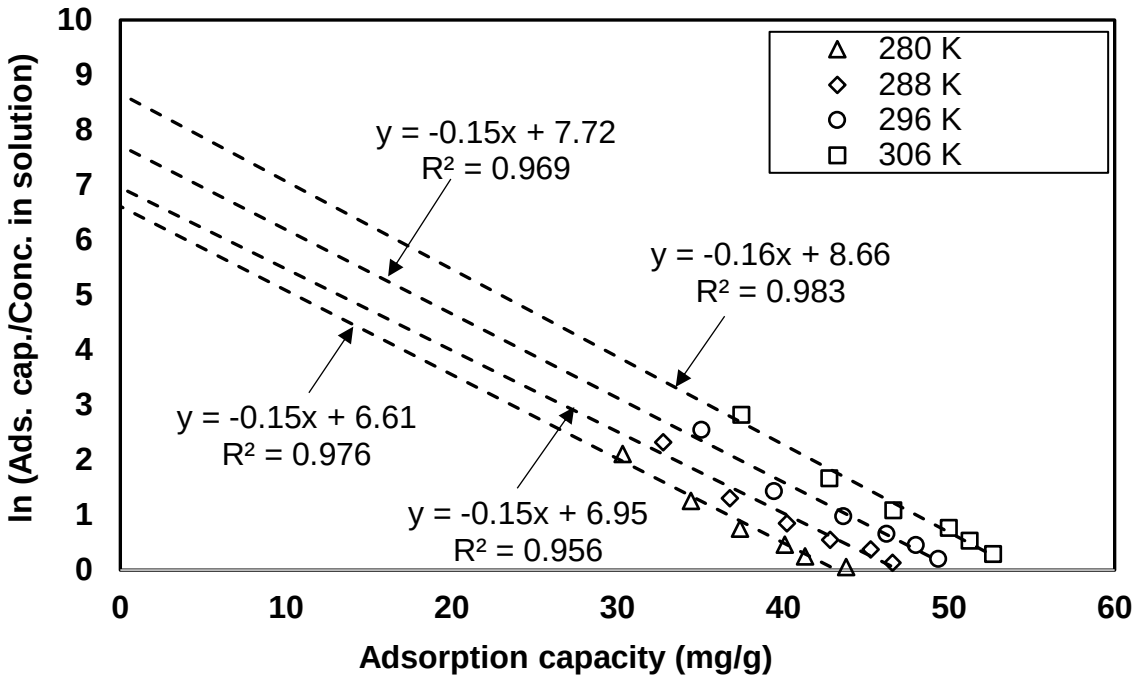

Figure D.6. Ln (adsorption capacity/concentration in solution) vs adsorption capacity plot for the adsorption of lincomycin on SAD activated carbon at different temperatures and pH 6.5

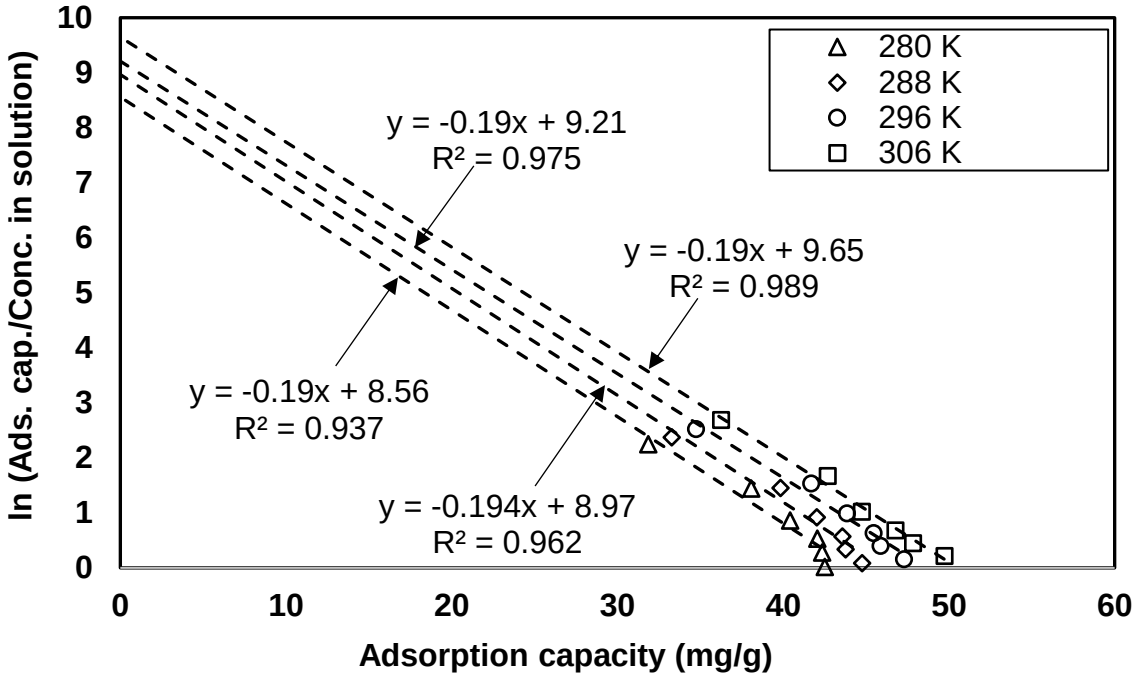

Figure D.7. Ln (adsorption capacity/concentration in solution) vs adsorption capacity plot for the adsorption of lincomycin on natural zeolite at different temperatures and pH 6.5

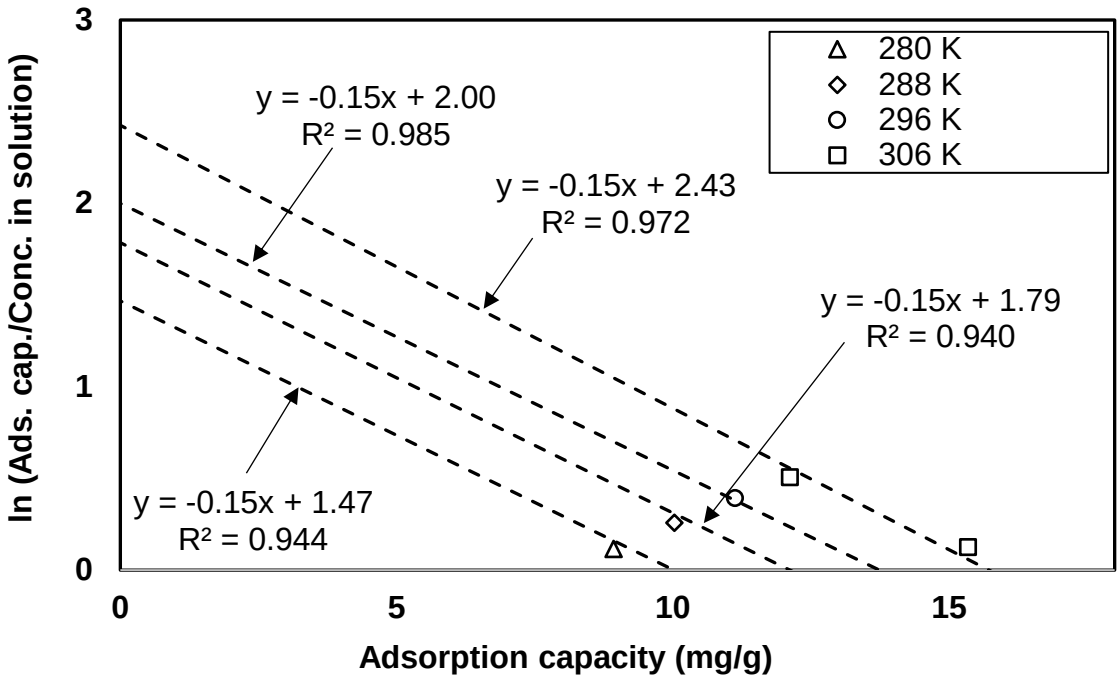

Figure D.8. Ln (adsorption capacity/concentration in solution) vs adsorption capacity plot for the adsorption of lincomycin on modified natural zeolite at different temperatures and pH 6.5

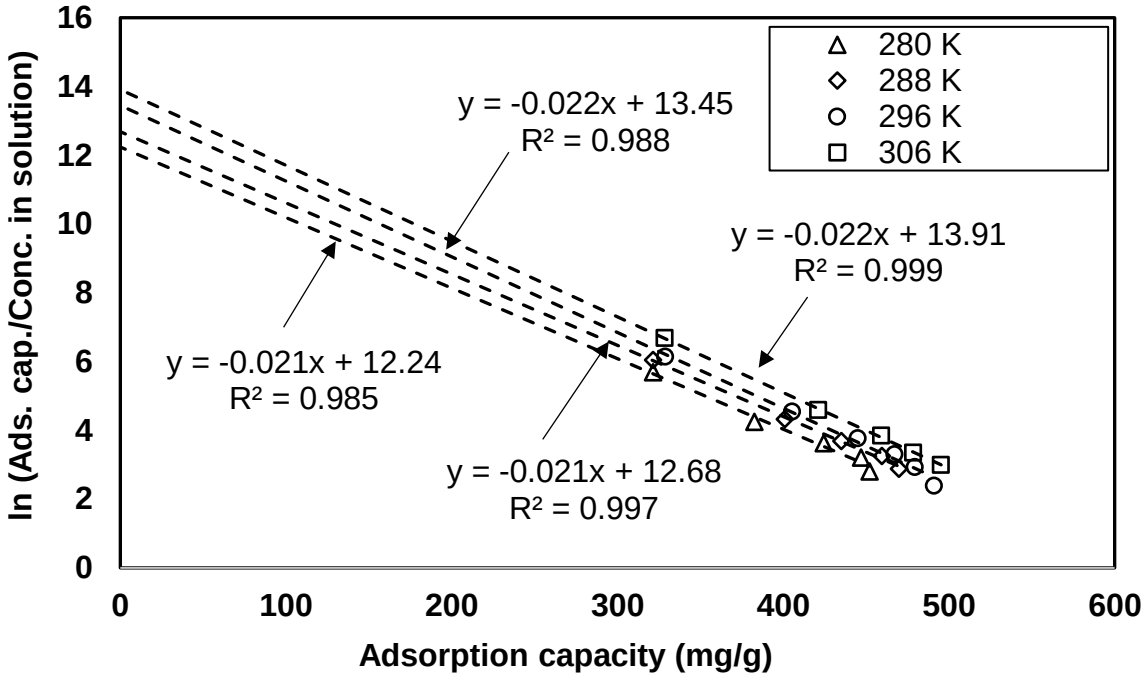

Figure D.9. Ln (adsorption capacity/concentration in solution) vs adsorption capacity plot for the adsorption of lincomycin on 1240 activated carbon at different temperatures and pH 10

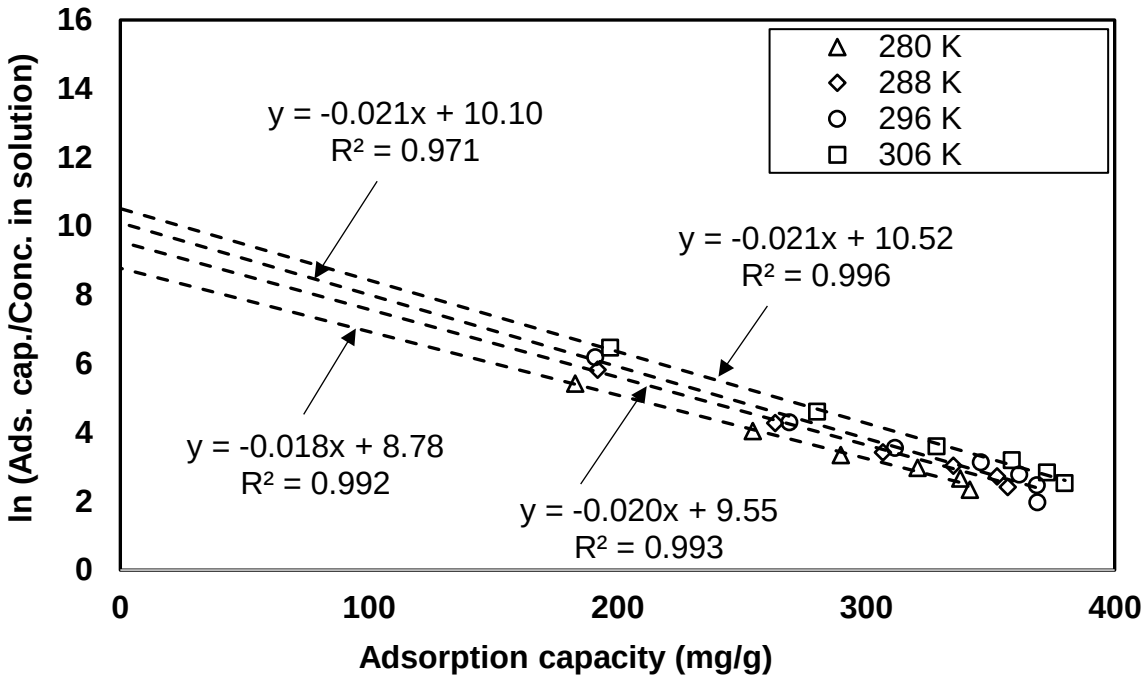

Figure D.10. Ln (adsorption capacity/concentration in solution) vs adsorption capacity plot for the adsorption of lincomycin on NR activated carbon at different temperatures and pH 10

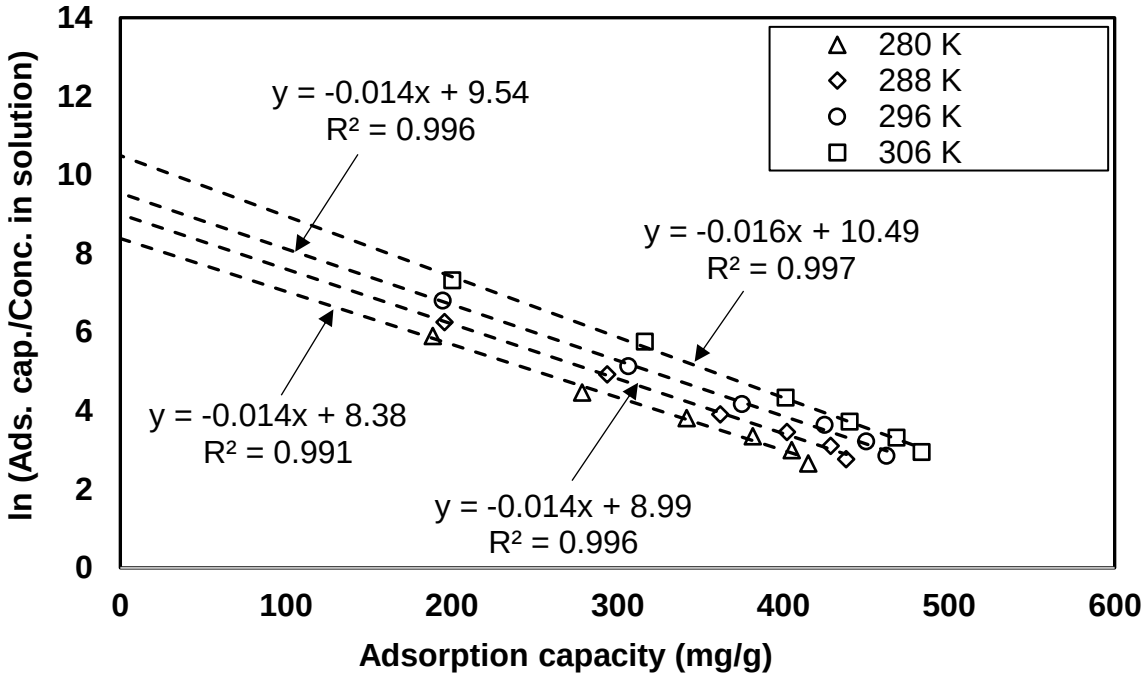

Figure D.11. Ln (adsorption capacity/concentration in solution) vs adsorption capacity plot for the adsorption of lincomycin on F400 activated carbon at different temperatures and pH 10

From the results presented in the plots ln(qe/Ce) vs qe it was possible to calculate the corresponding thermodynamic equilibrium constants (Kc) values. Results are presented in Table D.1 and Table D.2.

Table D.1. Thermodynamic equilibrium constants for the adsorption of lincomycin on activated carbons and natural zeolites at different temperatures and pH 6.5

Adsorbent	Temperature (K)	Ln(Kd) (L/g)	Kc*10^{-6}	Adsorbent	Temperature (K)	Ln(Kd) (L/g)	Kc*10^{-6}
1240	280	6.72	0.83	**NR**	280	8.74	6.23
	288	7.14	1.26		288	9.21	10.00
	296	7.69	2.19		296	9.64	15.3
	306	8.56	5.22		306	10.45	34.5
F400	280	7.00	1.10	**F300**	280	6.42	0.62
	288	7.48	1.77		288	6.59	0.73
	296	8.26	3.86		296	7.32	1.51
	306	8.74	6.26		306	8.02	3.04
SAN	280	6.59	0.73	**SAD**	280	6.61	0.74
	288	7.28	1.45		288	6.95	1.05
	296	7.90	2.70		296	7.72	2.25
	306	8.70	5.99		306	8.66	5.77
NZ	280	8.56	5.20	**NZH**	280	1.47	4.34E-03
	288	8.97	7.83		288	1.79	5.96E-03
	296	9.21	9.98		296	2.00	7.39E-03
	306	9.65	1.55		306	2.43	1.13E-04

Table D.2. Thermodynamic equilibrium constants for the adsorption of lincomycin on activated carbons and natural zeolites at different temperatures and pH 10.0

Adsorbent	Temperature (K)	Ln(Kd) (L/g)	$Kc*10^{-7}$
1240	280	12.239	20.6
	288	12.685	32.2
	296	13.448	69.1
	306	13.91	110
NR	280	8.7809	0.65
	288	9.5520	1.41
	296	10.101	2.43
	306	10.516	3.69
F400	280	8.3814	0.44
	288	8.9978	0.81
	296	9.5357	1.38
	306	10.492	3.60

APPENDIX E. Van't Hoff Plots for thermodynamic characterization of the adsorption of lincomycin on activated carbons and natural zeolite

Van't Hoff plots were used for determining the enthalpy and entropy changes using the slope and intercept of this trend respectively. Van't Hoff plots for the adsorption of lincomycin on activated carbons and natural zeolites at different pH values (1240, NR and F400) are presented below.

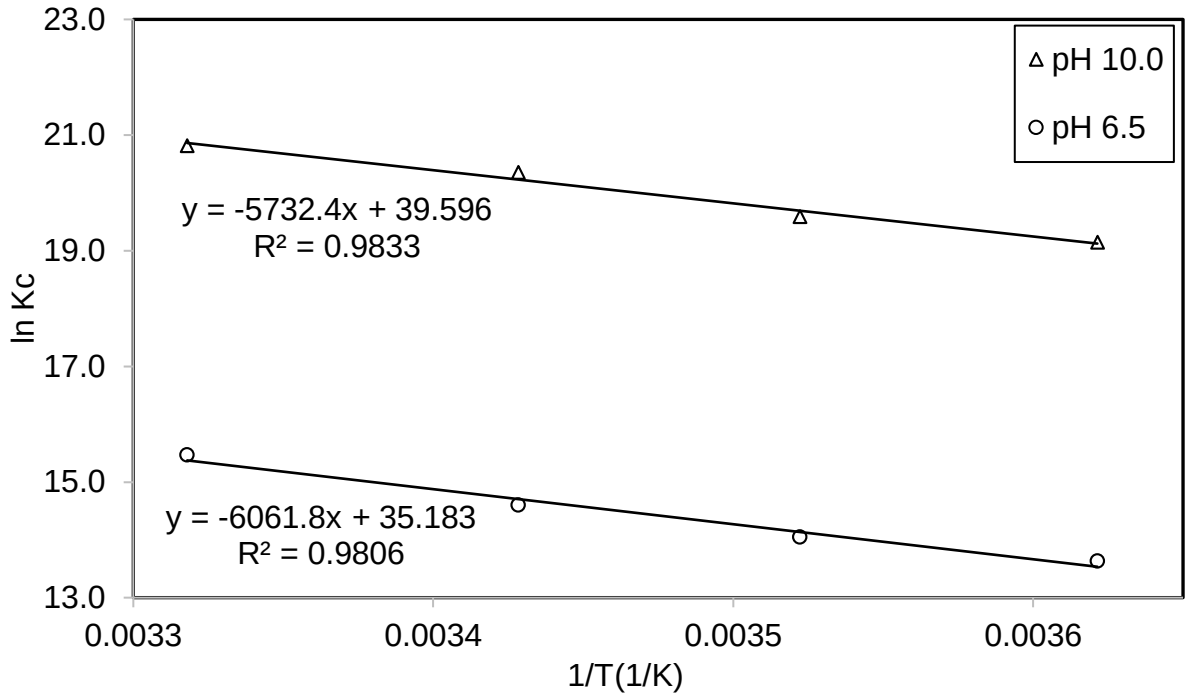

Figure E.1. Van't Hoff plot for thermodynamic analysis of adsorption of lincomycin on activated carbon 1240 at 280-306 K and pH values of 6.5 and 10

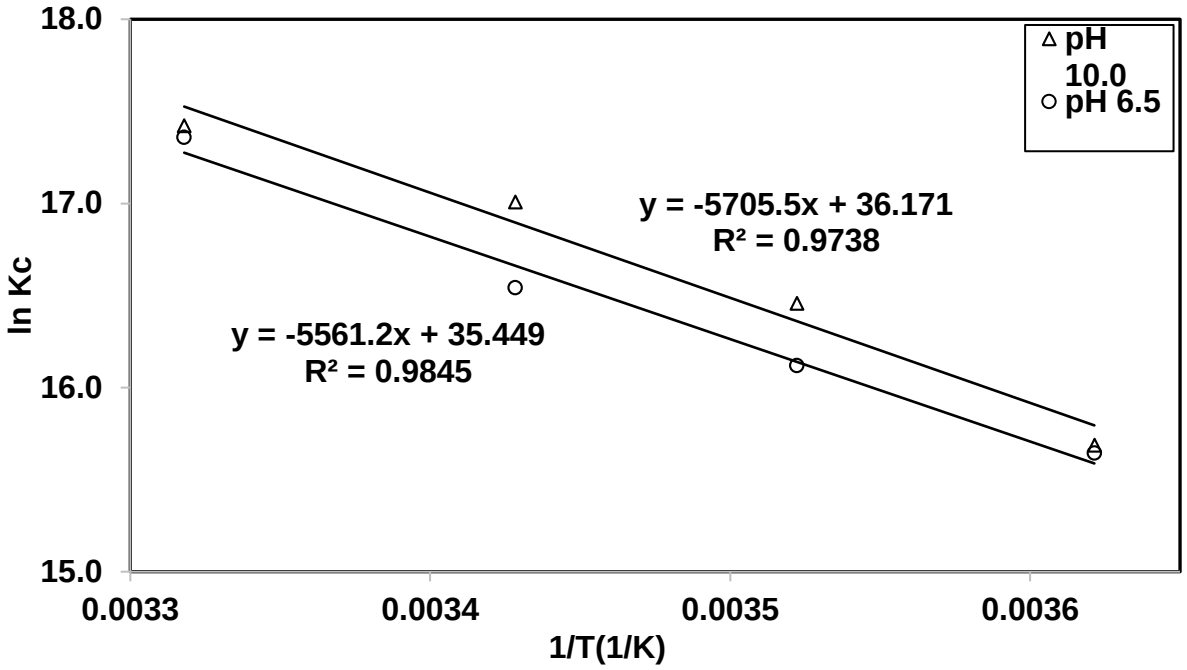

Figure E.2. Van't Hoff plot for thermodynamic analysis of adsorption of lincomycin on activated carbon NR at 280-306 K and pH values of 6.5 and 10

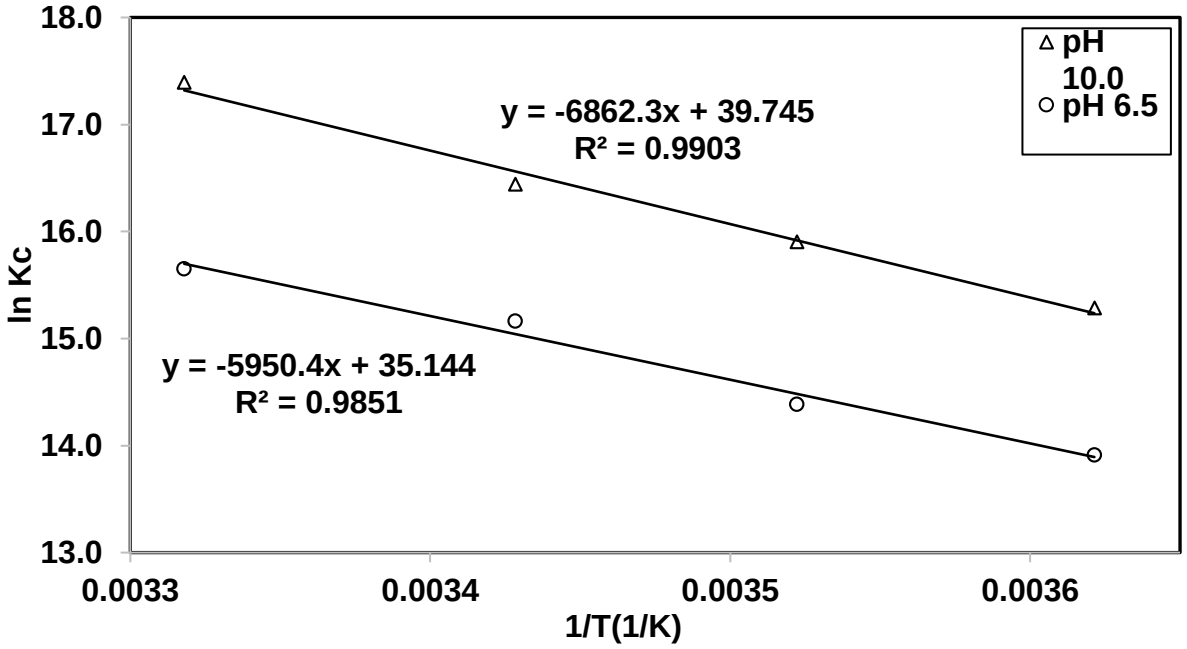

Figure E.3. Van't Hoff plot for thermodynamic analysis of adsorption of lincomycin on activated carbon F400 at 280-306 K and pH values of 6.5 and 10

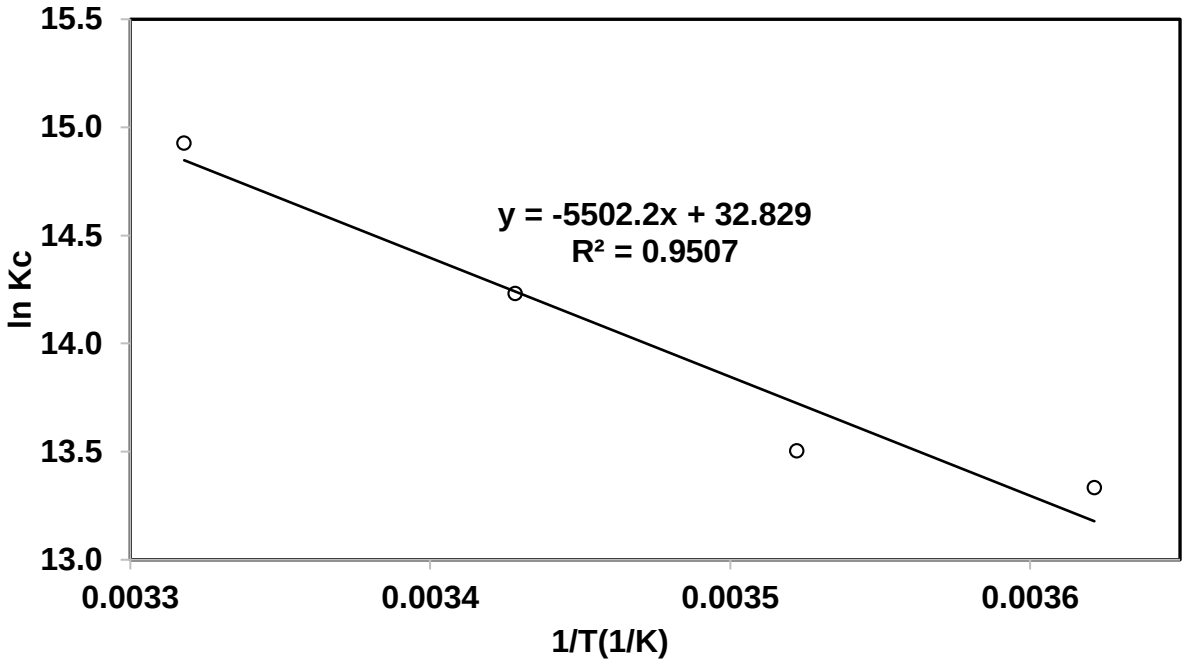

Figure E.4. Van't Hoff plot for thermodynamic analysis of adsorption of lincomycin on activated carbon F300 at 280-306 K and pH value of 6.5

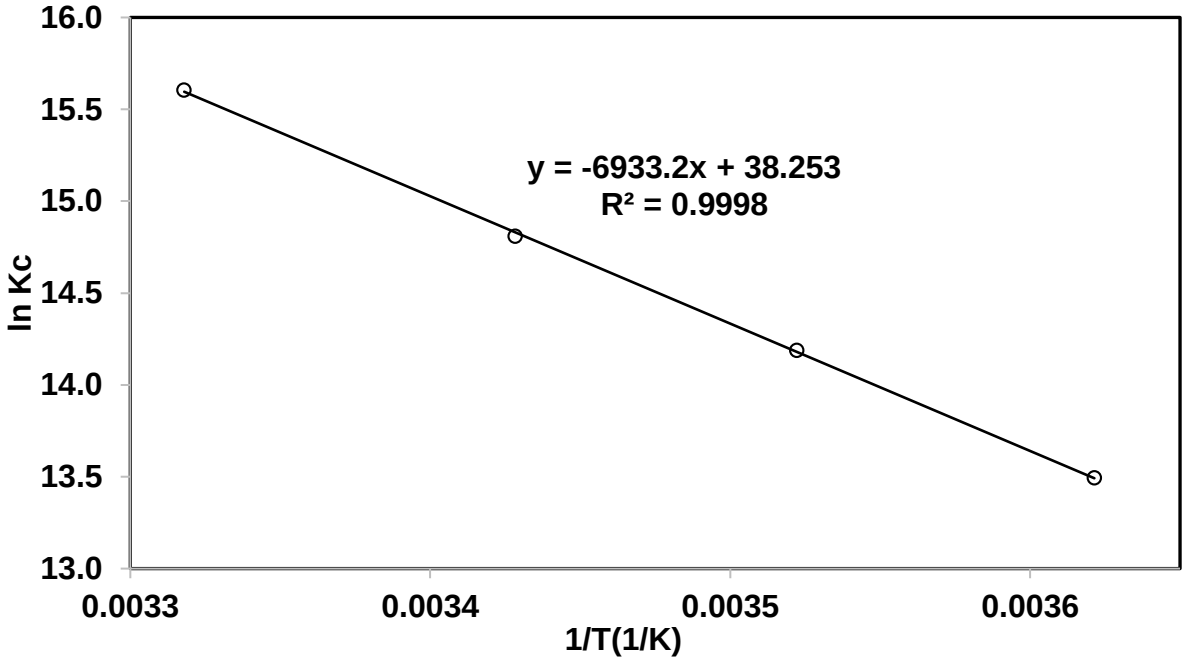

Figure E.5. Van't Hoff plot for thermodynamic analysis of adsorption of lincomycin on activated carbon SAN at 280-306 K and pH value of 6.5

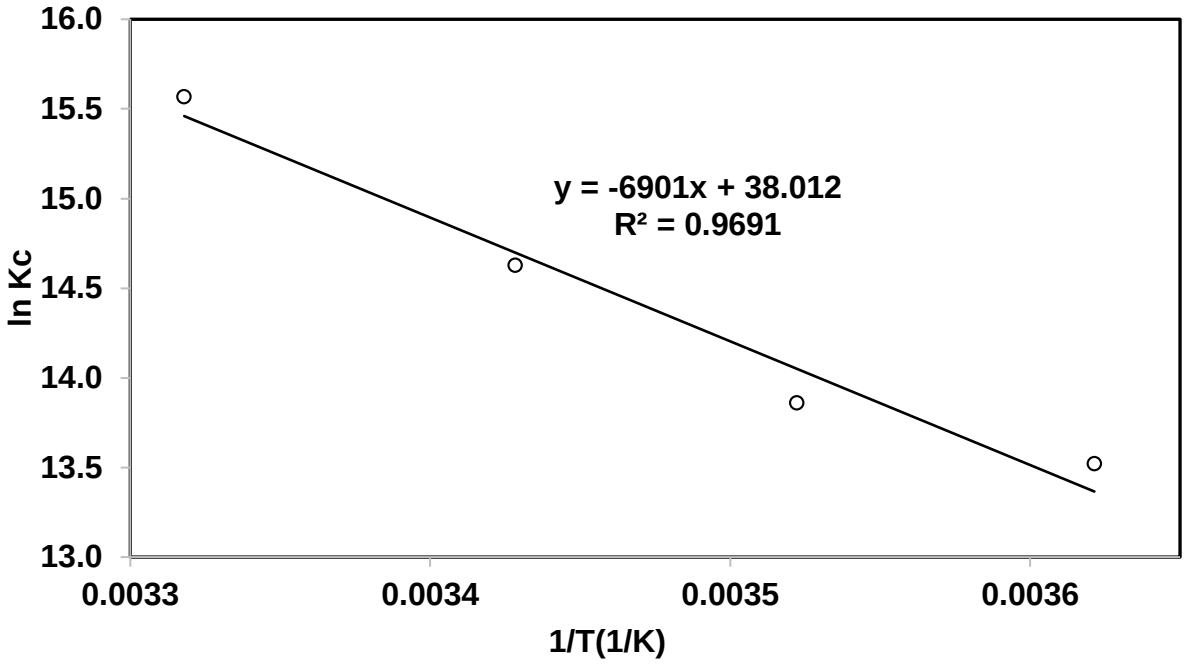

Figure E.6. Van't Hoff plot for thermodynamic analysis of adsorption of lincomycin on activated carbon SAD at 280-306 K and pH value of 6.5

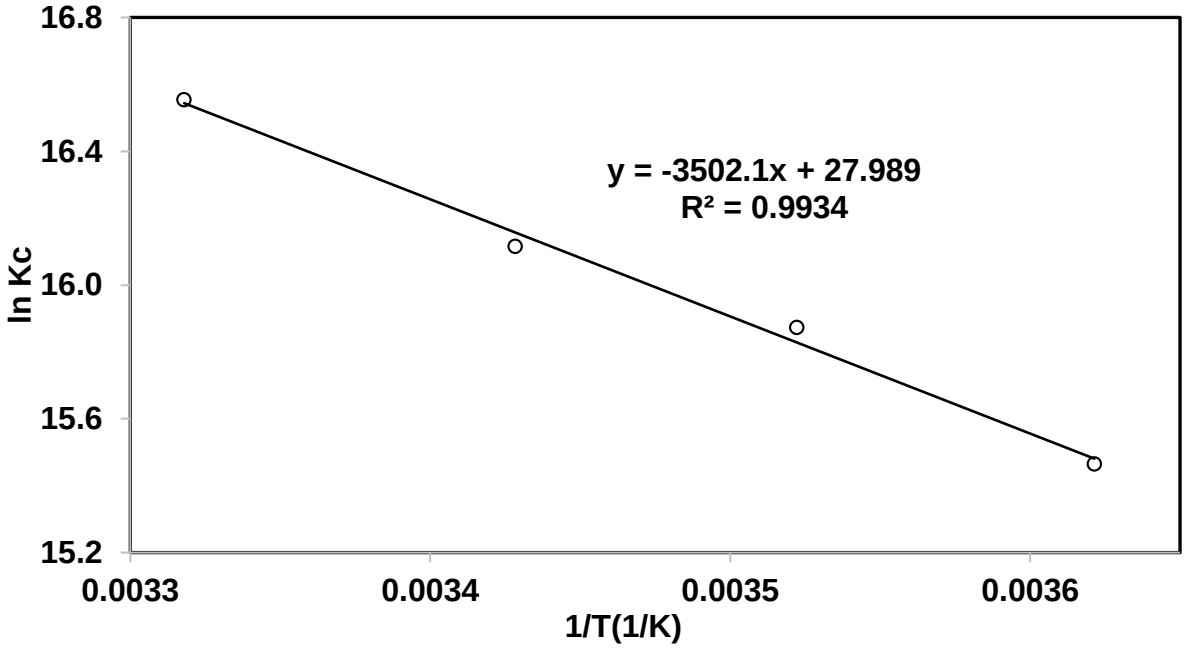

Figure E.7. Van't Hoff plot for thermodynamic analysis of adsorption of lincomycin on natural zeolite at 280-306 K and pH value of 6.5

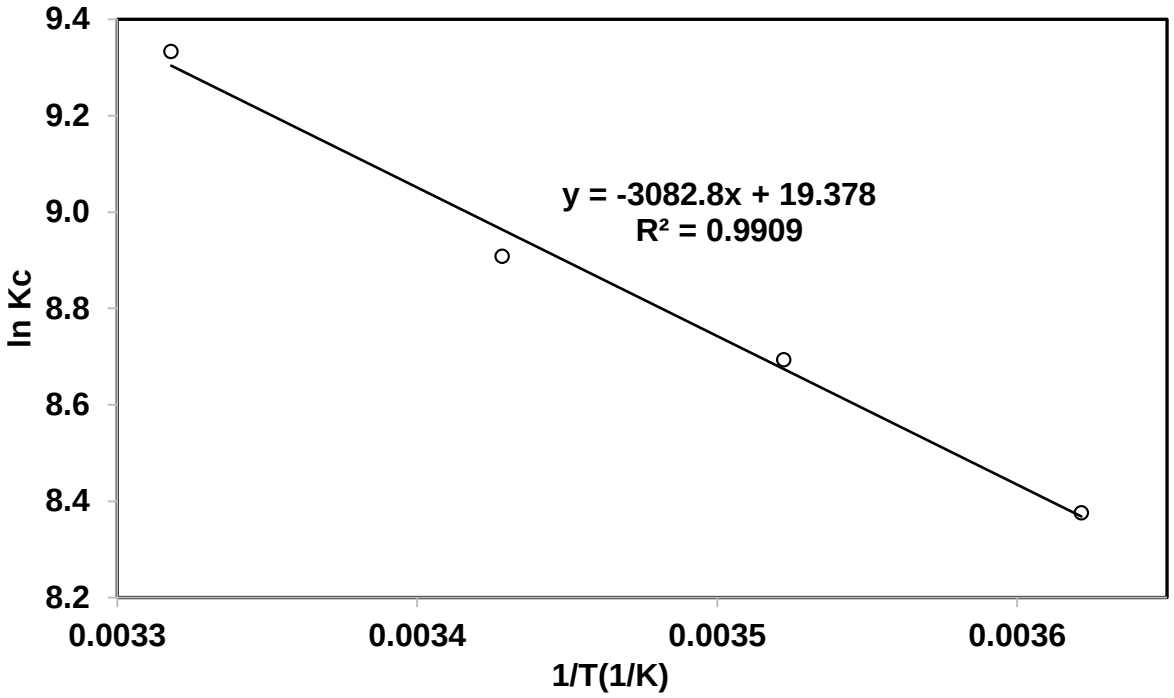

Figure E.8. Van't Hoff plot for thermodynamic analysis of adsorption of lincomycin on modified natural zeolite at 280-306 K and pH value of 6.5